THERMAL CONDUCTIVITY OF EPDM RUBBER COMPOSITES AS A FUNCTION OF FILLER CONCENTRATION AND TYPE.

by

ANDREW ODHIAMBO ODUOR

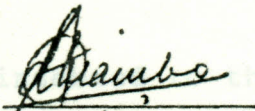A thesis submitted in partial fulfilment for the degree of master of science in Kenyatta University.

Physics Department.

1988.

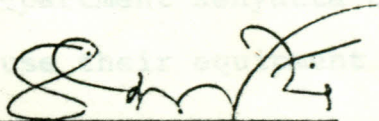This thesis is my original work and has not been
presented for a degree in any other University.

ANDREW ODHIAMBO ODUOR.

(B.Ed.)

This thesis has been submitted for examination with my
approval as the University supervisor.

Dr. SAMUEL K. KATIA,

DEPARTMENT OF PHYSICS,

KENYATTA UNIVERSITY.

ACKNOWLEDGEMENT

I wish to express my sincere gratitude to my
Supervisor Dr. S.K. Katia for introducing me to Polymer
Science and for his tireless and continuous
supervision and advice during the course of preparation
of this thesis.

I am greatly indebted to the management at Car
and General Company for their permission, that made
it possible for me to use their equipment at their
rubber factory and their kind offer of the raw
materials used in the preparation of the samples. My
sincere thanks are extended to Mr. Bondwari, the
Chief Chemist and the entire rubber factory staff,
for their assistance during sample preparation.

I would like to thank the Kenya Industrial
Research Development Institute, leather department;
the University of Nairobi, faculty of Mechanical
Engineering; the Appropriate Technology Centre;
and the Chemistry Department Kenyatta University
for allowing me to use their equipment in this study.

I wish to thank the Science workshop staff
at Kenyatta University for the assistance offered
to me during the construction of the guarded hot
plate apparatus used to test the samples in this
study. The cooperation of the technical staff in
physics department during thermal conductivity tests,

ABSTRACT

Thermal conductivities of EPDM (ethylene propylene diene monomer) rubber loaded with one of the following fillers: carbon black type N339, a reinforcing filler, kaolin, a non-reinforcing filler, and ground charcoal have been studied using a guarded hot plate apparatus designed at Kenyatta University. The hardness and tensile strength as well as the breaking energy of the composites have also been determined.

The results show that the thermal conductivity, k increases with increasing filler concentration in the composites. The thermal conductivity values also increase with increasing composite hardness. Thermal conductivity and tensile strength values were higher for the composites filled with a reinforcing filler than those filled with non-reinforcing ones. The high values are explained in terms of the filler-polymer interaction energies that are higher in composite filled with reinforcing fillers than those filled with the non-reinforcing ones.

Using several known thermal conductivity models, for bicomponent composites, the theoretical values of thermal conductivity were calculated for the various filler concentrations and compared with the experimentally determined values. None of these models, successfully predicted the experimental values of

thermal conductivity of rubber composites. In almost all the cases the theoretical values of k for kaolin, charcoal and carbon black samples are at variance with the experimental values. Explanation for this discrepancy is based on the fact that the polymer filler interaction-parameter which is different in the three fillers used, plays an important role in facilitating thermal conductivity in the composites. Besides other results, the conductivity-hardness and tensile strength results confirm this observation. As a major finding of this work, it is observed that the theoretical models available have been derived on the basis of conductivities of the individual components, they do not incorporate the interaction parameter which apparently plays an important role in rubber composites.

TABLE OF CONTENT

(iv)

LIST OF TABLES

Tables

LIST OF PLATES

LIST OF FIGURES

Page

APPENDIX 1 - TABLES

APPENDIX II - GRAPHS

CHAPTER ONE

1.0.0 INTRODUCTION

Natural and synthetic rubbers have many applications in technological development in modern societies, such as tyres, carpets, shoes, electrical and thermal insulations, etc. Some of these applications require that the rubber be mixed with inorganic fillers to act as either extenders or softeners. Some of the commonly used fillers are kaolin, carbon black, zeosil, micaceous earth, silica, etc. In the manufacture of electrical cables and wires, rubbers have become very important as insulators. It is normal for wires to heat up while conducting large currents. The consequence of heating can sometimes be so, serious, that it causes overheating which results in the rubber insulation breakdown and hence failure in the power. Such breakdowns are determined by the thermal properties of the composite insulating materials. Data concerning their thermal properties are required.

In this study the effect of filler concentration on the thermal conductivity of EPDM at a constant pressure and temperature range of about 393 - 403K, will be examined.

EPDM rubber is widely used in the manufacture of rubber products that are expected to be resistant to weather, light and heat, e.g. radiator hose pipe,

vehicle bumpers, roller covers, electrical wire insulations etc. For this reason a detailed understanding of the thermal properties of EPDM rubber composites is important. In this study EPDM rubber will be filled with, either kaolin or carbon black (N339) or charcoal (kahawa coal).

Generally, Ethylene-Propylene rubbers are resistant to breakdown on milling. In contrast to other rubbers, high proportion of carbon black and oil are incorporated, necessitating on occasions upside down mixing.

EPDM rubber does not possess tack, but in compounds with ENB (5-ethylene-norbornene) as the third monomer, after addition of a tacktifier and light treatment, good tack can be achieved.

During compounding oils are added to the composite, paraffinic and Naphthenic oils are preferred in large amounts because they are compatible with EPDM rubber. Generally, EPDM has excellent resistance to oxygen and ozone. It also has a low specific gravity of 0.86.

The charcoal (kahawa coal) used was bought from the local charcoal dealers. It was prepared from ground coffee hasks that were highly packed into cylindrical pipes and burnt in insufficient supply of air in a kiln. The density measured was 0.99 g/cm^3.

The carbon black used was provided by Car and General Company. It was type N339, from high abrassion furnace with a high structure. Its preparation methods are well documented (1). It had a DBP (Dibutylphthalate number) value of 124cm^3/100g , a density of 2.06 g/cm^3 (1) and a particle size of 26nm (1). The thermal conductivity coefficient associated with this carbon black was 1.59 W/mK and 1.73 W/mK at 303K and 343K respectively. These values are characteristic of amorphous carbon (2).

The kaolin used was manufactured by Athi River mining company and was provided by Car and General Company. It had a thermal conductivity value of 1.97 W/mK (3), a density of 2.61g/cm^3 (3), an oil absorption value of 36cm^3/100g (4), and a particle size of 45 microns (4).

In this study the effect of:

(i) filler concentration on the thermal conductivity of EPDM rubber composites at a constant pressure

(ii) temperature on the thermal conductivity of the rubber composites in the temperature range 293-403K

(iii) filler reinforcement properties on the

thermal conductivity of rubber composites

(iv) fillers on the breaking energy and tensile strengths of rubber composites and the influence of these values on the thermal conductivity of the composite,

will be specifically investigated. The thermal conductivity measured will be tested against some established models found in literature that may be used to calculate the thermal conductivity of composites.

CHAPTER TWO

2.0.0 LITERATURE REVIEW

In relation to this study, it is important to note the contributions of P. Anderson and G. Backstrom (5) in which the thermal properties of insulators were studied under pressure. They used the stationary radial flow method, using thermocouples for their temperature measurements.

The thermal properties of natural rubber as a function of temperature and pressure have been investigated by O. Sandberge and G. Backstrom (6). They determined the thermal conductivity and the heat capacity per unit volume up to 1.0 GPa., in the temperature range 130-340K.

A.B. Bashirov and A.M. Manukyan (7), studied the thermal conductivity k, of high density and low-density polypropylene, polyorthochlorostyrene and polyparachlorostyrene as a function of temperature and pressure. They observed k to increase with increasing omnidirectional pressure on polyparachlorostyrene and polyorthochlorostyrene. They attributed this increase to the decrease in the free volume, and also measured k for various temperatures for low and high density polyethylene, and observed a decline in k with increasing temperatures. The thermal conductivity sharply declined

at the melting temperatures, a result of the disruption

of the closely packed crystalline structure. They

observed a sharp increase in k for temperatures above

the melting temperatures, and attributed this to the

high elasticity of the polymer, a state characterized

by vibrationary motion of the monomer units (torsional and

vibratory), so that the polymer chain is able to bend

hence increase in the k values. The k values of high

density polyethylene were higher than those of the low

density polyethylene.

Thermal conductivity tensor in insulating materials

has been studied by Silas E. Gustafsson and Ernest

Karawachi (8). Using the hot strip method, they

determined the heat capacity and the thermal conductivity

along the principal directions of orientation of the

molecules. The temperature dependence of the thermal

conductivity of amorphous polymers have been reported by

"Reese (9)". He studied the dependence of k on temperatures

below the T_g of PMMA. The dependence of k of PMMA on

temperature through its T_g has also been reported by

Eiremann (10).

Thermal conductivity of some rubbers under pressure

have been studied by transient hot wire method by P.

Anderson (11). In that study the effect of fillers

on the thermal conductivity of various rubber composites

under pressure were described. It was found that the

thermal conductivity increased with increasing pressure at 300K. Experimentally determined data for the thermal conductivity of ethylene/propylene rubber composites filled with zinc oxide were tested against two models (Figs. 1 and 2). The theoretically determined values of k, did not satisfactorily agree with the experimental data. The experimental values were found to be higher than the theoretically determined values between filler volume fraction of 0 and about 0.25 (Fig. 1). Above this filler concentration the theoretical values were found to be higher than the experimentally determined values. The variance may have been caused by the influence of filler polymer interaction that was not accounted for in the calcualtion of k.

A review of thermal conductivity of polymers has been made by D.R. Anderson (12). Thermal conductivity of rubber composites is also given in the review. Attention was paid to natural rubber, perbunan N2810, Buna Huls 152 and Enjay Butyl 365, filled with philblack (carbon black) and vulkasil. In the review, thermal conductivity of rubber composite linearly increase with increasing filler concentration (13, 14) and with increasing sulfur content (15) .

Dauphinee (16, 17) has measured the thermal conductivities of the stretched and the unstretched
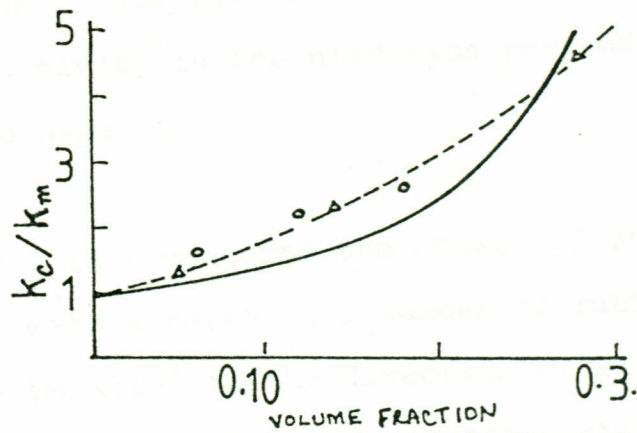
Fig. 1. Relative thermal conductivity at atmospheric pressure vs volume fraction of ZnO filler. △, ZnO in EPM rubber [7]; ○, ZnO in Silicon-organic rubber [19]
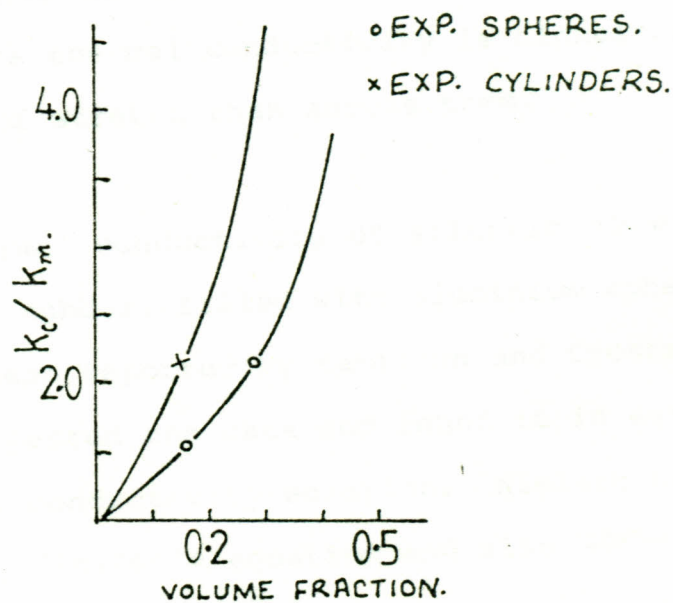
Fig. 2. Thermal conductivity of rubber composites consisting of aluminium spheres and aluminium cylinders. Solid lines are theoretical predictions from Nielsens model [14-16].

natural and GR-S rubbers. He observed lower values of thermal conductivity in the direction perpendicular to the stretched samples.

Tantz (18) measured the change of thermal conductivity with stretch on a number of rubber vulcanizates parallel to the direction of stretch. In all the materials investigated a considerable increase in the thermal conductivity with elongation was observed. The results of Dauphinee (16, 17) and Tantz (18), show the important role played by molecular and perhaps filler orientation in thermal transport through rubber composites. The thermal conductivity is highest along the direction of stretch than across them.

The thermal conductivity of silastic (Dow-Corning corp.) RTV-502 rubber, filled with aluminium spheres and rods has been reported by Hamilton and Crossers (19). They tested the data and found it in agreement with Hamiltons conductivity equation. Nielsen tested the data using Nielsen's equation and also showed agreement (20), (Fig. 2) .

It is important to note the unique method used to prepare the samples tested for k, by Hamilton and Crosser (19) . The mixture was prepared by stirring a weighed amount of particles into a measured volume of silastic (Dow-corning corp.) RTV-502 rubber and then

adding 3 drops of catalyst which accelerated the
vulcanization process. The fact that the mixture from
which the samples were prepared was simply stirred to
obtain good filler dispersion, guaranteed a constant
viscosity for all the mixtures prepared, and hence the
consistency with the theoretical results of Hamilton
and Neilsens. Milling or banbury mixing is known to
influence the viscosity of the mixed composite. This
has far reaching effects on the reinforcement
properties of the cured vulcanizate.

Atkins and Sullivan (21) developed an apparatus
for determining the thermal conductivity of rubber
composites. Using this apparatus they determined the
thermal conductivity of composites of cured butyl
stocks filled with various blacks at 40 phr loading
(Table 1). Despite the significant differences in the
effective thermal conductivities of the various blacks
of upto 50% (Table 2) (18), the difference in k of
the composites was hardly 10%. This was an indication
that, the effects of the elastomer vastly overshadows
those of the black in the effective k of the composites.

CARBON BLACK	THERMAL CONDUCTIVITY
Vulcan XC-72 (N472)	0.201
Sterling V (N660)	0.192
Sterling SO (N550)	0.192
Vulcan SC (N294)	0.187
Vulcan 6H (N242)	0.187
Vulcan 6 (N220)	0.187
Vulcan 3 (N330)	0.180
Vulcan 9 (N110)	0.180

CARBON BLACK	THERMAL CONDUCTIVITY
Vulcan C (N293)	0.180
Regal 600 (N219)	0.178
Regal 99 (N440)	0.178
Regal SRF (N761)	0.178
Sterling MT (N991)	0.170

TABLE 1   Thermal conductivity of Butyl stocks containing various Blacks in W/mK in the temperature range 308-373K (21).

CARBON BLACK	TYPE	THERMAL CONDUCTIVITY
N326	HAF-LS	0.0197
N330	HAF	0.0268
N347	HAF-HS	0.0306
EXP.	HAF-VHS	0.0343
EXP.	HAF-VHS	0.0452
N242	ISAF-HS	0.0285
N472	XCF	0.0352

TABLE 2   Thermal conductivity k for a series of HAF and ISAF blacks of different structures measured at constant pressures (22). Values of k are expressed in W/mK.

In this study, k of cured EPDM rubber composites filled with various fillers ie. charcoal, kaolin and carbon black (N339) will be determined. The results will be used to establish whether Hamilton, Nielsens and other models also hold in this case, where the samples are prepared by mixing EPDM rubber with the fillers on an open mill.

CHAPTER THREE

3.0.0 THEORY

In this section the following will be considered namely (a) Modes of heat transfer (b) Fouriers law (c) Models for predicting thermal conductivity of composites (d) General filler properties (e) Filler dispersion in composites (f) Rubber reinforcement and (h) Bound rubber.

3.1.0 MODES OF HEAT TRANSFER

There are three types of heat transfer processes, these are convective, radiative and conductive heat transfer processes. The convective heat transfer mode refers to energy transfer due to random molecular motion, and energy being transfered by bulk, or macroscopic motion of the fluid. Thermal radiation is energy emitted by matter that is at finite temperature, by electromagnetic waves. The higher the temperature of a body, the greater the total energy emitted.

When temperature gradient exists in a stationary medium, which may be a solid or a fluid, conduction of heat across the medium occurs. Conduction may be viewed as the transfer of energy from more energetic to the less energetic particles of a substance through thermal interaction between the particles. In solids with no interstitial voids conduction is the dominant

mode of heat transfer. In this discussion conduction
is assumed to be the main mode of heat transfer.

3.2.0 FOURIER'S LAW

The relationship between the heat transfer rate
by conduction and the temperature distribution is
given by Fourier's Law (23). For one dimensional plane
wall shown in Fig. 3, having a temperature distribution
T(x), the rate equation is expressed as

$$q = -k\,dT/dx \quad \ldots\ldots\ldots\ldots\ldots \quad 3.1.$$
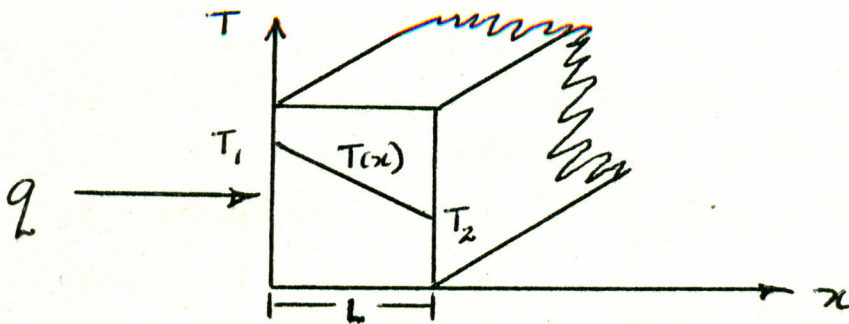
Fig. 3 One dimensional heat transfer by
conduction.

q = Is the heat flux (W/m^2) i.e. the heat
transfer rate in the x-direction per unit
area perpendicular to the direction of
transfer. It is proportional to the
temperature gradient dT/dx.

k = The proportionality constant, is a transport
property called the thermal conductivity, and
is a characteristic of the wall material.

The minus sign is a consequence of the fact that heat is transfered in the direction of decreasing temperature.

Fourier's law as written in equation 3.1 implies that the heat flux is a directional quantity. The direction of $\dot{q}$ is normal to the cross-section area A. The direction of heat flow will always be perpendicular to a surface of constant temperature called isothermal surface.

3.3.0 MODELS ON THERMAL CONDUCTIVITY OF BINARY COMPOSITES

The thermal conductivity of a polymer composite may be analyzed in terms of separate contributions from the filler and the matrix. Many relationships based either on experimental data, or theoretical models with various degrees of realism have been proposed.

The models that have been used to calculate or explain the thermal conductivities of materials can be classified into three groups (24).

(a) The Flux-law model: derives the temperature gradient of one of the following model systems (25,26,27):

(i) A regular array of spherical particles which may be in contact or dispersed.

(ii)   A random distribution of spheres dispersed
        in a matrix phase so that no interaction
        between the temperature fields of the
        particles occurs.

Fourier's law given by equation 3.1 is based on the
flux-law model.   Flux-law is inadequate in determining
temperature fields inside a body.

(b)   Ohm's-law model: The draw-back of Fourier's model
gave rise to Ohm's-law model (28,29,30,31,32,33) which
is derived from an electrical analogue of a system of
resistances, assuming a one dimensional heat transfer
through a unit cell of material.

     Russell (28) developed one of the early model
system using electrical analogy.   He considered two
extreme cases, they are

        (a)   a continuous split phase with isolated cubic
              filler phase and

        (b)   continuous filler phase with discontinuous
              cubic solid particles.

Using these two model systems Russell derived two
equations giving the relationship between the composite
conductivity, the volume fractions and conductivities
of the two components.   For a continuous matrix phase:

$$k_c = k_m \left[\frac{\phi^{2/3} + k_m/k_f (1-\phi^{2/3})}{\phi^{2/3} - \phi + k_m/k_f (1-\phi^{2/3}+\phi)} \right] \quad \dots\dots\dots\dots 3.2.$$

and for a continuous filler phase:

$$k_c = k_f \left[\frac{(1-\phi)^{2/3} + k_f/k_m (1-(1-\phi)^{2/3})}{\phi - (1-\phi)^{2/3} - 1 + k_f/k_m (1-\phi-(1-\phi)^{2/3})} \right] \quad \dots\dots\dots 3.3.$$

where k_c = composite conductivity.

k_m = matrix-phase conductivity.

k_f = filler-phase conductivity.

ϕ = volume fraction of the filler-phase.

It would be expected that the thermal conductivity of a real system would be better described by a combination of both these models, and would hence exhibit conductivity somewhere between the calculated values of equations 3.2 and 3.3.

Wyllie and Southwick (33) developed a three resistor model for calculating the electrical conductivity of an aggregate of conducting particle in a conducting electrolyte. These three elements were considered to be

(a) particles and electrolyte in series,

(b) particles in close contact, thus forming a continuous solid conducting path,

(c) the electrolyte filling the interstices.
This model is depicted in Fig. 4.
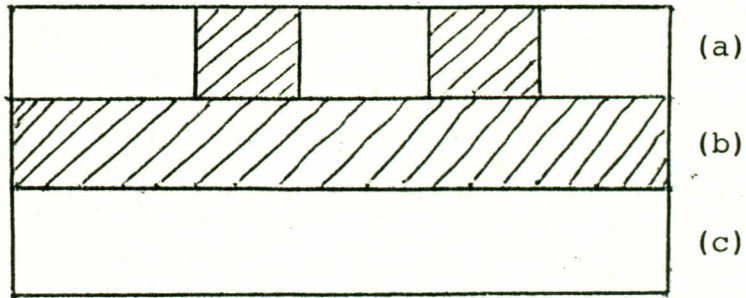
Fig. 4 The Wyllie and Southwick (33) three-element
resistor model. The letters refer to
texts above (the solid phase is shaded).

Woodside and Messmer (29) adopted this model for the
calculation of the thermal conductivities of two phase
systems and developed it to give a weighted mean
equation of the form,

$$k_C = \frac{ak_m k_f}{k_m(1-d) + k_f d} + bk_m + ck_f \quad \dots\dots\dots\dots\dots\dots 3.4.$$

where the terms a, b, c, and d are defined in Fig. 5.
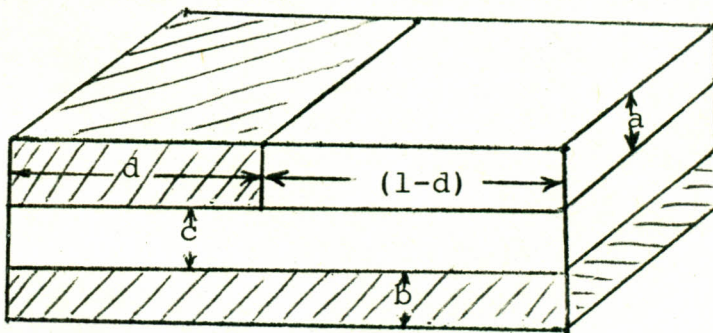
Fig. 5 The Woodside and Messmer three-element resistor
model. The letters refer to the text above.

Dul'nev and Zarichnak (31) derived an expression
similar to equation 3.4 with numerical values for
a to d (eq. 3.5).

$$k_c = \frac{2/3 k_m k_f}{k_m \phi + k_f (1-\phi)} + 1/3 (k_m (1-\phi) + k_f \phi) \qquad \ldots\ldots\ldots \quad 3.5.$$

In the early models, one phase (the filler)
considered as a spherical island in a continuum of
matrix of the polymer phase and the effective thermal
conductivity was calculated from eq. 3.6.

$$\frac{k_c}{k_m} = \frac{1+2\phi (k_f/k_m-1)(2+k_f/k_m)^{-1}}{1-\phi (k_f/k_m-1)(2+k_f/k_m)^{-1}} \qquad \ldots\ldots\ldots\ldots\ldots \quad 3.6.$$

Equation 3.6 is applicable only to dilute dispersions.
But Brailsford and Major (34), have extended the result
of this model to cover the full range of compositions,
by a random two-phase mixture in equation 3.7, and
assumes that, the overall conductivity of the composite
is equal to the average conductivity of the two phase
separately.

$$\frac{k_c}{k_m} = 1/4 \left[(3\phi-1) k_f/k_m + 2-3\phi + \right.$$
$$\left. \left\{ \left[(3\phi-1) k_f/k_m + 2-3\phi \right]^2 + 8k_f/K_m \right\}^{\frac{1}{2}} \right] \ldots 3.7.$$

(c)   There are many emperical relationships between the
effective conductivity of a material and the volume
fractions of its components and their conductivities.
A large number of these relationships take an equation
derived from a model and include an empirical value to
give the best fit to the available data. Chaudhary and

Co-workers (35) used a variation of the equation derived from the model shown in Fig. 5, which takes the form in equation 3.8-9.

$$k_c = (\phi k_f + (1-\phi) k_m)^n (\phi/k_f + (1-\phi)/k_m)^{n-1} \quad \ldots\ldots\ldots \quad 3.8.$$

$$n = \frac{0.5(1 - \log\phi)}{\log(\phi(1-\phi)k_m/k_f)} \quad \ldots\ldots\ldots \quad 3.9.$$

Other models have also been proposed to predict thermal conducitivity e.g.

(i)   The Nielsen's model (20, 37, 38) is a modification of the Kerner equation (39) and Halpin equation (40). It has been used to evaluate the modulus (shear, youngs or bulk), dielectrical and thermal conductivity of composites. The Nielsen's equation is given below.

$$\frac{k_c}{k_m} = \frac{1 + AB\phi}{1 - B\psi\phi} \quad \ldots\ldots\ldots \quad 3.10 \ (a).$$

where

$$\psi = 1 + \left[(1 - \phi_m)/\phi_m^2\right] \quad \ldots\ldots\ldots \quad 3.10 \ (b).$$

$$A = k_E - 1 \quad \ldots\ldots\ldots \quad 3.10 \ (c).$$

$$B = \frac{k_f/k_m - 1}{k_f/k_m + A} \quad \ldots\ldots\ldots \quad 3.10 \ (d).$$

and k_f = thermal conductivity of filler phase.

k_m = thermal conductivity of matrix phase.

k_E = Einsteins coefficient.

ϕ = volume fraction of filler phase.

ϕ_m = maximum filler packing.

A = takes into account factors, such as geometry

of the filler phase and poisson's ratio of the

matrix.

B = takes into account the relative conductivities

of the filler and matrix phases.

Thermal conductivity can also be predicted using

Hamilton's equation (41) based on the model of a

heterogeneous system and consists of a filler phase

dispersed in a matrix phase. The fillers may be of

different shapes, distributed in either regular or

irregular array. On this basis Hamilton (41), gave the

equation 3.11.

$$k_c = \frac{k_m \phi_m (dT/dx)_m + k_f \phi_f (dT/dx)_f}{\phi_m (dT/dx)_m + \phi_f (dT/dx)_f} \qquad \dots\dots\dots\dots\dots 3.11.$$

where $(dx/dT)_m$ and $(dx/dT)_f$ are the overall

temperature gradients in the matrix and

filler phase.

An average gradient ratio can be determined from the

theoretical work of Maxwell and Fricke (42,43) to be

of the form:

$$\frac{(dT/dx)_f}{(dT/dx)_m} = \frac{nk_m}{k_f + (n-1)k_m} \qquad \dots\dots\dots\dots\dots 3.12.$$

where n depends on the shape of the particles and upon

the ratio of the conductivities of the two phases.

From solutions of Laplace's equation in spherical

coordinates (36), equation 3.12 becomes

$$\frac{(dT/dx)_f}{(dT/dx)_m} = \frac{3k_m}{k_f + 2k_m}$$ .... 3.13.

for spherical particles. By substituting equation 3.13 into equation 3.11 Maxwell's equation is obtained.

$$k_c = k_m \left[\frac{k_f + 2k_m - 2\phi_f(k_m - k_f)}{k_f + 2k_m + \phi_f(k_m - k_f)} \right]$$ .... 3.14.

The use of these equations must take into account the following assumptions (24).

(a) The arrangement of the filler phase should be random.

(b) The filler particle sizes should be small in relation to the sample size.

(c) The filler and matrix should form a simple physical mixture.

3.4.0 GENERAL FILLER PROPERTIES

Raw rubber consists of a large number of flexible long-chain molecules possessing a structure which permits free rotation about certain chemical bonds along the chain. The crosslinks introduced randomly during vulcanization build up a three dimensional network. The basic element of such a

network is the portion of the molecule between two
adjacent crosslinks known as network chain.

Vulcanizates are normally reinforced by the
addition of fillers. The following fillers were used
in this study; charcoal (kahawa coal), kaolin and carbon
black (N339).

Reinforcing fillers have general properties
broadly classified as follows (44).

(i)   The extensivity factor, is the amount of
      surface area of the filler in contact with
      the polymer. In general the smaller the
      particles the bigger the surface area, the
      poorer the processibility and the higher the
      reinforcement. The area of interface between
      solid and elastomer in a compound, depends
      on the surface area per gram of the filler
      and also on the amount of filler in the
      compound.

(ii) The intensity factor is the specific activity
      of the solid surface per cubic centimetre of
      the interface. The filler surface activity
      also plays a very important role depending
      on the chemical groups present, which may in
      turn determine the adsorptive capacity of the
      polymer on the filler.

(iii) Geometric factors refer to the structure and porosity of the filler particles. The geometric characteristics determine the packing density of the filler in the composite. Non-spherical particles have a packing which is less dense than that of spheres leaving a greater volume of voids in between the particles.

Each of these properties affect the rubber matrix in which they are incorporated differently.

Adsorption measurements have shown that the adsorptivity of reinforcing black is not homogeneously distributed but concentrated at a number of sites of much greater activity than most of the surface. These sites only represent a small percentage, less than 5% of the total surface (45). Evidence of active sites is shown by heat treatment of carbon black through a process called graphitisation. This is known to destroy the activity of the sites, by recrystallizing the filler particle and a total loss of surface flaws in the lattice, which are believed to be responsible for the active spots (46). Graphitized carbon black results in poor mechanical properties when mixed in rubber.

There are two types of adsorptions; namely mobile and local adsorption. The adsorption energy on the

filler surface varies along the surface. This is
illustrated in Figs. 6(a) in which a rubber molecule
adsorbed at location A, needs an energy E to remove it
from the surface, but only the amount x of the small
energy barrier to move it to location B. This barrier
is of the same order as the thermal energy of the polymer
molecule. It implies that the adsorbed rubber segment
can freely move over the surface when stress is applied.
This is referred to as mobile adsorption. Local
adsorption is depicted in Fig. 6(b). A molecule located
at A, needs an energy E to remove it from the surface
and to move it from A, to B.

The potential energy profiles of a normal carbon
black and a graphitized carbon black surfaces are shown
in Fig. 7 (a) and (b) respectively (47). Fig. 7(a)
shows the heterogeneity of the surface of a reinforcing
carbon black as is depicted in the form of energy
troughs of varying depths. In general these troughs
are caused by defects in the crystal lattice or in the
case of carbon black, also by end effects at the edges
of the crystallographic plane layers. Fig. 7(b) shows
the effect of graphitizing carbon black, a process that
involves heating carbon black at the temperatures 2000-
2500°C. It has been shown that upon graphitisation at
3000°C carbon black looses a significant part of its
reinforcing characteristics (44).

The result of graphitisation is the observed

(a)

(b)

(c)
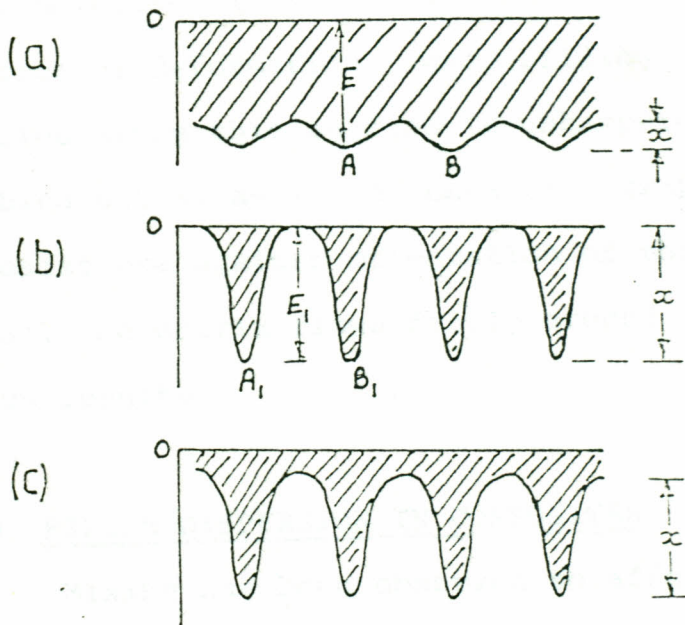
Fig. 6. Schematic representation of energy berrier to the translation of adsorbed molecules along the surface. From Ross and Oliver [46].

(a)

(b)
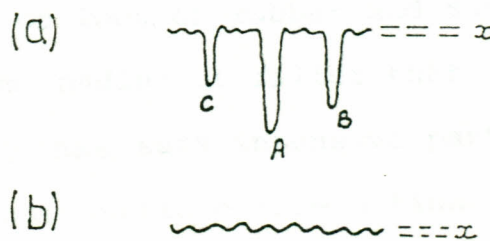
Fig. 7. Potential energy profile of (a) normal carbon black and (b) a graphitized carbon black surface; points A, B and C represent sites of high adsorptive energy in decreasing order. From Boonstra and Taylor [47].

decline in the modulus properties of the vulcanizate.
The main effect of high structured particles on modulus
is the resistance they offer against orientation of the
matrix molecules in the direction of flow lines during
extension or deformation. When sliding of polymer
molecules along this surface is unhampered by strong
adsorbing sites, as is the case with graphitized black,
the resistance against orientation of the particle is
minimal, the matrix flows freely around it and a low
modulus results.

3.5.0 FILLER DISPERSION IN COMPOSITES

Mixing has been observed to affect the ultimate
vulcanizate properties of the rubber composite, depending
on the extent of dispersion of the filler in the rubber
matrix. Boonstra (44) observed, that for a filler with
oil absorption of $1.25 \, cm^3/g$ the primary agglomerates has
a composition of 100g of rubber and 85g of filler. This
is the maximum loading of filler that is still dispersible.
Higher loading has such intensive particle-to-particle
contact and interparticle interaction that they are no
longer dispersible within a practical time. In a well
mixed batch the filler particles are well dispersed (Fig.
8(a)), a poorly dispersed batch has large lumbs that are
not dispersed (Fig. 8(b)).

Several methods have been devised to determine the
degree of dispersion (44,48), these include the monsanto
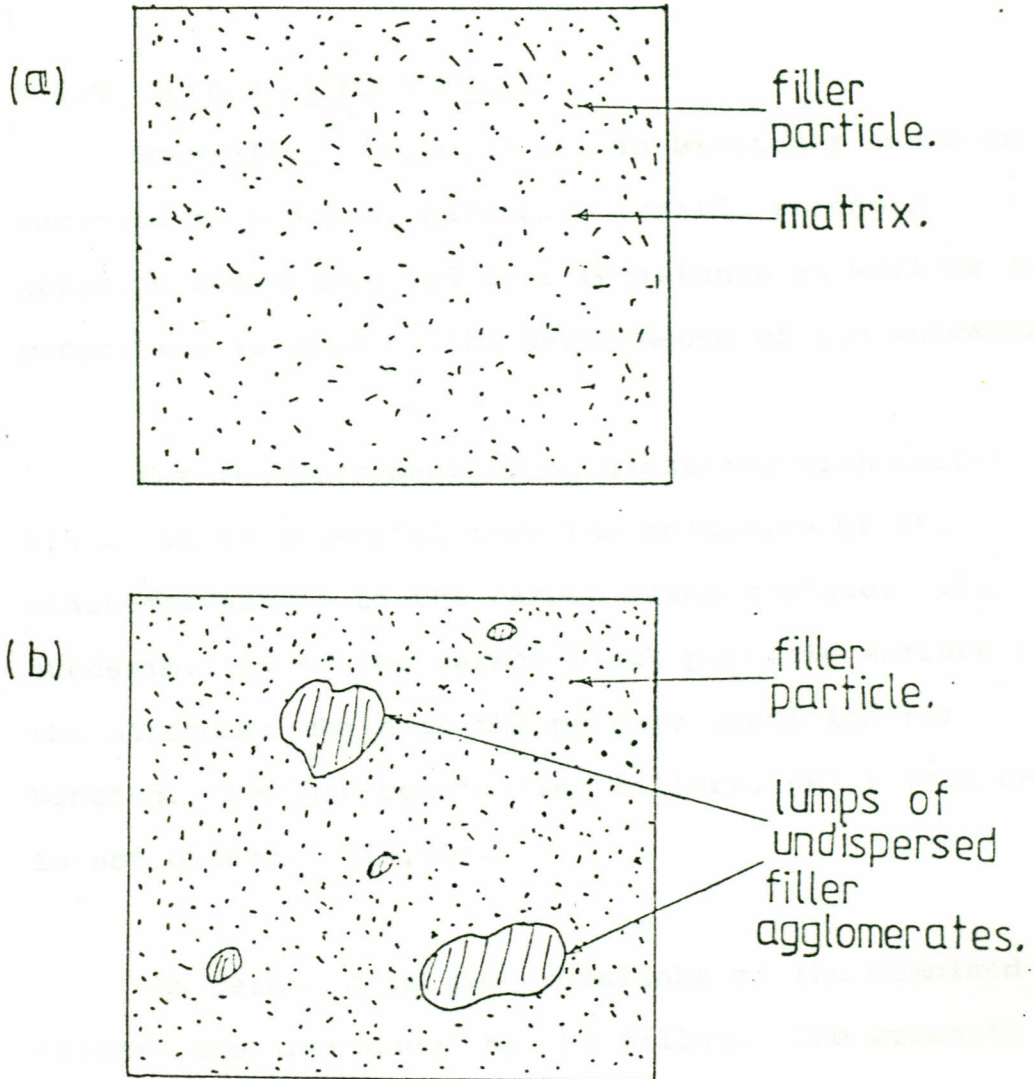
Fig. 8. a) A well mixed composite showing good filler dispersion.

b) A poorly mixed composite with lumbs of undispersed filler agglomerates.

rheometer (see section 4.1.3).

3.6.0 RUBBER REINFORCEMENT

Generally, reinforcement in elastomer shows an increase in modulus, hardness, tensile strength, abrasion resistance and tear resistance as well as other properties related to the performance of the vulcanizate.

For reinforcement of an elastomer with carbon black, it is essential that the molecules of the elastomer adhere to the carbon black surface. The accessibility of the carbon black particle surface to the elastomer chain is the primary condition for bonding. For non-reinforcing fillers, gel formation is not observed (49,50).

In carbon gels the crosslinks of the combined network are introduced by the filler. The strength of these crosslinks is the determining factor in the characteristics of the elastomer-carbon network which forms the reinforced vulcanizate. The essence of reinforcement by fillers is the interaction between particle and elastomer chains, particularly the strength of the bonds. The fundamentals of reinforcement are therefore, directly related to the nature and properties of the carbon-elastomer bonds.

3.7.0 BOUND RUBBER

When carbon black is mixed with rubber, rubber chain molecules became attached to reinforcing fillers, as a result of which they are no longer soluble in the usual rubber solvents. The rubber adhering to the carbon black is known as "bound rubber" or carbon gel (51).

Bound rubber is basically proportional to the surface area of the black accessible to elastomer chains. It depends on the physical and chemical activity of the surface of the black particles (48).

Graphitized black has a relatively inactive surface while the surface of reinforcing blacks is much more active as reflected in their bound rubber values.

Bound rubber formation is usually explained in terms of mechanical breakdown of polymer chain molecules that result in the appearance of free radicals at the newly formed chain ends. Reactive sites on the filler surface then combine with these free radicals to form the bound rubber (52).

CHAPTER FOUR

4.0.0   APPARATUS, SAMPLE PREPARATION AND EXPERIMENTAL
        PROCEDURES

4.0.1   INTRODUCTION

In this section the apparatus used will be
described, details will be given for those that were
built. Sample preparation will be described and finally
the experimental procedures adopted will be outlined.

4.1.0   APPARATUS

The following pieces of equipment were used in
this study: The guarded hot plate apparatus, compact
data logger, water bath temperature regulator, power
supply, digital multimeter, mixing mill, rheometer,
curing molds, hot press, wallace pocket hardness meter,
clicker, instron machine and the planimeter. The
construction and use of these pieces of equipment will
be briefly discussed.

4.1.1   THE GUARDED HOT PLATE APPARATUS

Various methods have been concieved on how to
measure the thermal conductivity of insulating materials
(21, 29, 53-56). There are two types of the guarded
hot plate apparatus, the square and the circular guarded
hot plate apparatus. In this study the circular guarded
hot plate apparatus was built to determine the thermal

conductivity of rubber composites of circular samples, and is described below.

The guarded hot plate apparatus used is similar in many respects to the type described by ASTM (56). The apparatus was made up of heaters, cooling and heating surface plates, cotton wool as the sample edge insulator and temperature detectors. The samples were held between the cooling and heating surface plates, by a clamp and enclosed in a water tight box.

(a) HEATERS

The heaters consisted of the metering and the guard heaters. The metering heater was an asbestos circular disc of radius 5.5 cm. The guard heater was a ring that was concentric to the metering heater with an internal radius of 5.7 cm and an external radius of 6.7 cm. The asbestos sheet used for both the metering and guard heater windings had a thickness of 0.16 cm. The ring had been cut out in parts such that some sections were left to hold it to the disc, as is illustrated in Fig. 9(a). The gap between the guard ring and the metering heater was 2 mm wide.

On to the asbestos circular disc and concentric ring was wound an element wire (constantan) of diameter 0.029 cm. The following assumptions were made about
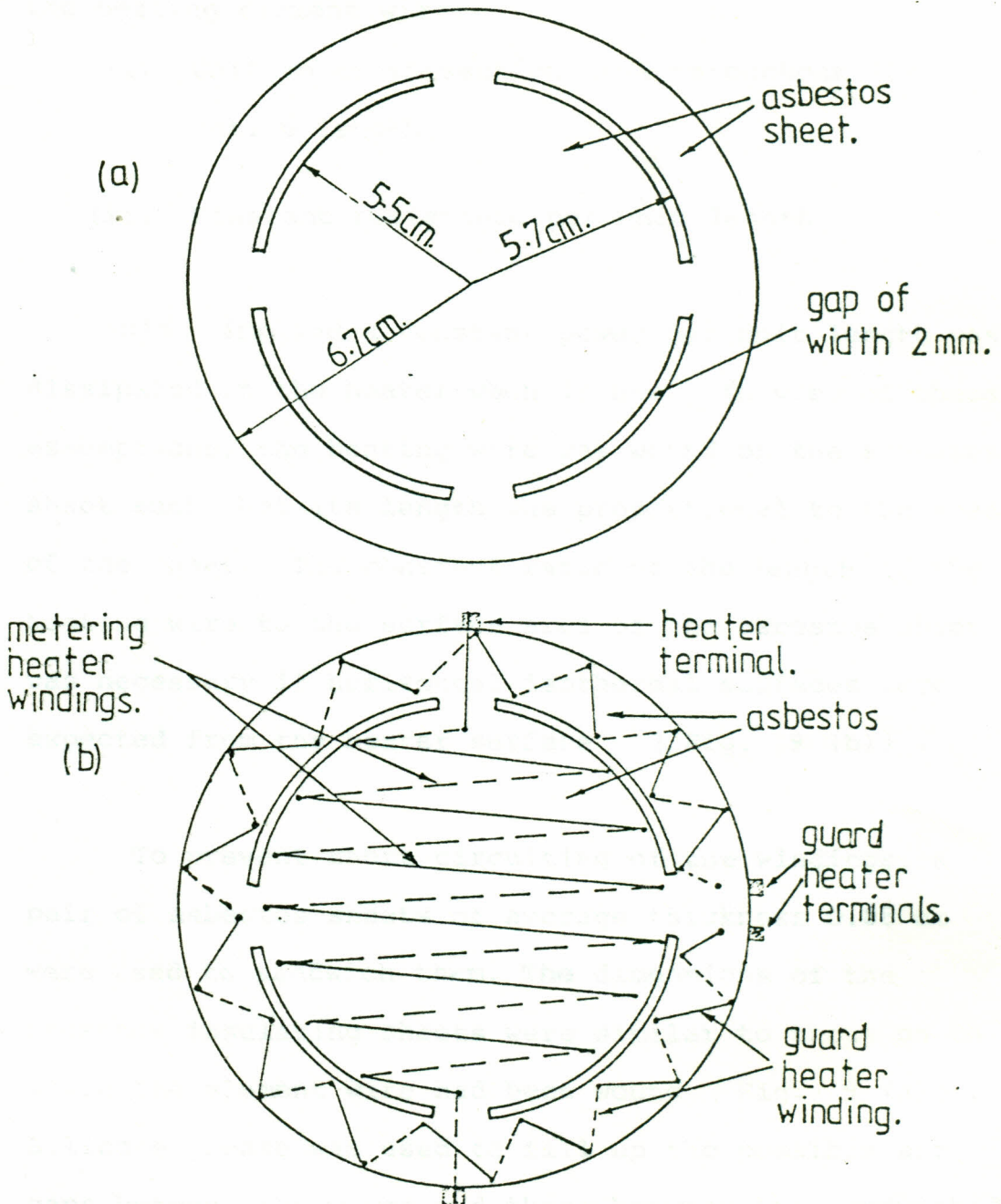
Fig. 9 . a) Asbestos sheet of thickness 0·88mm, used to sandwich the heater windings.
b) Asbestos sheet of thickness 0·16cm, with metering and guard heater windings.

the heating element wire:

(i) Uniform cross-section area throughout its entire length.

(ii) Constant resistance per unit length.

This implied a constant power per unit length was dissipated in the heater when in use. In view of these assumptions, the heating wire was wound on the asbestos sheet such that its length was proportional to the area of the sheet. The constant ratio of the length of the heating wire to the surface area of the asbestos sheet was necessary if horizontal isothermal surfaces were expected from the heater surface (Fig. 9 (b)) .

To prevent short circuiting of the windings, a pair of asbestos sheets of average thickness 0.88 mm were used to sandwich them. **The** dimensions of the asbestos insulating sheets were similar to those on to which the element wire had been wound (Fig. 9 (a)) . Silicone grease was used to fill up the possible air gaps between the wires,and those between the sandwiched sheet and the heaters. Silicone grease was used because of its inert properties and high thermal conductivity value. The gap between the metering and the guard section was filled with silicone rubber to avoid convective and radiative heat transfers from one section to the other.

(b)   SURFACE PLATES.

Two types of surface plates were used, the heater
surface plates and the cooling surface plates. The
heater surface plates comprised of the metering and the
guard surface plates. The metering surface plate was a
disc made from a copper sheet of thickness 0.071 cm
and radius 5.5 cm. Concentric to this disc was the
guard surface plate also made from a similar copper
sheet, but had an internal and external radii of 5.7cm
and 6.7 cm respectively (Fig. 10a). A gap of 2 mm
was left between the metering and guard surface plates.
The surface areas of the asbestos sheets used for the
heaters, and the heater surface plates were the same
(Fig. 9 (a)).

The pair of metering and guard surface plates
sandwiched the heaters (Fig. 11). The cooling surface
plates were two circular discs made from copper plates
of thickness 0.2 cm. They were of radius 6.7 cm. The
samples were placed between the heater surface plates
and the cooling surface plates, when in test (Fig. 12
and   Fig. 10 b).

(c)   TEMPERATURE DETECTORS

Type J-thermocouples of diameter 0.49 mm were used
to measure the temperatures on the surface of the samples.
On each of the metering and cooling surface plates two
thermocouple junctions were placed to sensor the
temperature (Fig. 12) . Each junction was positioned

(a)

5.5 cm.

5.7 cm.

6.7 cm.

guard heater surface plate.

metering heater surface plate.

gap of width 2mm.

(b)

6.7 cm
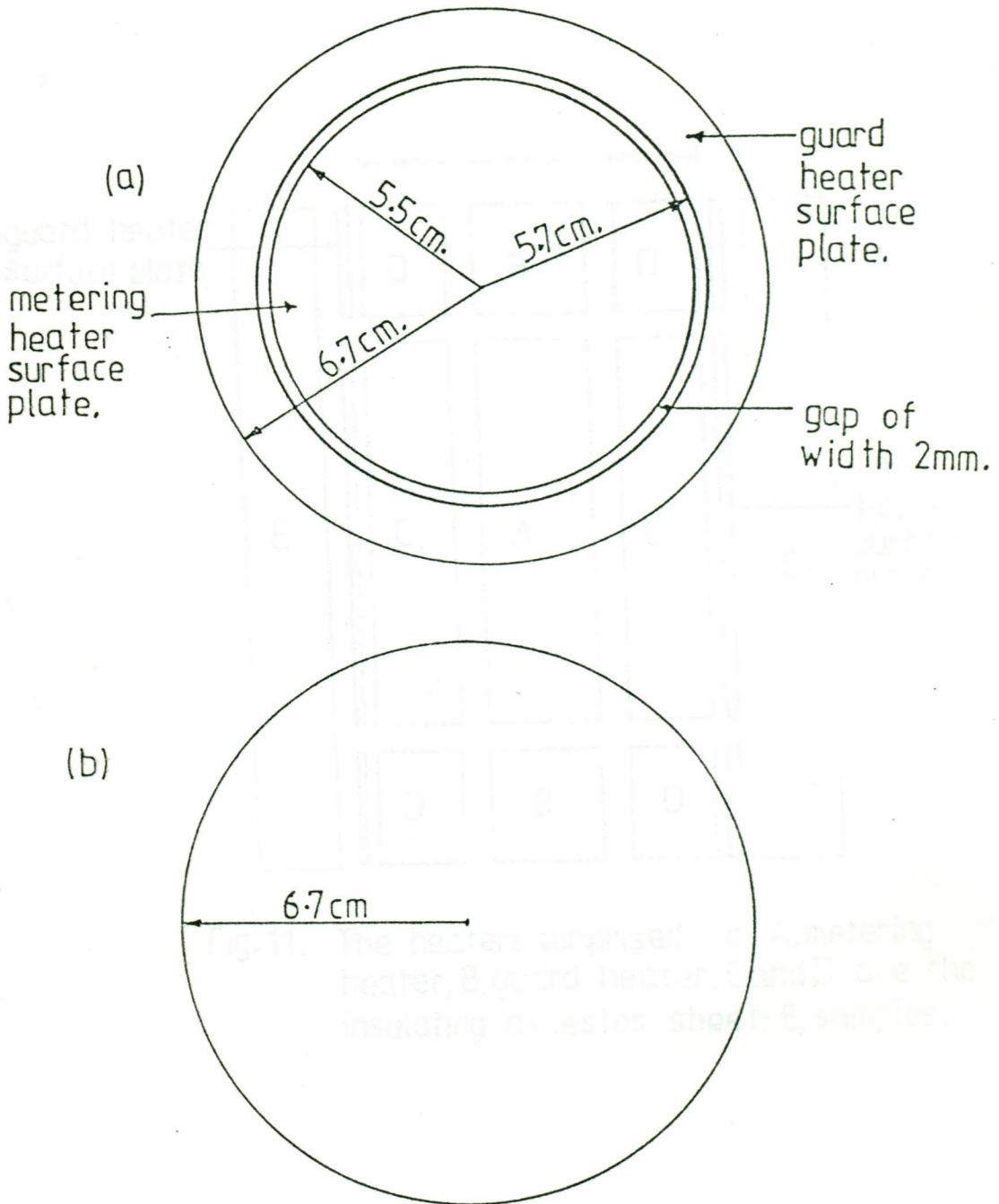
Fig.10.   a) Metering and guard heater surface plates.

b) Cooling surface plate.
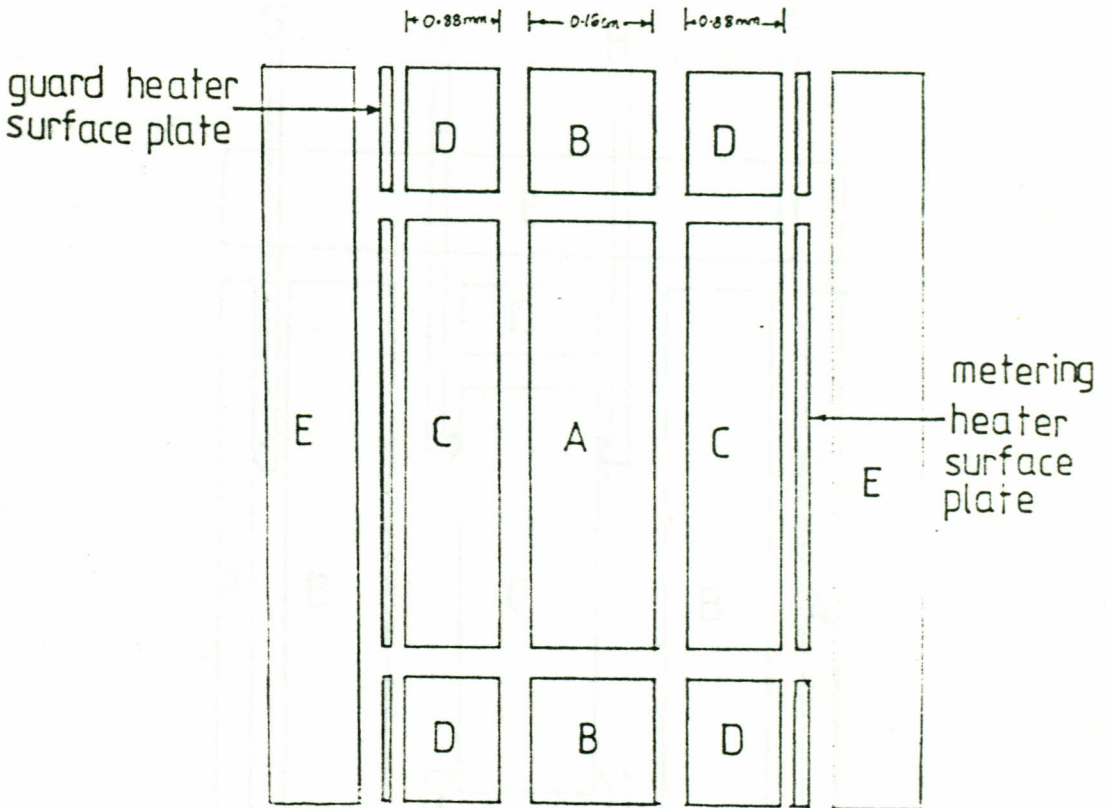
Fig. 11. The heaters comprised of A, metering heater; B, guard heater; C and D are the insulating asbestos sheet; E, samples.

Fig.12. The Guarded hot plate apparatus: A, surface cooling plates; B, test samples; C, metering surface plates and heater; D, guard surface plates and heater; E, cotton wool for lagging; F, differential thermocouples; G, thermocouples on cooling surface plates; H, thermocouples on metering surface plates.

along the diameter d, of the plates at d/3 and 2d/3 through holes of diameter 1.0 mm. Small grooves were cut next to the holes on these plate surfaces, so as to accommodate the junctions (Fig. 13). These junctions were positioned such that one side was firmly held on the groove surface using a thin film of araldite resin, the other side was exposed so as to monitor temperature changes on the surface of the sample. The araldite also insulated the thermocouples against electrical contacts on the plate surface. These thermocouple wires were protected from contact with water by enclosing them in plastic sleeves. They were connected to the compact logger 3430 by means of which (see section 4.1.13) temperatures were measured.

(d) UNBALANCED DETECTORS

Differential thermocouples were mounted to monitor temperature imbalances between the metering and the guard heaters. Thermocouple type K of diameter 0.29 mm was used. Nine junctions were placed on each plate, i.e. the guard and metering surface plates. Holes of diameter 1.0 mm were drilled 4.0 cm apart along the internal arc of the guard rings and 3.8 cm along the edge of the arc of the metering heater surface plate (Fig. 14). The junctions were placed along the edge, facing the gap between the metering heater and the guard heater surface plates.

Thermocouple junction.

Copper plate.

small groove to accommodate a thermocouple junction using a thin film of araldite.

Thermocouple wires.
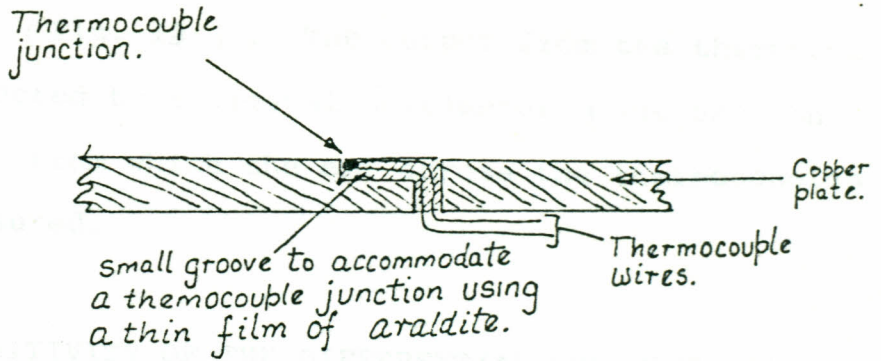
Fig. 13. Position of junction in the groove.

GUARD HEATER SURFACE PLATE.

5.7cm.

5.5cm.

6.7cm.

METERING HEATER SURFACE PLATE.

OUTPUT CONNECTED TO THE DIGITAL MULTIMETER TO MEASUE EMF.
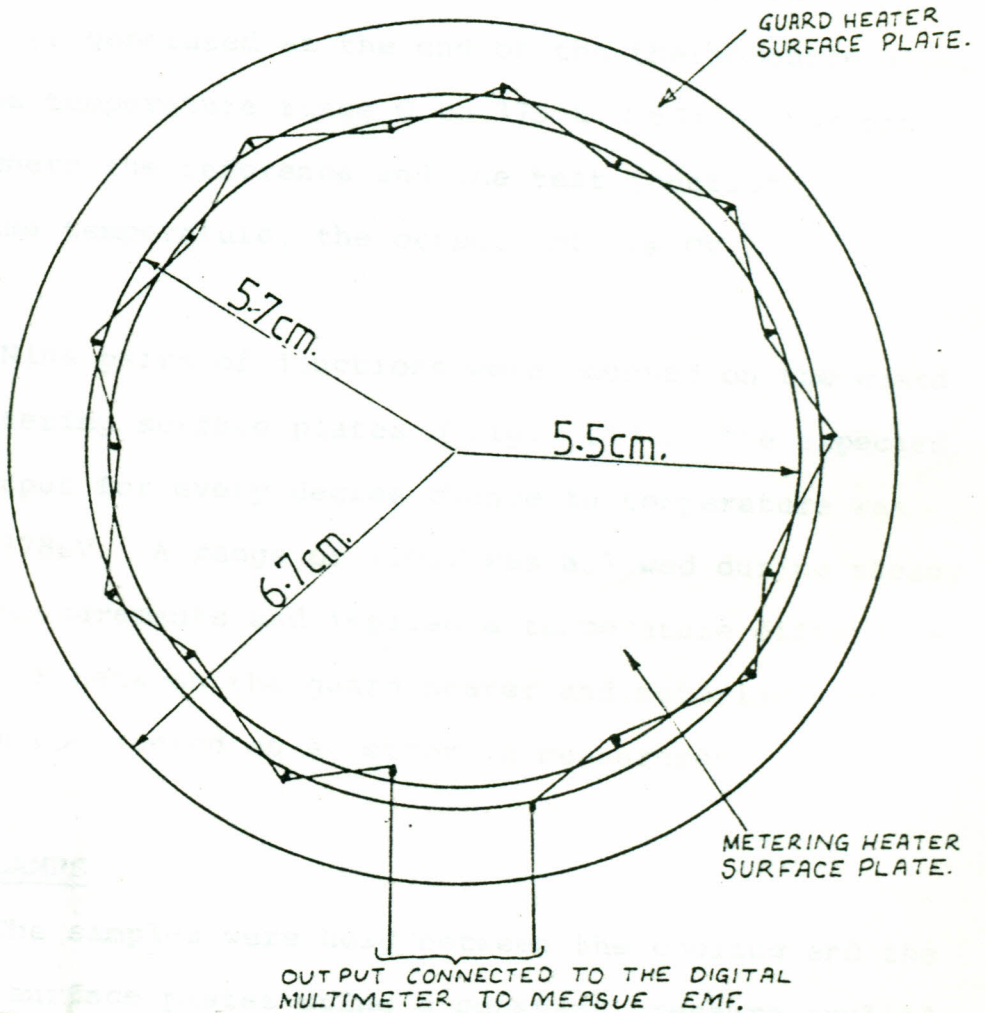
Fig. 14. Differential thermocouple arrangement.

The junctions were held by a thin film of araldite (Fig. 13) . The output from the thermocouple was connected to a digital multimeter (see section 4.1.12), from which the emf across the thermocouples were measured.

(e) SENSITIVITY OF THE DIFFERENTIAL THERMOCOUPLE

For every degree centigrade difference between the test and reference junction, of K type thermocouple, 42 µV is generated at the end of the thermocouple wires, for the temperature range 0 to 373 K (57) . For the case where the reference and the test junctions is at the same temperature, the output emf is 0V.

Nine pairs of junctions were mounted on the guard and metering surface plates (Fig. 14) . The expected emf output for every degree change in temperature was about 378µV. A range of ±10µV was allowed during steady state measurements and implied a temperature difference of 0.03 K between the guard heater and metering heater, and was considered as an error in measurement.

(f) CLAMPS

The samples were held between the cooling and the heater surface plates using a constant pressure applied by two crossbars made from mild steel, with holes drilled at their tips of diameter 7 mm (Fig. 15)..
The crossbars sandwiched the guarded hot plate apparatus
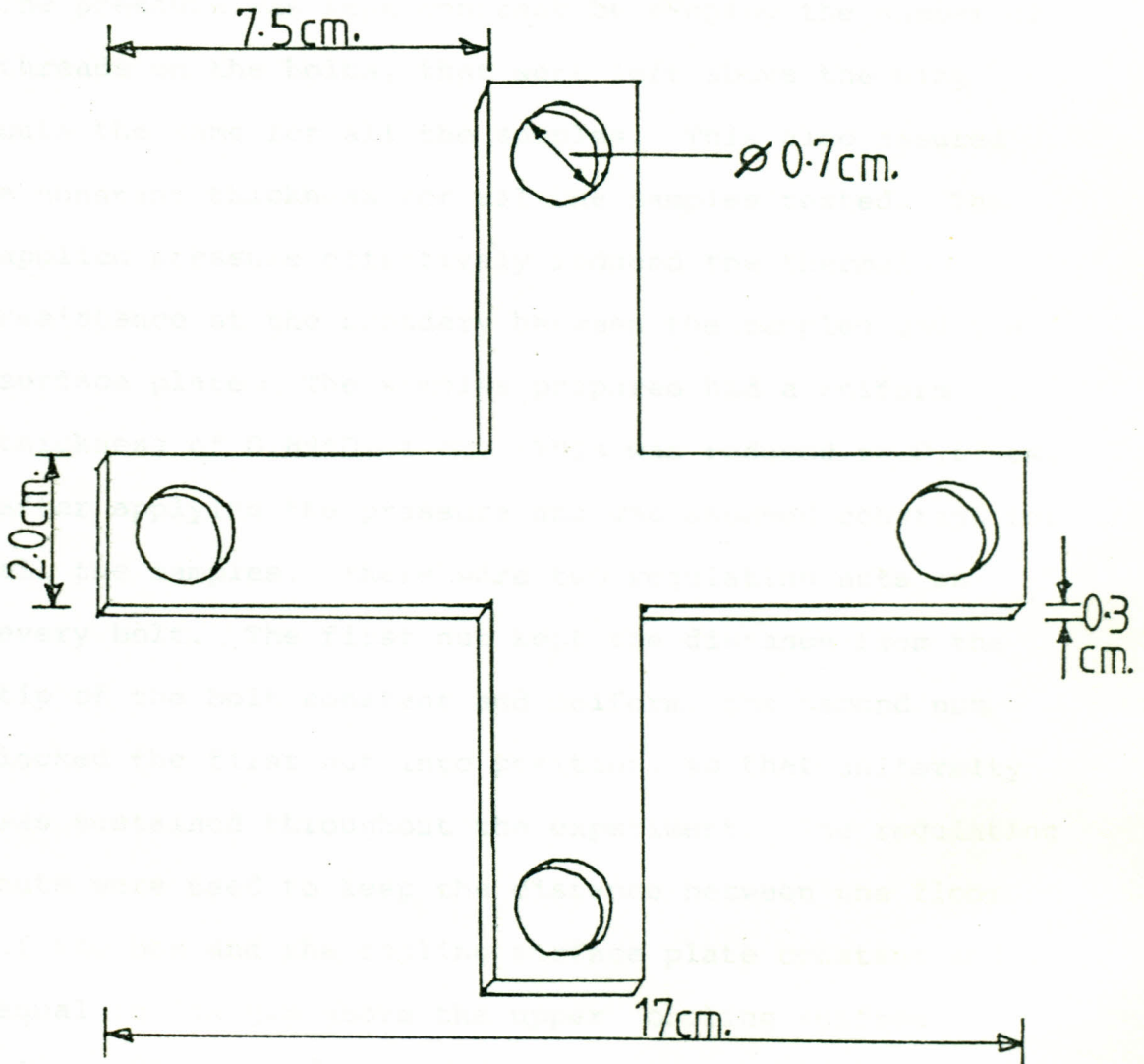
Fig. 15 . Crossbar used to clamp the samples in the guarded hot plate apparatus.

with the samples. The pressure was applied by
tightening the wing nuts on the bolts that went through
the holes. The bolts were similar and equal in size.
The pressure was kept constant by keeping the number of
threads on the bolts, that were left above the wing
nuts the same for all the samples. This also assured
a constant thickness for all the samples tested. The
applied pressure effectively reduced the thermal
resistance at the boundary between the samples and the
surface plates. The samples prepared had a uniform
thickness of 0.89 ± 0.01 cm. This was reduced to 0.87 cm,
after applying the pressure and was assumed constant for
all the samples. There were two regulating nuts on
every bolt. The first nut kept the distance from the
tip of the bolt constant and uniform, the second nut
locked the first nut into position, so that uniformity
was sustained throughout the experiment. The regulating
nuts were used to keep the distance between the floor
of the box and the cooling surface plate constant and
equal to the gap above the upper cooling surface
plate (Fig. 17).

(g) LAGGING

To minimize the edge heat losses from the samples,
cotton wool was used for lagging. The cotton wool was
enclosed in a cylindrical paper cardboard, with a
radius of 9.0 cm, a height of 2.5 cm and a hollow bottom
of radius 6.8 cm (Figs. 12 and 17).
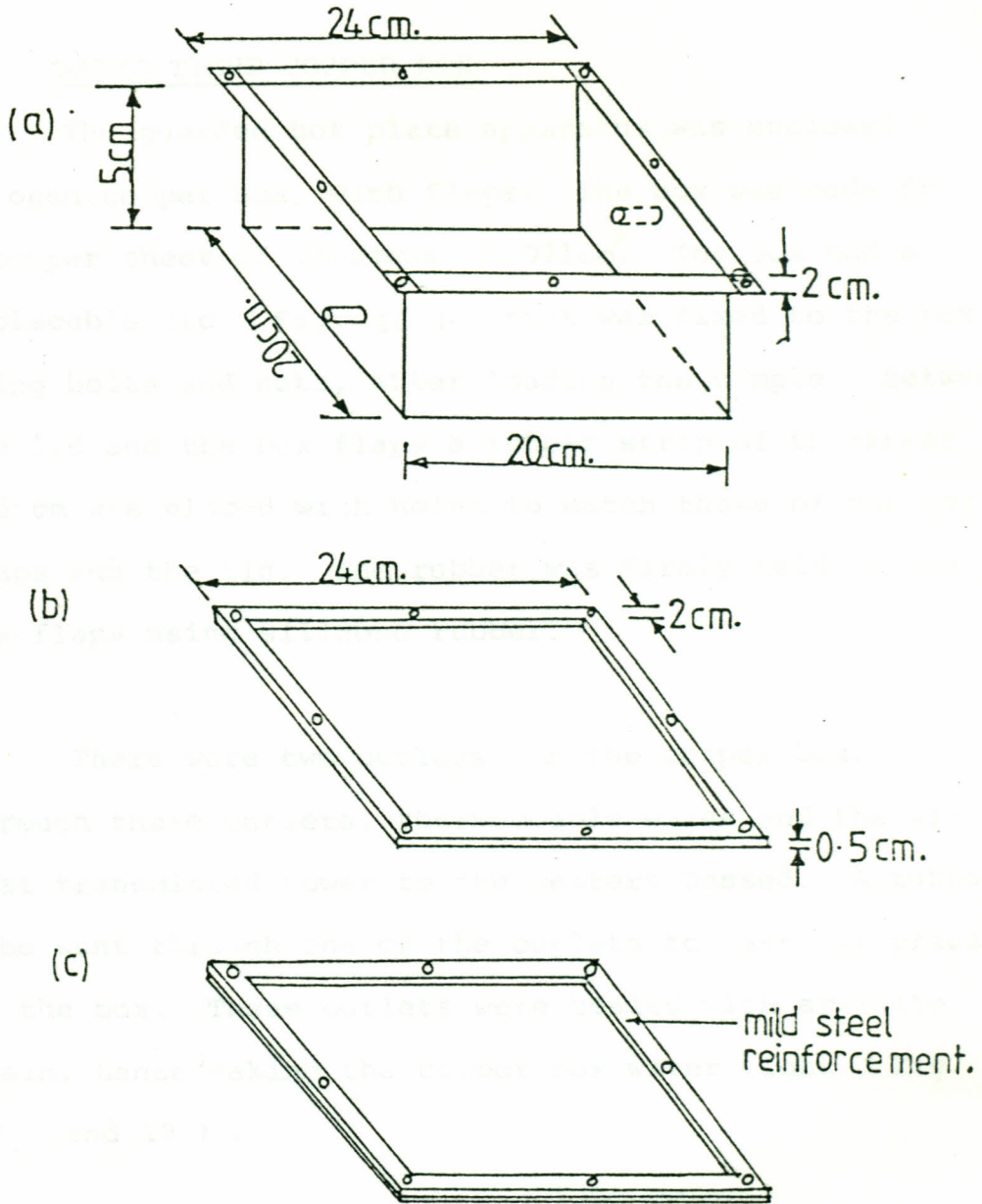
Fig. 16.   Copper box used to enclose the guarded hot plate apparatus a) copper box without lid b) rubber strip c) lid reinforced with mild steel.

(h)   WATER TIGHT COPPER BOX

The guarded hot plate apparatus was enclosed in an open copper box, with flaps. The box was made from a copper sheet of thickness 0.071cm. The box had a replacable lid (Fig. 16) , that was fixed to the box using bolts and nuts, after loading the sample. Between the lid and the box flaps a rubber strip of thickness 0.5 cm was placed with holes to match those of the box flaps and the lid. The rubber was firmly held to the box flaps using silicone rubber.

There were two outlets on the copper box. Through these outlets, thermocouple wires and the wires that transmitted power to the heaters passed. A rubber tube went through one of the outlets to ease air pressure in the box. These outlets were sealed with araldite resin, hence making the copper box water tight (Fig. 17 and 19) .

(i)   COOLING SYSTEM

The box enclosing the guarded hot plate apparatus was submerged in water, in a water bath. The box was supported by a metallic support. The water was circulated and its temperature regulated, using a water bath temperature regulator, type Techne TE-8J (Fig. 17).

(j)   ELECTRICAL CIRCUIT

The electrical circuit shown in (Fig. 18) , was
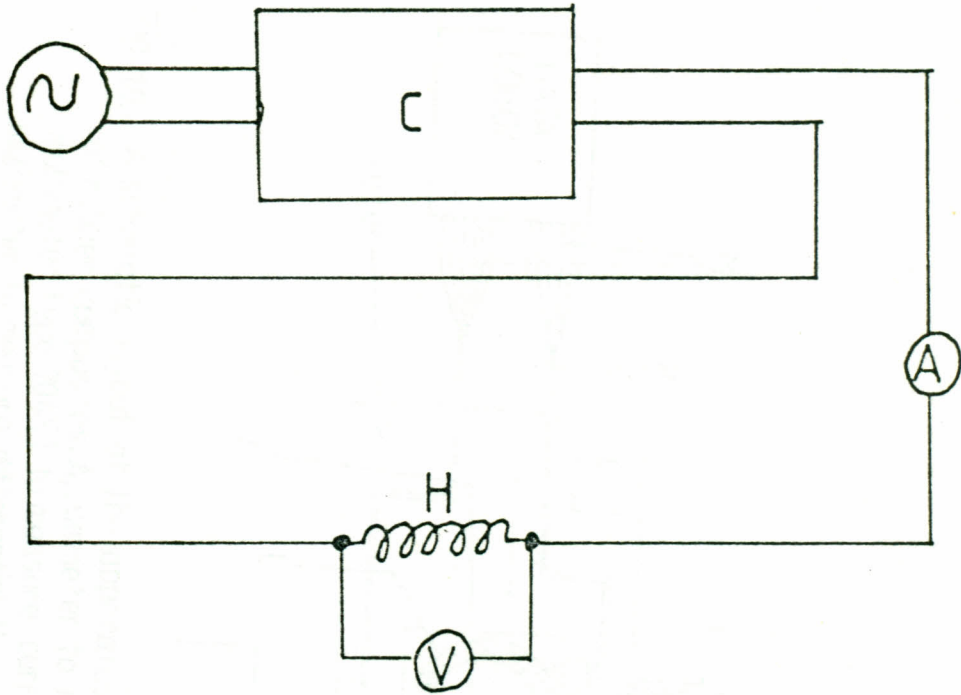
Fig. 18.   The electrical circuit used
seperately for the metering
and guard heaters; V, voltmeter
(compact data logga 3430); A,
ammeter (digital multimeter 7045);
C, power supply; H, heaters.
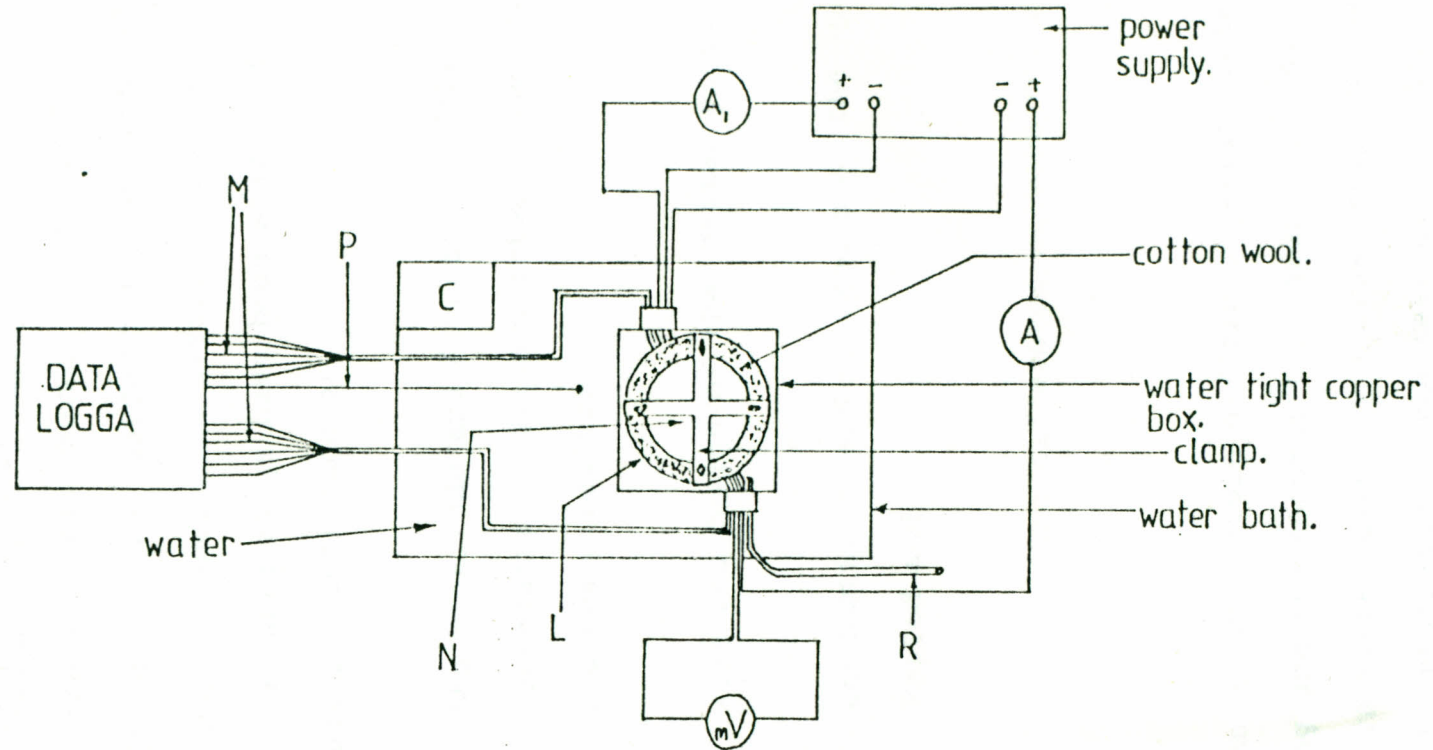
Fig. 19. A schematic layout of the apparatus used in determining the thermal conductivity of rubber composites. A_1, ammeter to measure guard heater current; A, ammeter (digital multimeter type 7045) to measure current through the metering heater; mV, digital multimeter to measure differential thermocouple output; M, thermocouple wires used to measure the voltage across the heaters; L, manila paper enclosure to keep cotton wool in contact with sample edges; N, guarded hot plate apparatus; C, water bath temperature regulator (type TE-8J); R, rubber tube to ease pressure in the cotton box.

used in isolation for both the guard and metering
heaters, the power supply was used as the source of
power. The circuits for the metering and guard heaters
was similar.

(k)   PRECAUTION AGAINST ERRORS

The errors in the thermal conductivity
measurements using the guarded hot plate apparatus,
caused by small tmeperature differences between the
test area and guard rings have been studied (58-62).
They include the influence of

(i)   the magnitude and direction of the
temperature imbalance between the metering
and guard heaters.

(ii)   size and design of the heater plate.

(iii) conductivity and thickness of the specimen
tested and

(iv)   temperature difference between hot and
cold plate.

When a temperature difference exists between the
guard ring and the central test area, not only will
heat be transfered directly accross the gap, but also
heat which originated in the test area of the heater

plate, will be conducted through the specimen towards the guard ring. It is the sum of these two heat flows i.e. the heat flow directly across the gap and that which is displaced out of or into the central test area of the samples which is termed "error heat flow", and which results in an error in the measured conductivity. The total error heat flow is expressed below (eq. 4.1).

$$q = q_o + ck \qquad \ldots\ldots\ldots\ldots\ldots \qquad 4.1$$

where

q_o = the heat transfer directly across the gap.

ck = the error heat flow through the specimen themselves, c is a constant and k is the thermal conductivity of the specimen.

The following steps were taken to minimize the effect of the major error heat flow:

(i) The edge heat losses from the samples were reduced by lagging the sample edges with cotton wool (Figs. 12 and 17).

(ii) The effect of heat losses across the gap and through the samples that may result from large temperature differences across the gap, were minimized, by limiting the temperature across the gap to 0.03 K, using the differential thermocouple on the heater

surface plates (Fig. 14).

·(l) DETERMINATION OF EQUILIBRIUM TIME

The equilibrium time (i.e. the shortest time for the apparatus to reach thermal steady state), was determined by taking temperature readings from the junctions positioned at the heating and cooling surface plates (Fig. 12), at 5 minutes interval, using the compact logga. This was done from the time the heaters were on, while the water bath temperature was regulated at 303 K. The temperature of the guard ring surface plates was kept at about equal value to the metering surface plates by manually adjusting the guard ring heater current. The emf., across the differential thermocouples was kept at a value less or equal to ± 0.010mV.

From the temperature readings of the cooling and metering surface plates, a graph of temperature gradient across the samples versus time was plotted (Fig.20), from which the equilibrium time was determined. From these curves steady state appears to have been attained after about 3 hours from the time the heaters were switched on.

(m) CALIBRATION OF THE GUARDED HOT PLATE APPARATUS

PMMA was used to calibrate the guarded hot plate apparatus described above, by determining its thermal conductivity at 303 K (see section 4.3.1). A value of
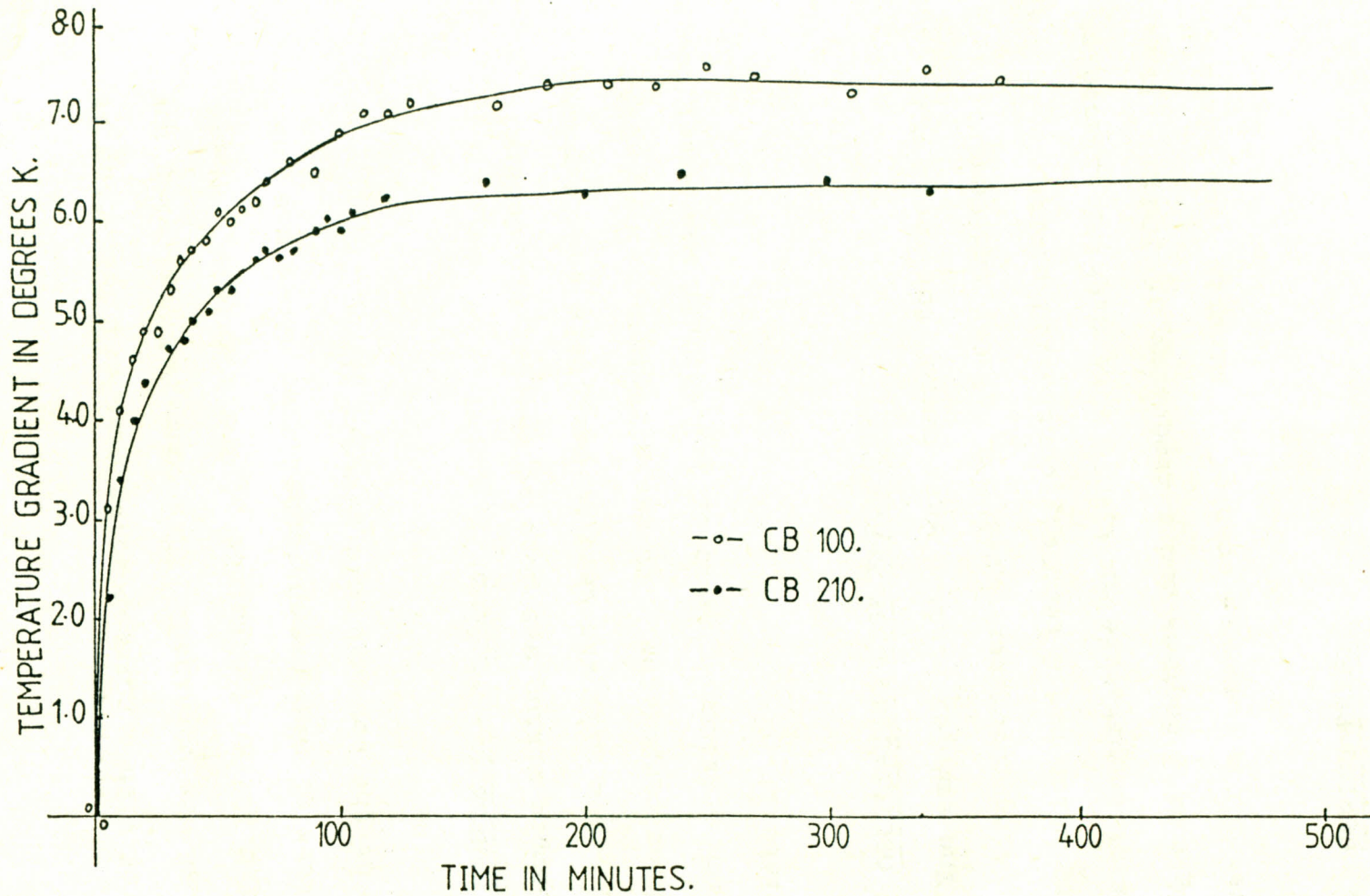
Fig. 20. Temperature gradient Vs.time curves to determine the equilibrium time of the guarded hot plate apparatus. The metering heater dissipated heat at 7.2W.

0.190 W/mK with a corresponding standard deviation of 0.008 W/mK was obtained. This compared well with the value of 0.187 W/mK obtained at 302.4 K (63). The temperature of measurement considered above was the average of the hot and cold plate.

4.1.2 SAMPLE MIXING MILL

Sample mixing was done at the Car and General Company. The mill was used to masticate and compound the rubber composites. It was a 24 inch, single gear mill with a friction ratio of 1:1.15, and was water cooled (see plate 1).

4.1.3 OSCILLATING DISK RHEOMETER

The samples studied were tested for their cure times using rheometer model 100, at Car and General Company which had a remotely controlled plotter. It had a platent temperature of 433 K. The disk oscillated at an angle of 3 degrees and a frequency of 100 Hz. It was set for a complete scan of 12 minutes (see plate 2).

4.1.4 CURING PRESS

This equipment is also at Car and General Company. It was used to cure the rubber composite samples under pressure. The platent temperature was kept constant at 423 K by steam. A ram pressure of 750 Psi was exerted through a hydraulic press.
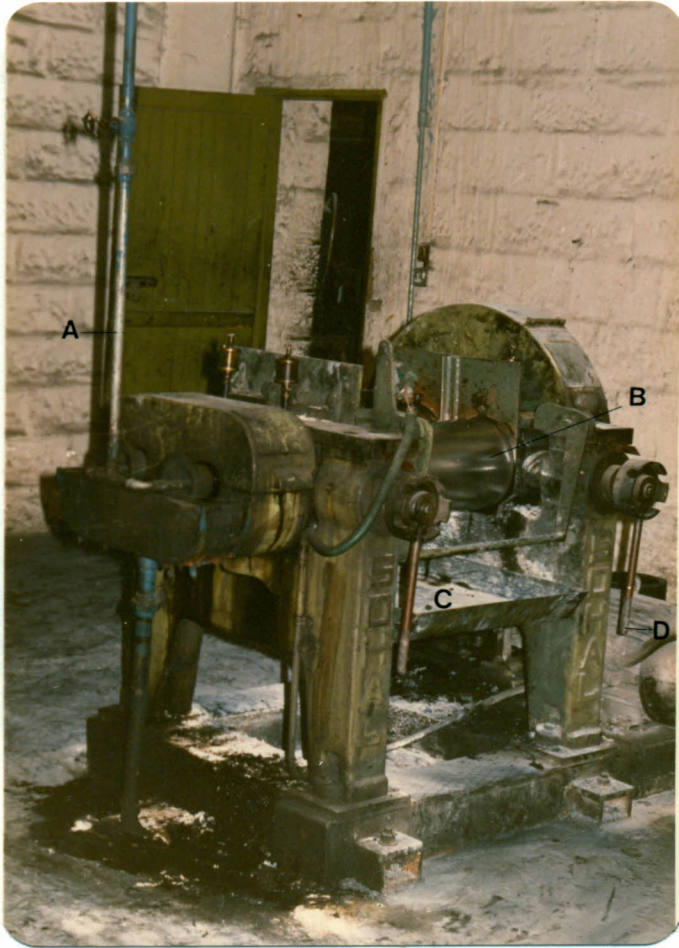
Plate 1. The mixing mill used to mix the rubber

composite samples.

A, pipe with cold water to cool the mills.

B, one of the two roll mills.

C, metal tray to collect droppings from the

mill.

D, handle for adjusting the mill nip.

(Courtesy, Car and General Company, Kenya).
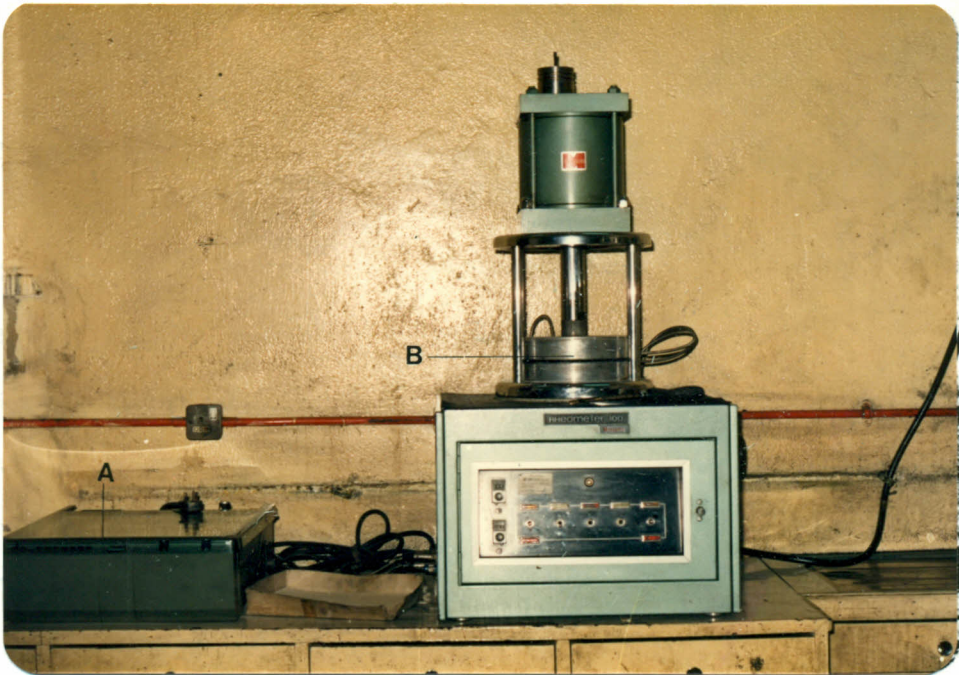
Plate 2.   The oscillating disk rheometer used to test

the cure properties of rubber composites

tested.

A, the remotely controlled plotter.

B, ram with oscillating disk inside.

(Courtesy, Car and General Company, Kenya).

4.1.5 PLANIMETER

This instrument was used to measure the area in a closed loop. It was callibrated by tracing the path of a loop whose enclosed area was known. It was used to determine the area under the stress-strain curves.

4.1.6 WALLACE POCKET HARDNESS METER

The wallace pocket hardness meter was used to determine the hardness of the rubber composites. It had a detachable counterweight for approximate adjustment of the instrument. It was callibrated in International Rubber Hardness Degree (I.R.H.D.).

4.1.7 GRINDING MILL

This equipment is at the Chemistry Department, Kenyatta University. The grinding mill was used for grinding charcoal made from coffee hasks. It was a christy lab mill type 8, with sieve mesh of 1 mm apperture.

4.1.8 CURING MOLD

Two molds were used to cure the samples for thermal and tensile tests. They were of thickness 0.89 cm and 0.25 cm, for curing rubber composite sheets to be tested for thermal conductivity and tensile tests respectively. They were made from mild steel. Each mold was sandwiched between two flat surface plates also

made from mild steel (Fig. 21).

4.1.9 INSTRON MACHINE

This equipment was used to determine the tensile strength and breaking energy of the rubber composites. It is at the Strength of Materials Laboratories in the Department of Mechanical Engineering, University of Nairobi and had a load cell of 2.0 kg.

4.1.10 CLICKER AND DUMB BELL SHAPED DIE

These equipments are at the Kenya Industrial Research Development Institute. The clicker was used to press the dumb bell shaped die and stamp out samples from the tensile sheets, that were used to make tensile tests. The dumb bell shaped samples had a width of 6.0 mm and a guage length of 33 mm.

4.1.11 WATER BATH TEMPERATURE REGULATOR

The Techne type TE-8J thermoregulator was used to control the water bath temperatures with the temperature range of 273 K to 358 K, to an accuracy of 0.1 K (see Fig. 17 and 19).

4.1.12 DIGITAL MULTIMETER

The solartron digital multimeter type 7045 was used to measure the current going through the metering heater to an accuracy of 1 mA and the emf across the differential thermocouple, to an accuracy of $1\mu V$
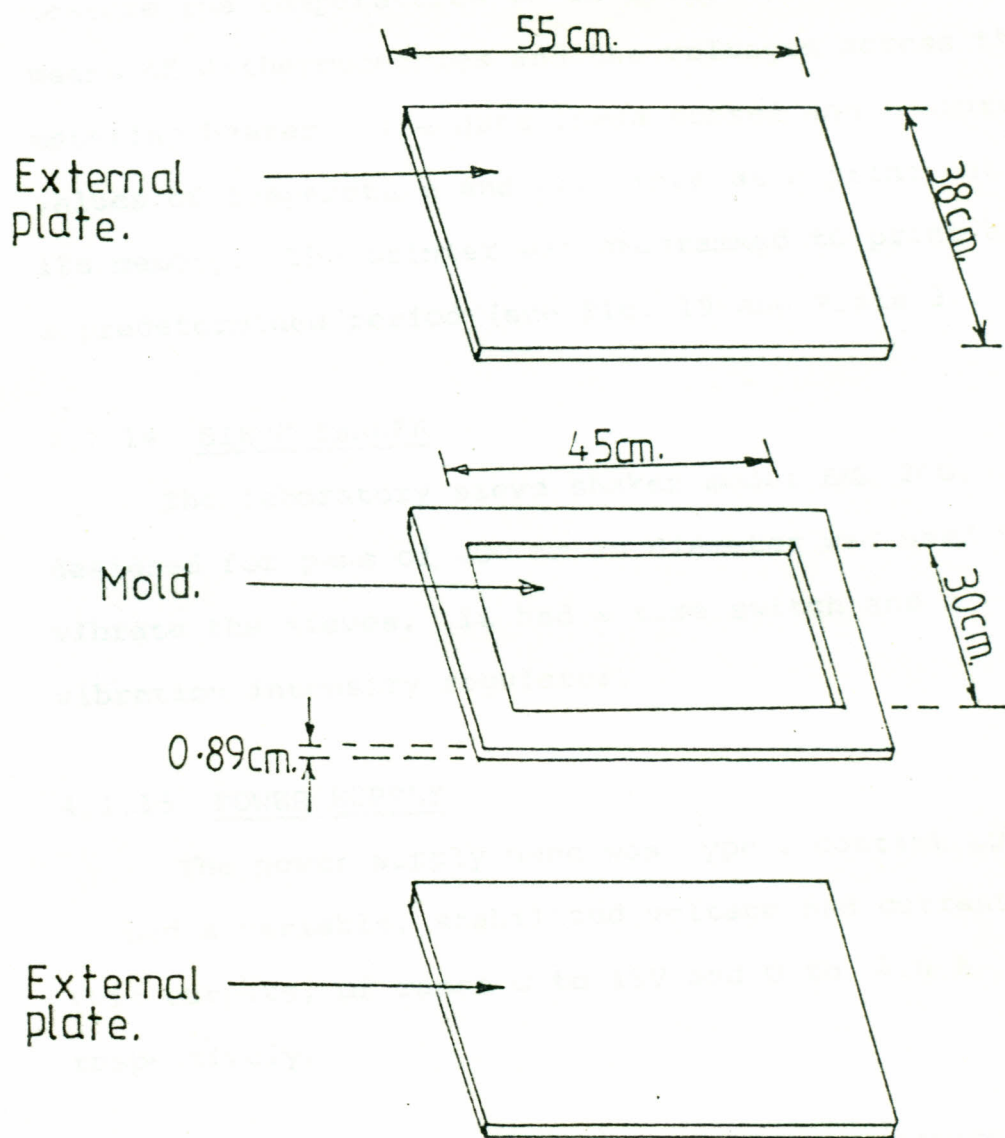
Fig. 21 Mold and external plates for samples tested for thermal conductivity.

see Fig. 19 and plate 2.

4.1.13 COMPACT DATA LOGGA

The solatron compact logga 3430 was used to measure the temperatures to an accuracy of 0.1 K, by means of J-thermocouples and the voltages across the metering heater. The data logga sensed and measured values of temperature and gave them as a print out from its memory. The printer was programmed to print after a predetermined period (see Fig. 19 and Plate 3).

4.1.14 SIEVE SHAKER

The laboratory sieve shaker model EML 200, designed for pans of 200 mm in diameter was used to vibrate the sieves. It had a time switch and a vibration intensity regulator.

4.1.15 POWER SUPPLY

The power supply used was type : coutant LQT 200. It had a variable, stabilized voltage and current, twin outputs, of range 0 to 15V and 0 to 2.0 A respectively.

4.2.0 PREPARATION OF THE SAMPLES AND THE CHARCOAL USED AS A FILLER

The samples tested in this study were prepared by mixing EPDM rubber with fillers namely carbon black N339, kaolin and charcoal. EPDM, carbon black and kaolin were generously donated by Car and General Company, while charcoal was bought, ground and graded
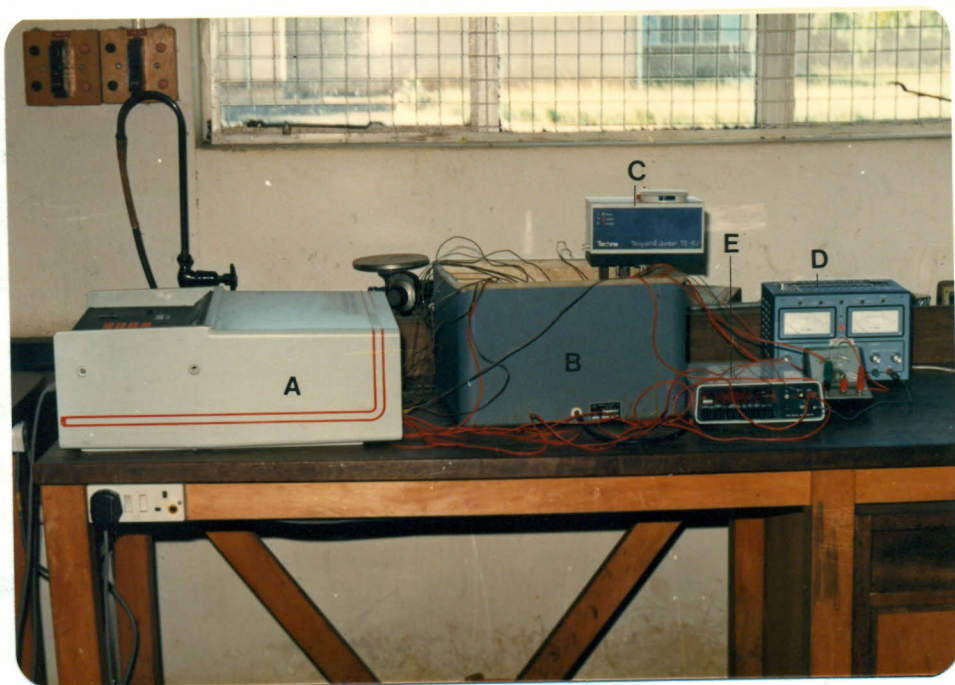
Plate 3. The apparatus used to determine the thermal
conductivity of rubber composites.

A, solatron compact logga 3430.

B, water bath, in it is the water tight copper
box, enclosing the guarded hot plate
apparatus.

C, water bath temperature regulator (TE-8T).

D, Power supply.

E, solatron digital multimeter 7045.

as described below.

4.2.1 THE PREPARATION OF THE CHARCOAL (KAHAWA COAL) USED AS A FILLER

Charcoal prepared from coffee hasks, was bought from the local charcoal dealers. It was ground using the laboratory mill (section 4.1.7). The ground charcoal powder was sieved through sieves numbers 22, 85,100,170,200 and collected in a pan after passing through sieve number 300. The shaking was done by means of a laboratory sieve shaker type EM 200, for one and a half hours. The powder was collected and graded depending on the sieve size they stopped at.

GRADE	PARTICLES STOPPED AT SIEVE NUMBER	NOMINAL APERTURE IN MICRONS
1	passed through sieve 300	$x \leqslant 53$
2	300	$53 \leqslant x \leqslant 76$
3	200	$76 \leqslant x \leqslant 89$
4	170	$89 \leqslant x \leqslant 152$
5	100	$152 \leqslant x \leqslant 178$
6	85	$178 \leqslant x \leqslant 699$

TABLE 3. Shows the criterion used for grading the charcoal fillers used.

The nominal aperture of the sieve was considered as representing the particle size distribution of the charcoal fillers.

4.2.2 SAMPLE PREPARATION

(a) INTRODUCTION

The physical and thermal properties of polymers depend not only on thermal properties of each compound but also on their preparation methods and thermal history. For this reason a description of the method used to prepare the samples tested for mechanical and thermal properties in this study is outlined. The formula describing the chemical composition of the composite rubber is reproduced for all the fillers used. The sample preparation procedure adopted here is similar to that one normally used in industry at Car and General Company, both on methodology and composition except for a few test ingredients.

The samples tested were prepared from EPDM rubber (ethylene-propylene-diene monomer), compounded with fillers, curing agents and oil. Before compounding mastication was done.

(b) MASTICATION

Mastication of the rubber was done on an open mill at a temperature range of 338 K to 358 K. Mastication reduced the rubber to a gummy mass as it was subjected to severe mechanical work. This is normally accompanied by a marked decrease in the molecular weight of rubber (63). This makes it easy to add ingredients

to the rubber, during compounding.

(c) COMPOUNDING

Compounding of the masterbatch involved the
addition of the ingredients at different stages during
mixing on the open mill. A filler concentration of 20
phr (parts by weight of the filler per hundred parts of
rubber) and flexon oil of concentration 80 phr were
first incorporated into the masticated rubber. The
following chemicals were next added to the masterbatch;
Zinc oxide, used as an activator during curing, stearic
acid, used as a medium for optimum performance of the
accelerators, TMTM (Tetramethyl thiuram monosulfide)
and MBT (Mercaptobenzothiazole) were both used as
complimentary accelerators to produce faster cure than
can be separately obtained (64).

(d) SAMPLES

After completion of the compounding process, the
masterbatch was divided into portions, such that each
portion contained 1.0 kg of EPDM rubber. To each of
these pieces, more fillers were added, so as to obtain
the intended volume fraction of the filler in the
respective samples. Finally insoluble sulfur was
added and well mixed. This procedure was repeated for
all the samples prepared.

The table below gives a typical composition of each rubber sample.

INGREDIENTS	PARTS OF RUBBER BY WEIGHT
EPDM	100.0
MBT	1.5
TMTM	1.0
ZINC OXIDE	5.0
STEARIC ACID	1.0
FLEXON LIGHT OIL	80.0
INSOLUBLE SULFUR	1.5
FILLER	VARIED

TABLE 4   The composition of the rubber compound.

The formula and processing method described above was consistent for all the fillers used.

For convenience the samples prepared were coded as follows : carbon black filled EPDM rubber compounds were coded   CB, the number next to it, to the right indicates the filler loading in parts of rubber by weight e.g. CB20 means that the filler loaded is carbon black at 20 phr. The others are as follows:

FILLER	CODE
NO FILLER	A
KAOLIN	K
CHARCOAL	C
CARBON BLACK	CB

TABLE 5.   The letters correspond to the filler in the composite.

In the case of charcoal, different particle sizes were attempted. The number written to the left of C indicates the particle size (see section 4.2.1), while the one to the right indicate the filler concentration in the composite.

(e)   DETERMINATION OF STATE OF CURE

Rubber must be cured before it attains the desired physical and thermal properties. The curing period has to be accurately assessed to avoid undesired properties which may result from undercure or overcure.

There are numerous methods of determining the state of cure of rubber composite. In this study the Monsanto rheometer model 100 (see section 4.1.3) was used to measure the cure times.

Before curing pieces of the compounded samples, they were tested for their ability to cure, and also to determine the degree of dispersion of the fillers and other ingredients in the compound. This was done by running monsanto rheographs for several pieces of the same compound, cut randomly from the compounded sample. Cure curves of CB150 and K150 are shown as examples in Figs. 23 and 24 respectively.

EPDM Compounds have a matching modulus mode of overcure as is shown in Fig. 22. This suggests that curing process does not come to an end by the removal of the samples from the molds, but continues at low rates whenever the sheet is subjected to some heating.

The continuity of vulcanization during thermal conductivity determination, may easily influence the k values determined. Sulfur vulcanization is an exothermic chemical process (66), and thermal conductivity taken at high temperatures must take into account the possibility of overcuring.

(f) CURE TIME

The scotch time required to raise the temperature of the inside of a thick sheet of rubber which is a poor conductor of heat, while curing in the press, is longer compared to the isothermal cure in the rheometer. This calls for a procedure of determining the optimum cure time.
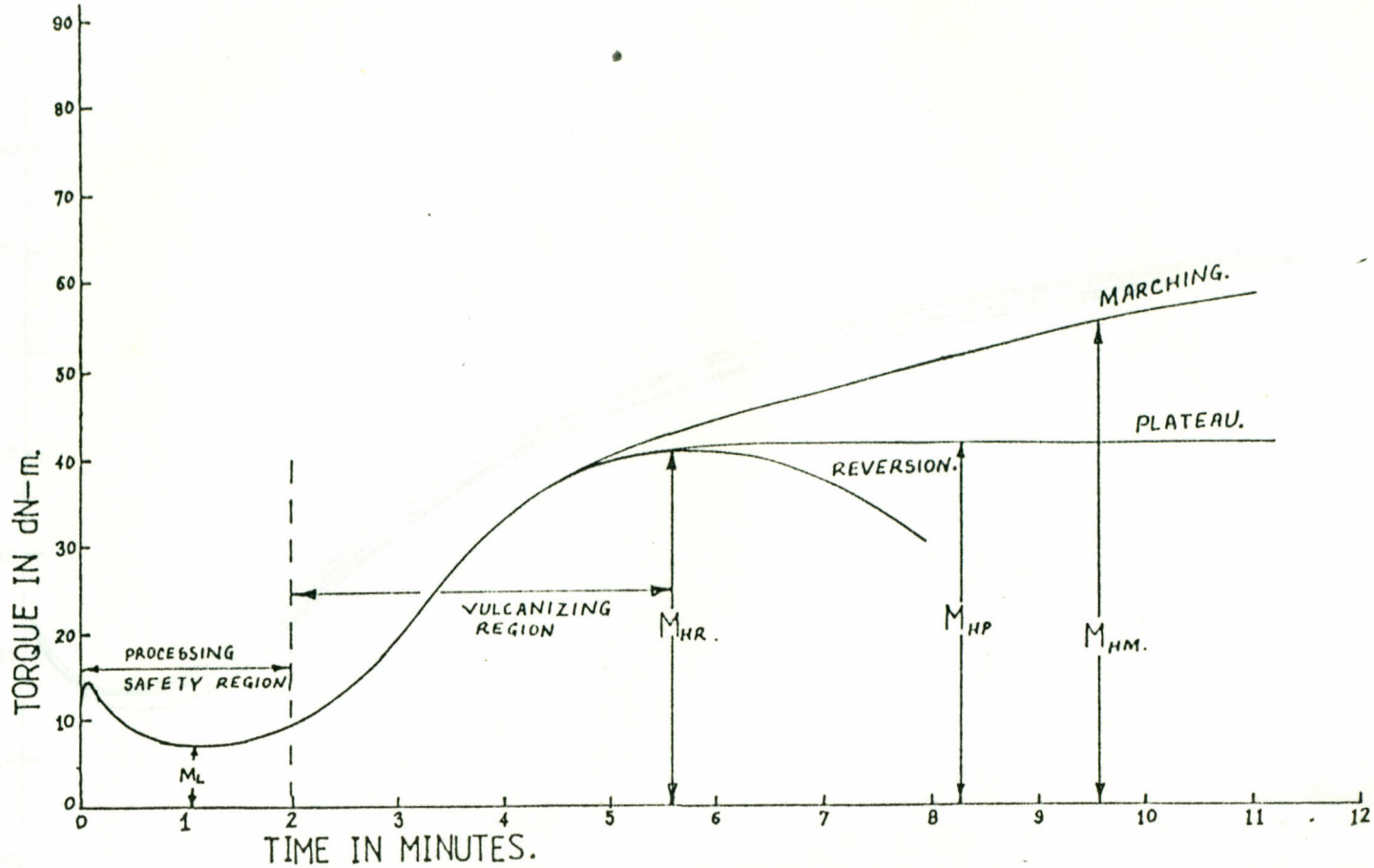
Fig. 22. Cure curve showing the various sections of cure.

M_L, min. torque; M_{HM}, max. torqure at specified time of matching modulus;
M_{HP}, max. of plateau cure; M_{HR}, max. torque of reversion cure.

67

Fig. 23. Cure curves of sample type CB150.
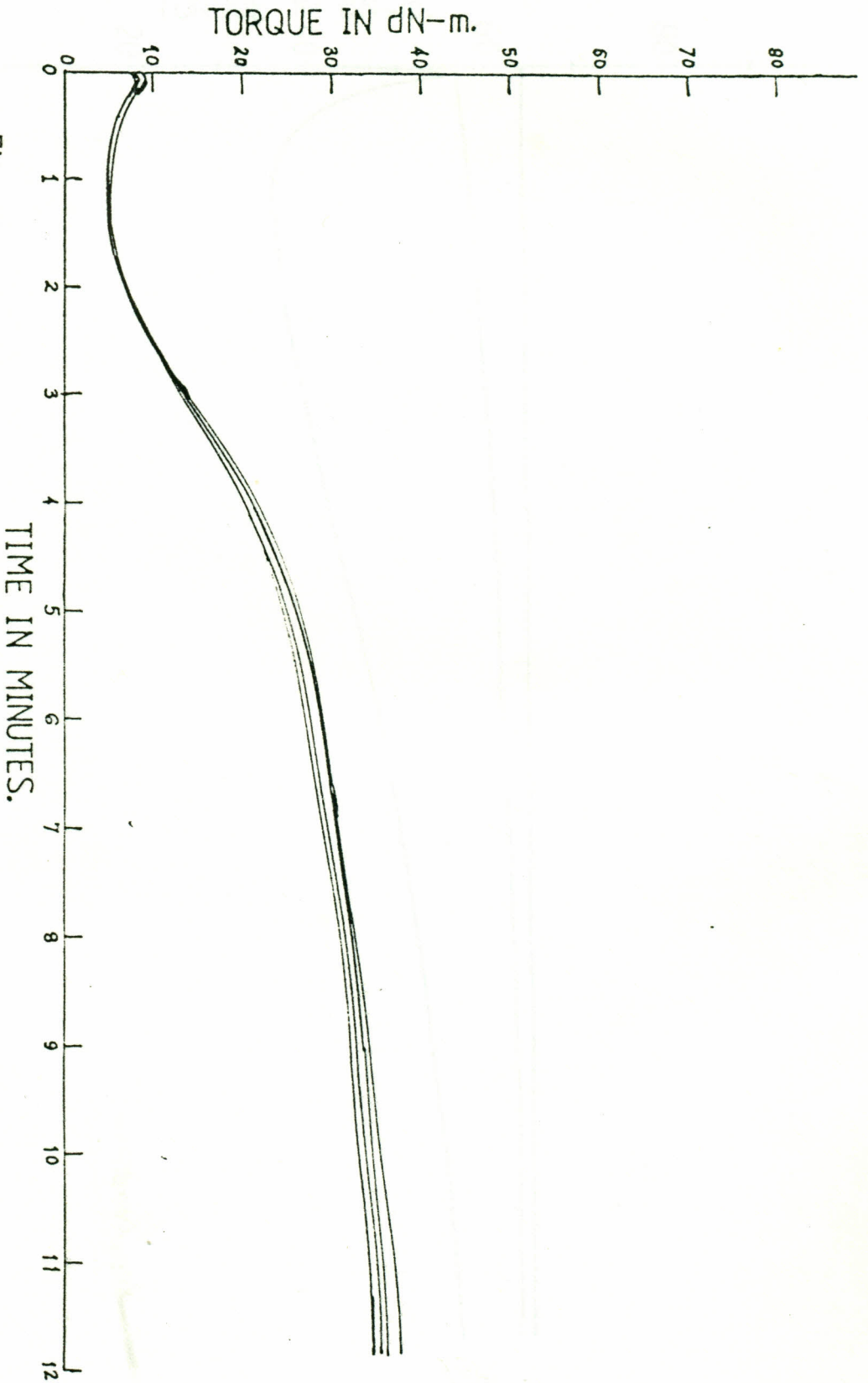
Fig. 24. Cure curves of sample type K150.
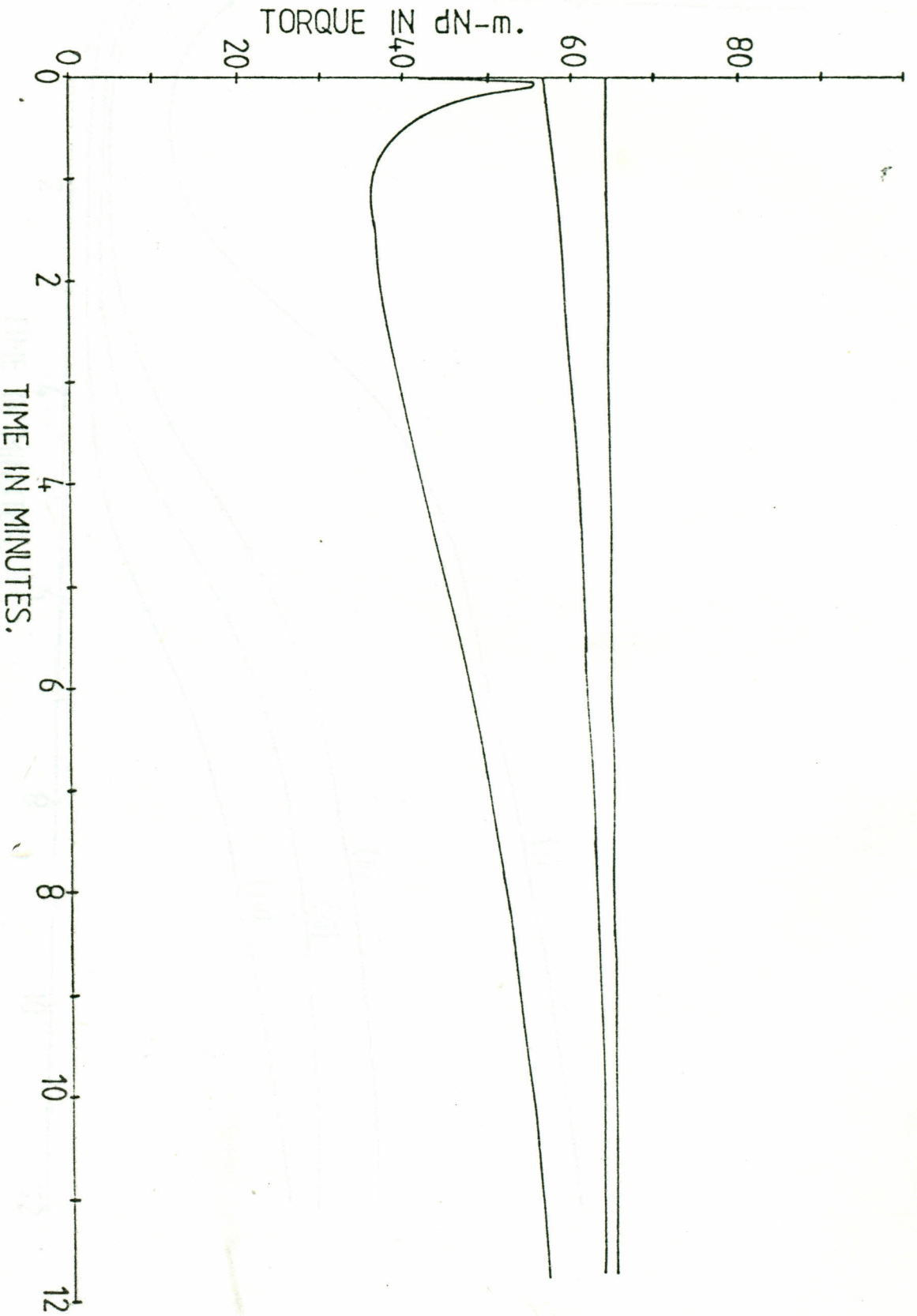
Fig. 25. Cure curve of sample type CB210, cured for 36 minutes.
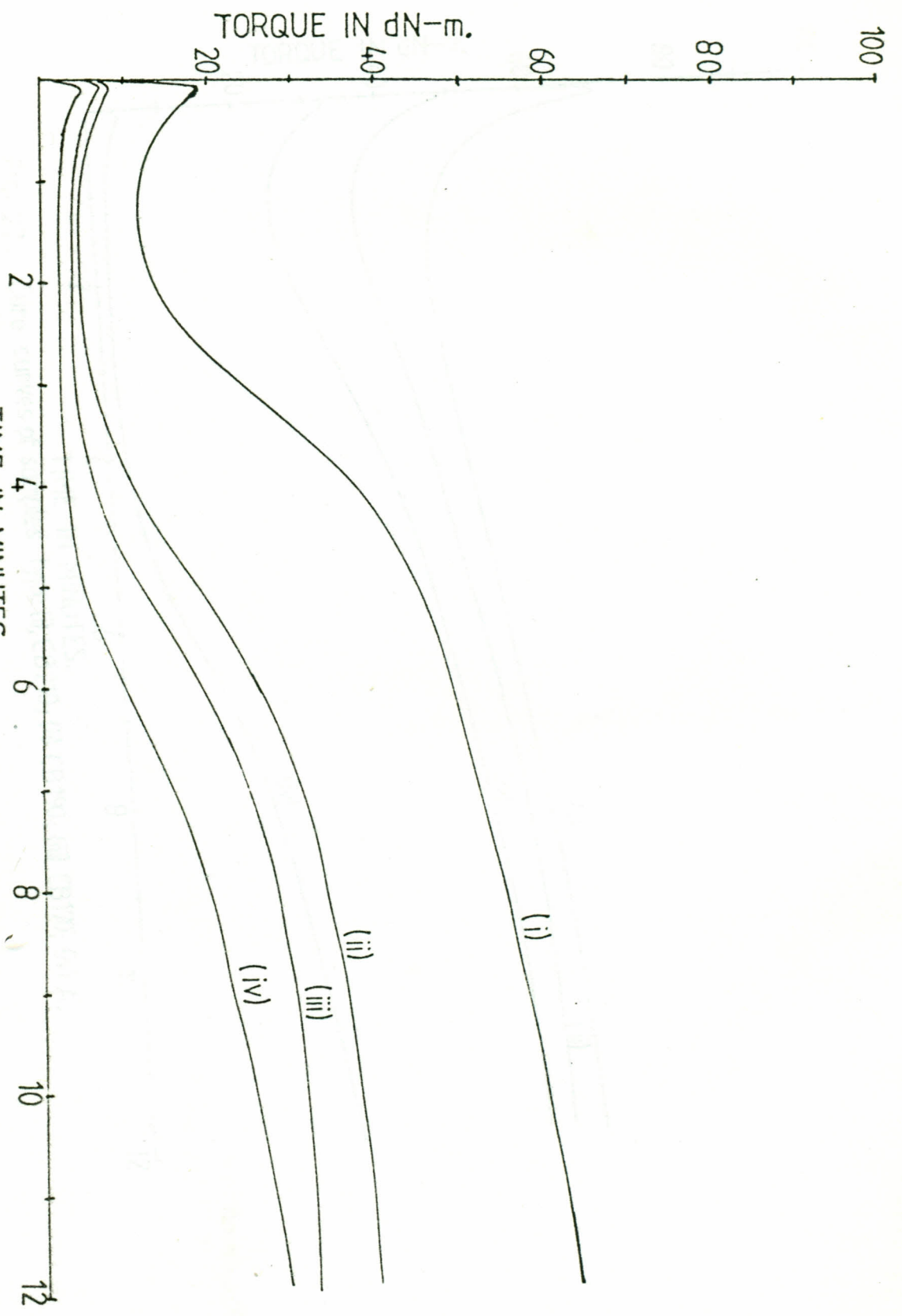
Fig. 26. Cure curves of samples types (i),CB80; (ii),CB40; (iii),CB20;(iv),A.
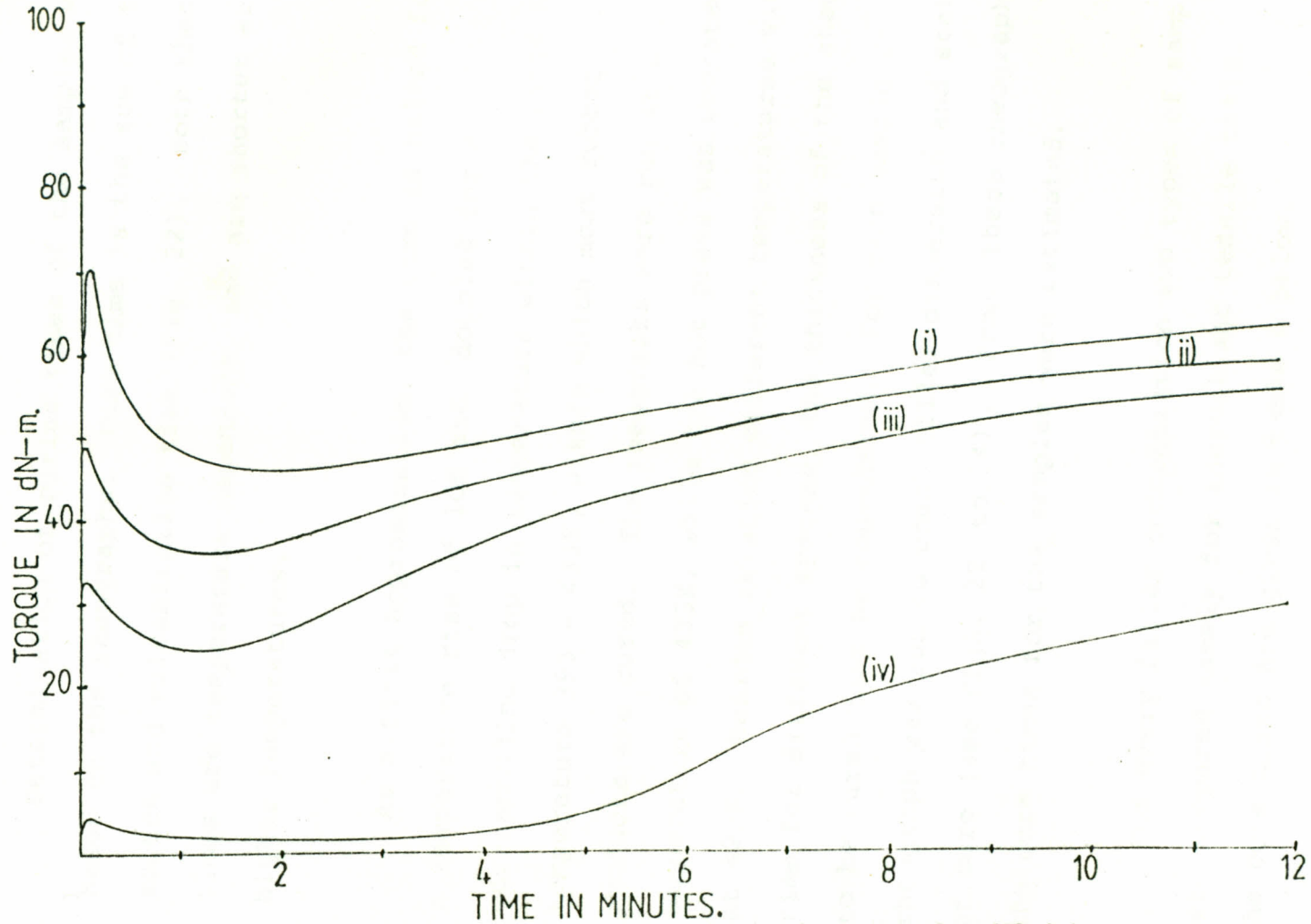
Fig. 27 . Cure curves of samples type (i), CB 210; (ii) CB 190; (iii) CB 170; (iv) A.

Determination of curing times of the samples was based on the rheographs. Cure time is the sum of the scotch and vulcanization time (Fig. 22). Both these times are temperature dependent, and are shorter at higher temperatures.

As a first approximation, the time is halved for a temperature rise of 10K and doubled for a corresponding drop in temperature within the range of temperature 393 - 433K, within which most rubber products are cured. The rheographs were run at a temperature of 433K, while the hot press was operated at 423K. Besides relating different temperatures with time for different systems, the thickness of the sheet to be cured must be considered. For each sample a rheograph was run to check filler dispersion and state of cure (see Figs. 22 to 24). From these rheographs the cure times for the samples were estimated.

For every filler concentration two types of samples were prepared namely for thermal and tensile tests. The cure times are given in table 6 below.

SAMPLES	CURE TIMES OF SHEETS FOR,	
	THERMAL TESTS IN MINUTES	TENSILE TESTS IN MINUTES
CB20	25	15
CB40	25	15
CB80	25	15
CB100	25	15
CB120	25	15
CB135	25	15
CB150	25	15
CB170	30	24
CB190	30	24
CB210	30	24
K20	20	10
K40	20	10
K50	20	10
K60	20	10
K80	20	10
K100	20	10
K120	20	10
K135	20	10
K150	20	10
K170	20	10
K190	20	10
K210	20	10
IC20	15	10
IC40	15	10
IC50	15	10
IC60	15	10
IC80	15	10
2C50	15	10
4C50	15	10
5C50	15	10
6C50	15	10

TABLE 6   Sample types prepared and their cure times.

1C100 and 1C120 were also attempted, but they were too weak to be tested for tensile strength and thermal properties.

After cure tests, the rubber composite was prepared to fit the molds in which they were cured. The composite was milled to a uniform sheet that was slightly thicker than the mold thickness. Rubber being a viscoelastic polymer undergoes relaxation of its chains after subjecting them to severe shear forces during milling. For this reason, the rubber composite was left for at least 12 hours at 295K so as to recover it's "nerve" and then cut to fit the molds. This procedure was repeated for all the samples. It is important to note that nerve effect, affects only those samples with low reinforcing filler concentration and not those with high reinforcing filler concentration (67).

Molds were used for curing the rubber composite samples. One mold was used to prepare samples of average thickness 0.89±0.01 cm, (see Fig. 21). These were the samples tested for thermal conductivity. The other mold of a similar design was used to prepare samples for determining tensile strengths of the rubber samples. They were of average thickness 0.25 cm.

The mold covered with two surface plates on either sides were first pre-heated to an average temperature of 423K before filling it with the

unvulcanized rubber compound. The filled mold, covered with the surface plates was placed in a hot pneumatic press, operating at 750 Psi. The press plates were kept at a constant average temperature of 423K by pressured steam, and cured for times shown in table 6.

(g) SAMPLES TESTED FOR THERMAL CONDUCTIVITY AND HARDNESS

Three pairs of samples were cut from each cured molded rubber composite sheet. Each sample was a circular disc of radius 6.7 cm and a thickness of about 0.89 cm, the thickness being equal to that of the mold, then kept in a desicator so as to keep them free from moisture. Raw rubber absorbs moisture, vulcanized rubber absorb relatively small quantity of moisture (68). The remaining portions were used to determine the hardness of the composites using the Wallace hardness meter.

(h) SAMPLES TESTED FOR TENSILE STRENGTH

Specimen for tensile strength test were obtained from the cured molded sheets at least 12 hours after cure. Using a dumb bell shaped knife and a clicker to press the knife, dumb bell shaped samples were cut. Four specimen were sampled per sheet, one pair was cut such that it was perpendicular to the other. This was done to eliminate a possible effect of grain boundaries and orientation of the rubber chains on the tensile test results, that may have been brought about during

the final milling. The samples were tested for modulus and tensile strengths on the instron machine. The thickness of the dumb bell shaped samples were determined at the centre and the two ends along the guage length, using a thickness guage.

4.3.0 EXPERIMENTAL PROCEDURES

In this section the various methods used to collect data in this study will be outlined. They included methods used to determine the thermal conductivity, hardness and tensile strength of the samples.

4.3.1 DETERMINATION OF THERMAL CONDUCTIVITY

There are many methods of determining the thermal conductivity of materials. They are broadly divided into two types, the transient (29,52,54,69), and the steady state methods (55,70). In this study the steady state method was used. The guarded hot plate apparatus described in detail in section 4.1.1, was used in the determination of thermal conductivity of the rubber composites. The two samples of radius 6.7 cm and thickness 0.89 cm were sandwiched between the surface plates, as is shown in Fig. 12 and clamped with the wing nuts and bolts such that six threads from the end of the bolts were visible on the wing nuts. The sample

edges were lagged with cotton wool (section 4.1.1 g).
The guarded hot plate apparatus was enclosed in the
water tight copper box (section 4.1.1 (h)). The box
was supported on a metal support made from mild steel
and placed in a water bath (section 4.1.1 (i)). The
water bath was then filled with water to a level where
the copper box was completely submerged (Fig. 17).
The water bath temperature regulator was then set on
at the desired temperature to regulate the water.

The power to the metering and guard heater was
drawn from the power supply (see section 4.1.15). The
current was adjusted to the desired value and was
measured by means of the digital multimeter. The current
to the guard heater was adjusted such that the emf.
from the differential thermocouple was kept at a value
less or equal to $\pm 10 \mu V$ and was monitored using the
digital multimeter. After three hours, the emf. from
the differential thermocouples was found to be stable,
with occasional small deviations, that were controlled
by manual adjustment of the current to the guard
heaters. The system was left for a further two hours
after which it was assumed steady.

The temperatures were measured using the compact
logga type 3430, programmed to print out junction
temperatures at one minute intervals. Each data logger
print out contained the voltages of the metering and
guard heaters and the temperatures at the junctions.

15 print outs were collected and the corresponding currents measured using the digital multimeter. The data was manually fed to a computer and merged to a program to calculate the average thermal conductivity from eq. 3.1. The standard deviation σ of the thermal conductivities determined was also calculated. The values of the σ was used as a condition for the measured k. For values of σ higher than 0.006, fresh values were collected and k determined again. This was done for every value of k determined. The results are shown in Table 7 .

4.3.2   DETERMINATION OF HARDNESS

The hardness values of all the samples prepared were determined using the wallace pocket hardness meter, at a room temperature of 295K. It was first calibrated in an upside down position using a counterweight and an allen key.

The samples prepared for thermal conductivity measurements were tested for hardness at least twenty four hours after cure. The wallace hardness meter was used upright and pressed evenly on the surface of the sample such that the feet just sat on the sample surface. The deflection was read immediately and recorded. This was repeated for various positions on either sides of the sample. The average value was considered the hardness value (in I.R.H.D.) of the

composite. The values corresponding to the hardness of the various samples studied are shown in Table 7.

4.3.3. TENSILE TESTS

The tensile properties were determined using the instron machine. The thickness of the samples were determined at the two ends and the centre, using a thickness guage with an accuracy of ±0.01 mm. The instron machine was first calibrated, the chart speed was adjusted to 5cm/min, and the loading speed to 10cm/min, by replacing the corresponding gears. The samples were then loaded on the jaws of the instron machine such that the jaws were aligned with the lines that marked the ends of the guage length. The jaws were then manually adjusted such that their distances apart were equal to the guage length of the sample, and the load scale pointer at zero. The instron machine was then motorized and a force-elongation curve plotted on a graph paper. These tests were carried at a room temperature of 298 K.

CHAPTER FIVE

5.0.0 EXPERIMENTAL RESULTS.

In this section the experimental results of; thermal conductivity, hardness, tensile strength and breaking energy as a function of filler concentration of the fillers used will be presented. The rheographs corresponding to certain samples and the theoretical values of k, determined using the models reviewed above will also be given.

5.1.0 Thermal conductivity

Thermal conductivity values of the different rubber composites are given below.

(i)   Table 7 shows the k values at 303K and 343K for the various samples loaded with carbon black, kaolin and charcoal. It also contains the hardness values determined at 295K.

(ii) Figs. 28 and 29 show curves of k, as a function of filler volume fraction for kaolin and carbon black filled composites. These figures correspond to the results in table 7.

(iii) Fig. 30 shows both curves of k, determined at 303K and 343K for kaolin and·carbon

THERMAL CONDUCTIVITY RESULTS

SAMPLE TYPE	FILLER VOLUME FRACT.	THERMAL CONDUCTIVITY IN W/mK AT		HARDNESS VALUES IN I.R.H.D.
		303K	343K	
A	0	0.170	0.155	< 30
K20	0.071	0.193	0.180	32
K40	0.133	0.218	0.190	34
K50	0.161	0.235	0.200	37
K60	0.187	0.230	0.210	36
K80	0.235	0.245	0.237	40
K100	0.277	0.272	0.250	43
K120	0.315	0.291	0.269	40
K150	0.365	0.295	0.309	43
K170	0.395	0.316	0.347	45
K190	0.421	0.335	0.362	47
K210	0.446	0.332	0.384	49
CB20	0.088	0.232	0.210	44
CB40	0.163	0.270	0.264	54
CB80	0.280	0.345	0.330	76
CB100	0.327	0.355	0.349	83
CB120	0.368	0.390	0.370	85
CB150	0.421	0.419	0.397	85
CB170	0.452	0.432	0.419	87
CB190	0.480	0.434	0.451	86
CB210	0.505	0.450	0.464	89
1C60	0.375	0.173	0.162	35
1C50	0.333	0.174	0.177	35
1C80	0.444	0.180	0.181	40
4C50	0.333	0.170	0.179	36
5C50	0.333	0.185	0.176	37
6C50	0.333	0.199	0.169	34

Table 7 (a) Thermal conductivity results of the composites of kaolin, carbon black and charcoal determined at 303K and 343K.

(b) The hardness values are also given, determined at 295K.
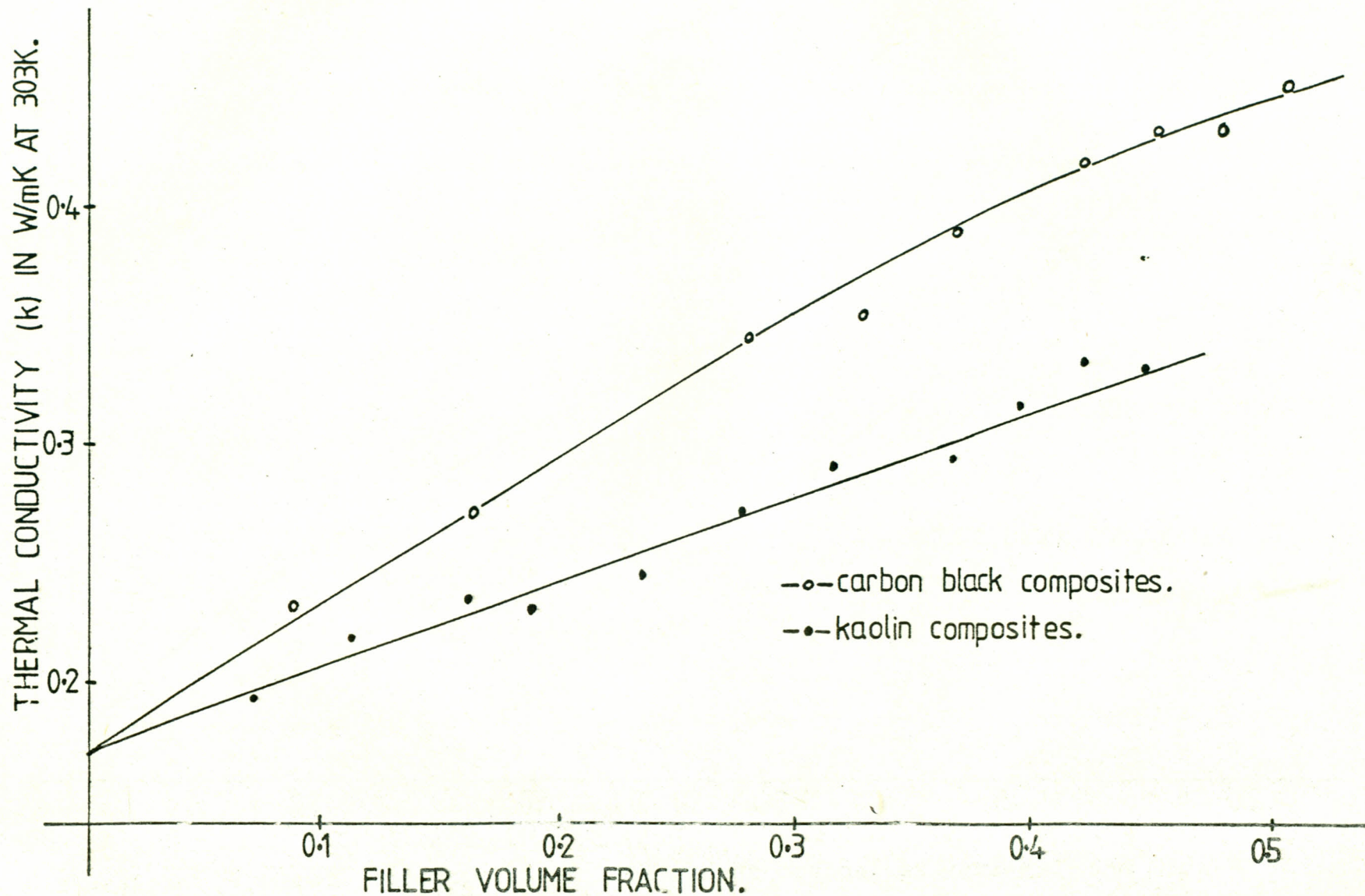
Fig. 28   Thermal conductivity of EPDM rubber composites versus filler fraction
at 303.
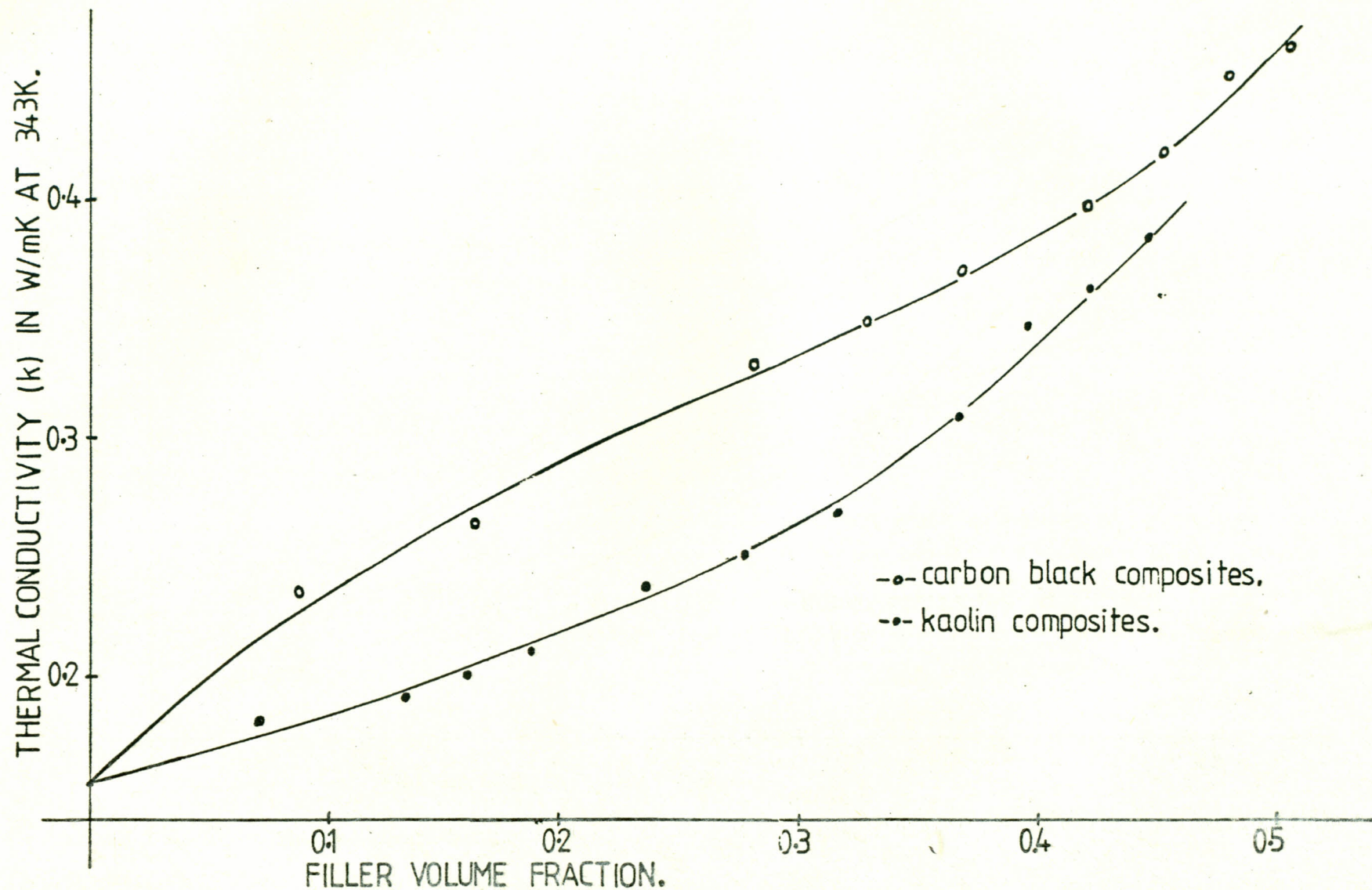
Fig. 29   Thermal conductivity of EPDM rubber composites versus filler volume
fraction at 343K.
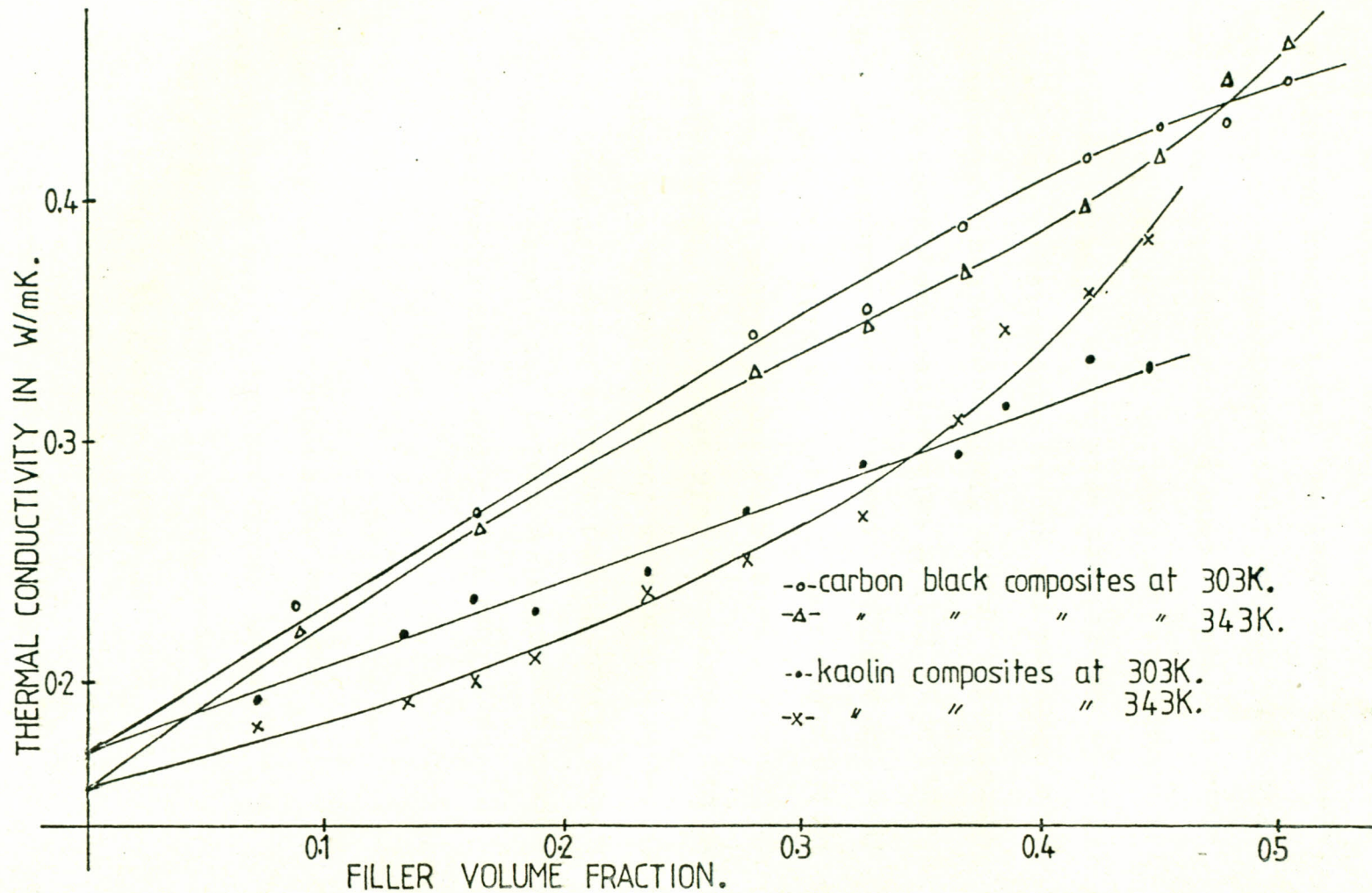
Fig. 30. Thermal conductivity of EPDM rubber composites versus filler volume
fraction at 303 and 343K.

black filled rubber composites.

(iv)   Thermal conductivity, as a function of
temperature, of samples types A, K100,
K210, CB100 and CB210, are given in Table 8
and the corresponding curves are shown in
Fig. 31.

The filler free rubber composites had the lowest
thermal conductivity while, the thermal conductivities
of the filler loaded samples increased with increasing
filler concentration for both kaolin and carbon black,
at the temperature 303K and 343K. The k values of
carbon black were found to be higher than those of
kaolin composites for all the filler concentrations
(Fig. 28 and 29). The k, values measured at 303K as a
function of filler volume fraction showed a linear
increase for carbon black composites. Similar results
were observed for kaolin composites. When the k values
for the two fillers were taken at 343K, upsurges in k,
at about a filler fraction of 0.32 for kaolin and
about 0.47 for carbon black composites were observed
(Fig. 30). Below the concentrations at which the
upsurges were observed, the k values determined at
303K were higher than those determined at 343K.

Thermal conductivity linearly decreased with
increasing temperature as is shown in the regression

THERMAL CONDUCTIVITY OF RUBBER COMPOSITES
AS A FUNCTION OF TEMPERATURE

SAMPLE TYPE	TEMPERATURES OF MEASUREMENT OF k (K)	k (W/mK)
A	303.2	0.170
	321.2	0.163
	339.2	0.155
	344.4	0.177
	369.8	0.153
	403.1	0.143
CB100	303.2	0.355
	321.8	0.350
	340.1	0.349
	364.1	0.348
	395.6	0.331
CB120	303.8	0.428
	323.8	0.432
	342.5	0.425
	369.2	0.411
	395.8	0.402
K100	303.8	0.272
	321.8	0.267
	339.8	0.269
	353.1	0.277
	370.4	0.259
K210	302.4	0.332
	321.3	0.334
	244.1	0.309
	356.7	0.326
	386.9	0.305
	409.7	0.290

TABLE 8 Thermal conductivity as a function of temperature of the samples type A, CB100, CB210, K100 and K210.
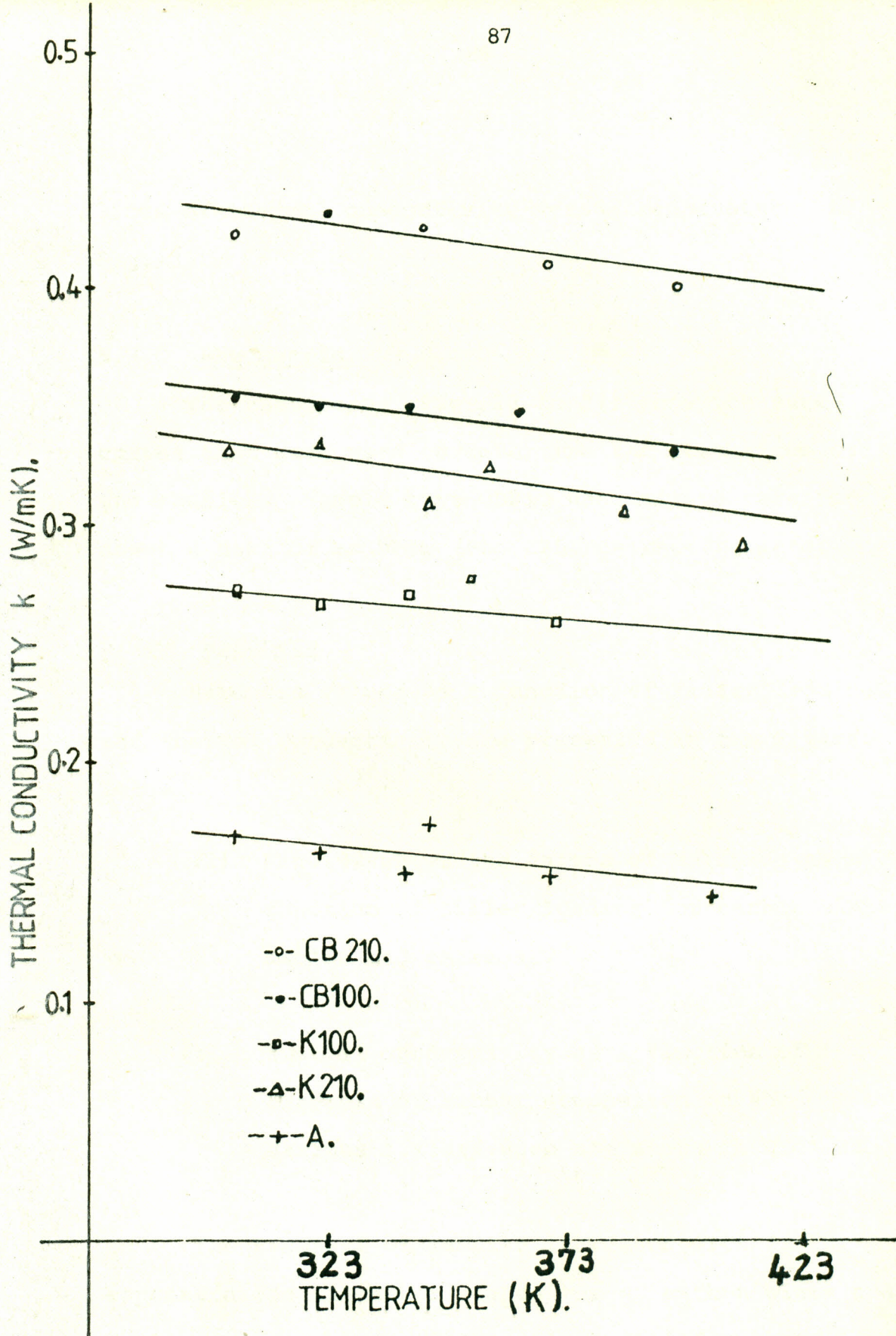
Fig. 31   Thermal conductivity versus temperature for different samples.

lines of thermal conductivity versus temperature in Fig. 31.

5.2.0 Rheographs

The rheographs (Figs. 23 to 27) show the cure curves that were used to determine the cure times of the samples. Sample type CB210 was left to cure for about a half of an hour (Fig. 25) on the rheometer.

5.3.0 Hardness

Hardness values as a function of filler loading and thermal conductivity are presented in the Figures below.

(i)   Fig. 32 shows the curves of hardness as a function of filler loading for carbon black, kaolin and charcoal.

(ii) Thermal conductivity as a function of hardness of rubber composites of the various fillers used are shown in Fig. 33.

The hardness of samples increased with filler concentration in rubber composites of carbon black and kaolin, as expected. Carbon black filled rubber composites exhibited higher hardness than kaolin or charcoal for the same filler concentration (Table 7 and Fig. 32). Charcoal filled rubber composites showed very little change in hardness due to
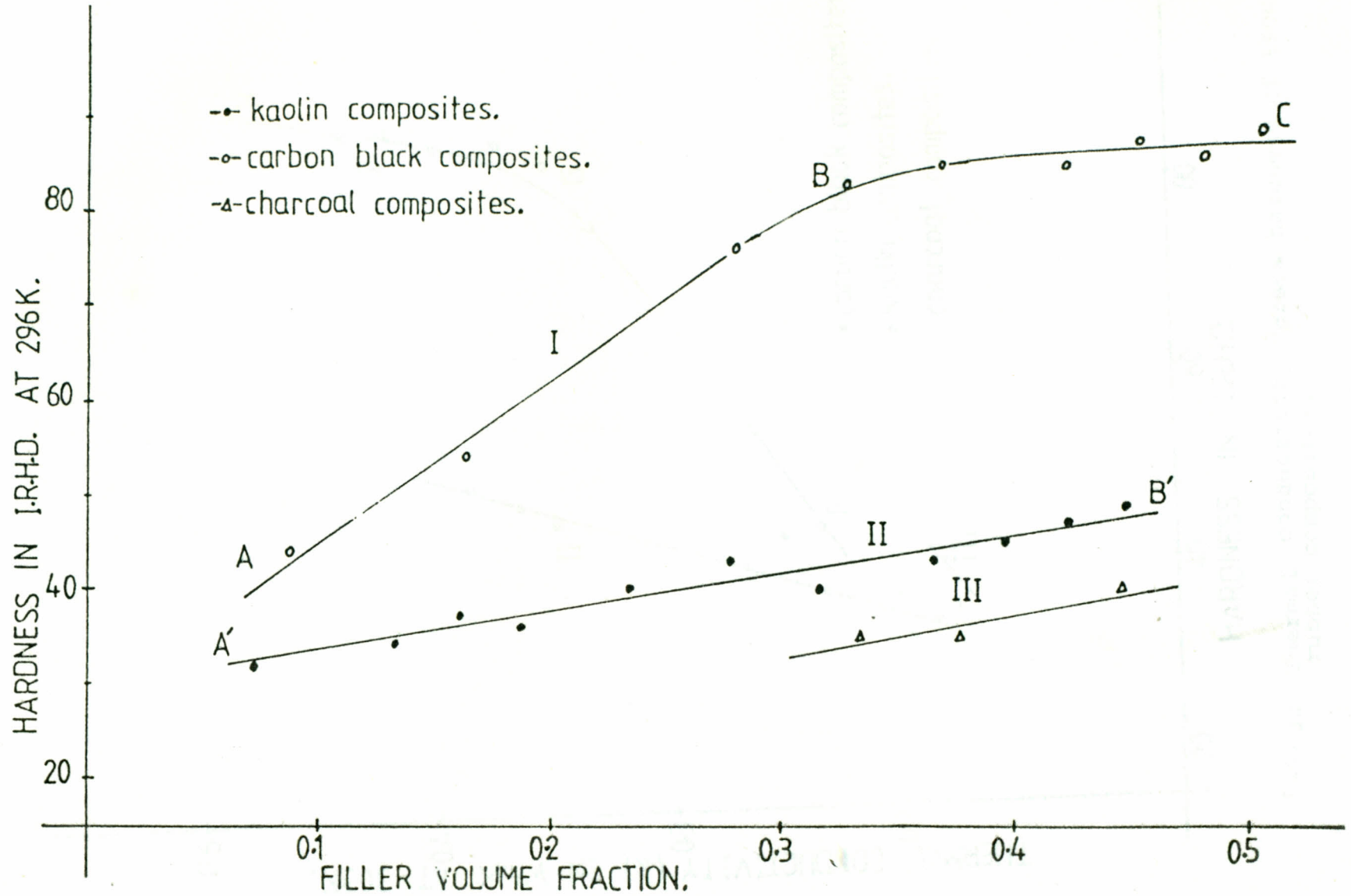
Fig. 32   Hardness of EPDM rubber composites versus filler volume fraction.
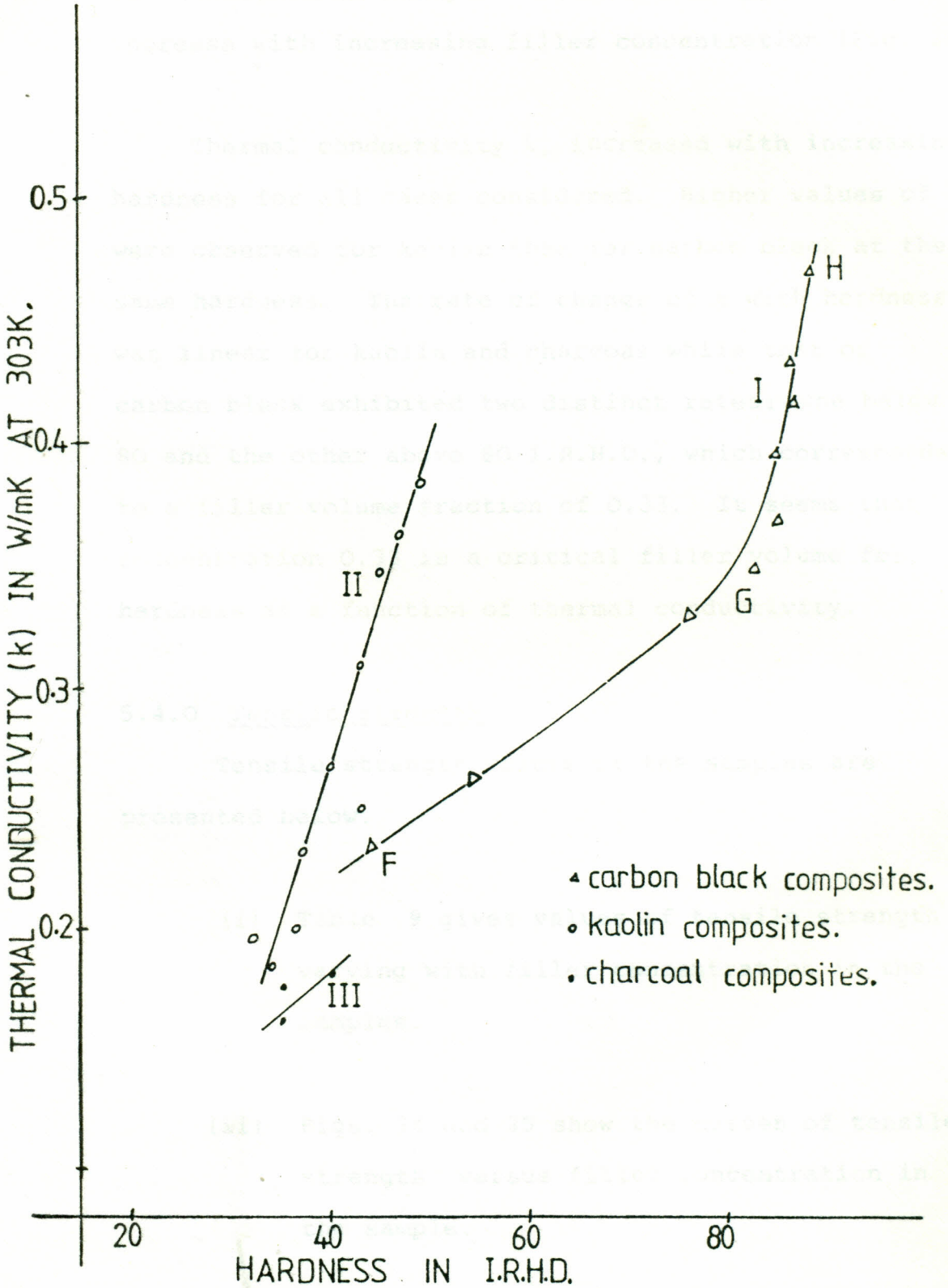
Fig. 33 Thermal conductivity versus hardness of EPDM rubber composites.

to concentration change. The hardness appeared to increase with increasing filler concentration (Fig. 32).

Thermal conductivity k, increased with increasing hardness for all cases considered. Higher values of k, were observed for kaolin than for carbon black at the same hardness. The rate of change of k with hardness was linear for kaolin and charcoal while that of carbon black exhibited two distinct rates; one below 80 and the other above 80 I.R.H.D., which corresponds to a filler volume fraction of 0.33. It seems that concentration 0.33 is a critical filler volume for hardness as a function of thermal conductivity.

5.4.0 Tensile strength

Tensile strength values of the samples are presented below.

(i) Table 9 gives values of tensile strength varying with filler concentration in the samples.

(ii) Figs. 34 and 35 show the curves of tensile strength versus filler concentration in the sample.

Tensile strength increased with increasing filler concentration to a maximum then declined as the

SAMPLE TYPE	FILLER VOLUME FRACT.	TENSILE STRENGTH (MPa)	BREAKING ENERGY (N/m²)
A	0	1.0	1.7
CB40	0.163	4.82	10.7
CB60	0.226	12.40	15.3
CB80	0.280	16.23	15.3
CB100	0.327	20.64	27.8
CB120	0.368	18.29	17.0
CB135	0.396	16.59	17.5
CB150	0.421	13.31	23.2
CB170	0.452	12.77	15.9
CB190	0.480	9.73	8.4
CB210	0.505	17.52	5.5
K20	0.071	1.32	2.5
K40	0.133	1.41	3.6
K80	0.235	2.26	11.2
K100	0.277	2.86	14.0
K120	0.315	3.30	19.2
K135	0.341	2.64	21.8
K150	0.365	3.84	22.4
K170	0.394	3.15	23.4
K190	0.421	3.16	13.6
K210	0.446	2.61	1.1
IC20	0.167	1.67	5.0
IC40	0.286	1.88	9.9
1C50	0.333	2.64	15.4
1C60	0.375	2.39	14.8
1C80	0.444	3.30	23.7
2C50	0.333	1.05	1.9
4C50	0.333	1.39	4.1
5C50	0.333	1.33	2.7
6C50	0.333	1.16	0.8

TABLE 9: Tensile strength and Breaking energy are given as a function of filler concentration.
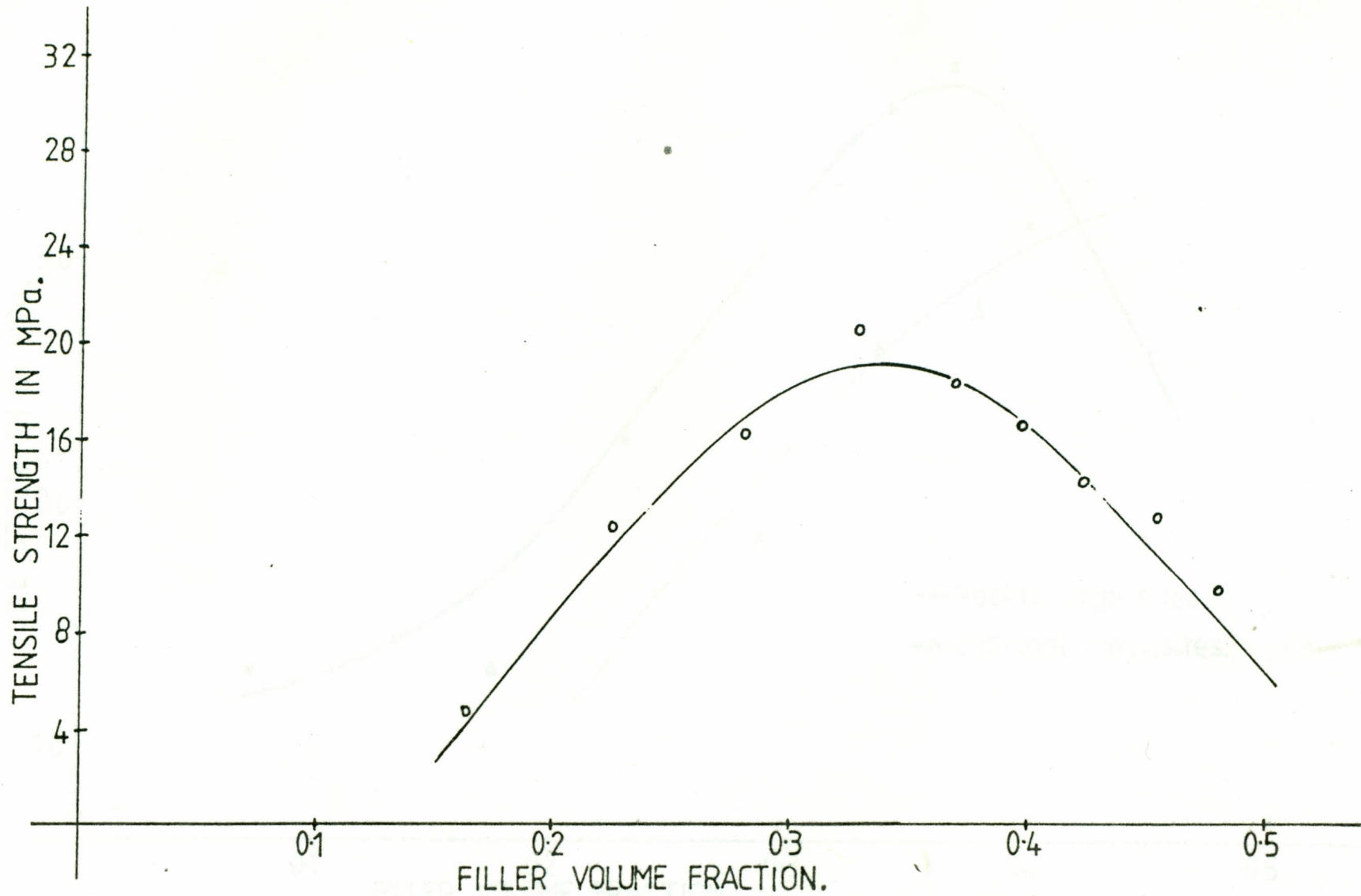
Fig. 34   Tensile strength of EPDM rubber composites (filled with carbon black N339) versus filler volume fraction.
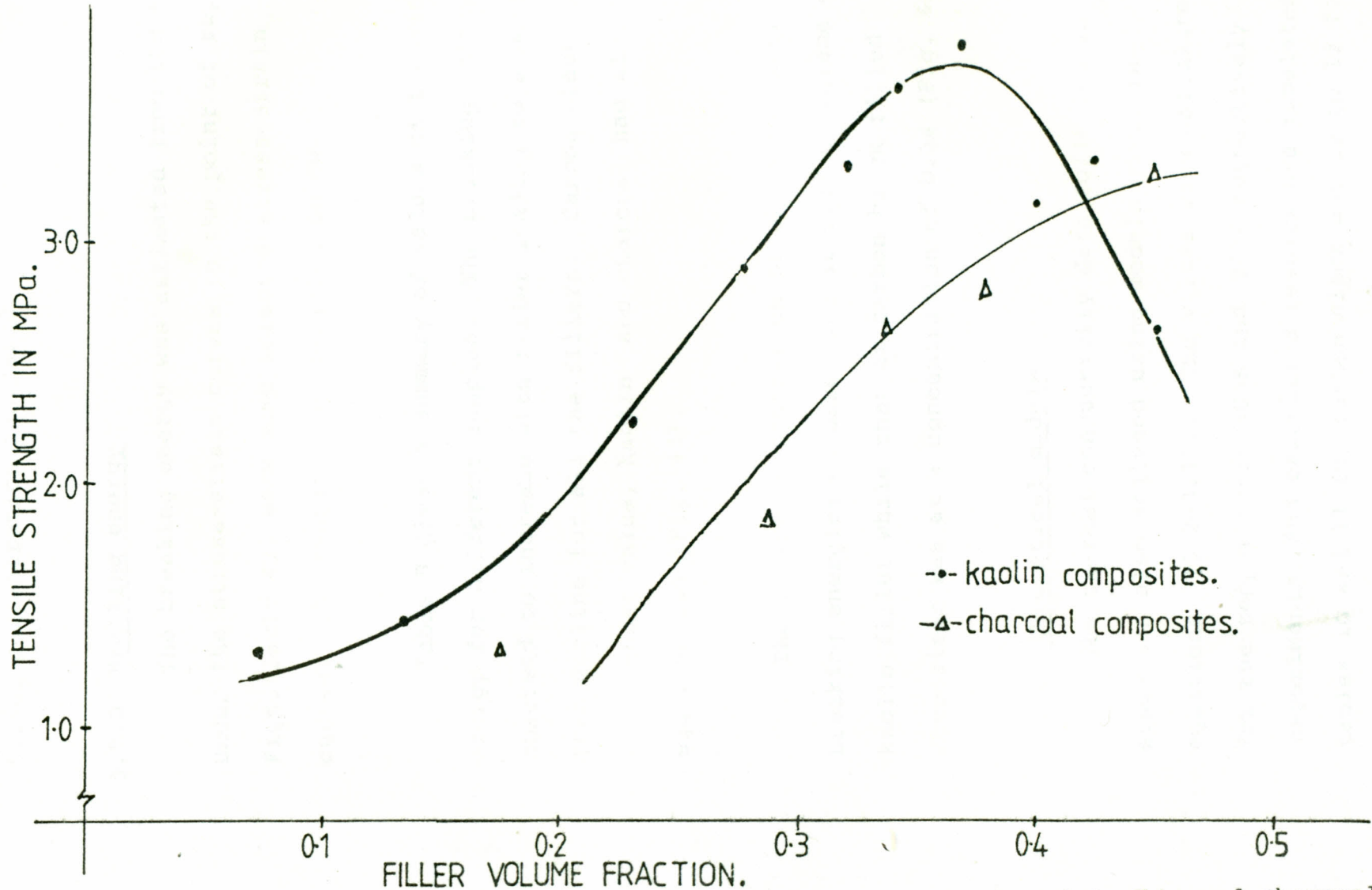
Fig. 35   Tensile strength of EPDM rubber composites (filled with kaolin and charcoal) versus filler volume fraction.

Nielsen's model given in equations 3.10 was also tested to predict the thermal conductivity of rubber composites in this study at 303K and 343K. The maximum packing fraction of carbon black (P_f) was given as 0.64 (36) and that of the constant A given by A = 1.5, (36). In the case of kaolin k_E = 4 and P_f = 0.52 (3). Figs. 44 to 53 show the curves of the theoretical and experimental values of conductivity versus filler volume fraction at 303K and 343K, for the various models tested.

filler concentration increased.

5.5.0 Breaking energy

The breaking energy was estimated from the area
under the stress-strain curves to the point of rupture.
Figs. 36 to 42, show some selected stress-strain
curves. The results are described below.

Table 9 gives a summary of values of breaking
energy for different samples. The breaking energy was
observed to increase with filler loading to a maximum
then decline for all the fillers. Carbon black had
the highest value, kaolin and charcoal had almost
equal values (Fig. 43).

The filler concentration at which the maximum
breaking energies occurred was at 0.37 by volume of
kaolin filler while that of carbon black filled
composites was at a concentration of 0.34 (Fig. 43).

5.6.0 Theoretical models

The thermal conductivity data collected in this
study was also analysed using models given in
equations (3.2-3.17). The values were calculated
for the temperatures 303K and 343K respectively. The
experimental and calculated results are tabulated in
tables 10 and 11 for carbon black and 12 to 13 for
kaolin at the temperatures 303K and 343K.

6.0.0. DISCUSSION

In this section the experimental results will be discussed. They will also be compared to the theoretical values predicted by some thermal conductivity models found in literature. Conclusions will be drawn from the discussion and recommendations for further work given.

6.1.0 (a) EFFECT OF CROSSLINKING, BOUND RUBBER AND PACKING DENSITY ON THE THERMAL CONDUCTIVITY OF EPDM RUBBER COMPOSITES

The thermal conductivity k, of filler free EPDM rubber composite was found to be lower than that of the filled composite (Figs. 28 and 29). This observation may be explicable if one assumes that heat transfer in the binary system i.e. rubber and filler, is governed by the thermal conductivities of the individual phases, and that the thermal conductivity of the filler is higher than that of the polymer phase. The thermal conductivity of the polymer matrix is further governed by structural and chemical nature of the polymer such as the amorphousness and crystallinity of the polymer. In a polymer, heat transfer can be thought of as being transmitted through the vibrations of the chains and crosslinks. The path along the backbone of a polymer molecule is

an easier route for heat transfer than the path running from units on one molecule to another (71). The path of high heat conduction therefore follows the conformation of the polymer molecule, which in rubber is essentially random. As a consequence of this, thermal conductivity of filler free rubber composite is very low.

Incorporation of fillers into the gum compound increases the effective thermal conductivity k, of the rubber composites. This increased with increasing filler concentration (Figs. 28 and 29). The increase in k with filler concentration may be the effect of increasing crosslinking density which may have resulted from increasing filler concentration in the composite (72). Increasing crosslinking density increases short thermal paths across the sample thus increasing the thermal conductivity of the composite.

Increase in the crosslinking density is equivalent to increasing the molecular weight of the rubber composite (72), and the increase in the molecular weight increases k (71).

By increasing the filler concentration, the average distance between the neighbouring filler particles is reduced. This increases the packing density of the filler thereby affecting the filler-polymer interactions. At very high filler

concentrations filler-filler interactions increases, minimizing the filler-polymer interactions. Both the filler-filler and strong filler-polymer interactions create short thermal paths that results in increasing thermal conductivity of the rubber composites.

The k values of carbon black filled rubber composites were found to be higher than those filled with kaolin or charcoal measured at the same temperature and filler concentration (Figs. 28 and 29). The apparent differences in k, between the composites can be attributed to the characteristic properties of the individual fillers. Carbon black (N339) used was the finest with a mean diameter of 26nm, while kaolin had a mean diameter of 45 microns, and the finest grade of charcoal used had a mean diameter of 53 microns. This difference in particle size means that a larger surface area per unit filler volume fraction was availed for filler-matrix interaction in carbon black composite than for kaolin or charcoal. Increasing the number of filler-polymer chain interactions perhaps by the higher number of chain adsorption on the carbon black, than in kaolin and charcoal, may be one of the reasons for the observed difference in k.

The differences in k, for carbon black, kaolin and charcoal filled composites may also be attributed to the nature of the surface activity of the fillers.

Carbon black has a more active surface than kaolin, because of a higher density of active sites on the carbon black surface that have high adsorption energy, than in kaolin (44). This is responsible for the high percentage of bound rubber formed in carbon black filled rubber composites (44). The presence of bound rubber also implies that strong filler-polymer coupling forces exist, thus facilitating thermal transmission by providing strong thermal contacts and hence increasing k. In kaolin and charcoal filled rubber composites, bound rubber is much lower than that in carbon black composites and exhibits low k values for equal filler concentrations than those filled with carbon black.

The upsurge in k values at high carbon black and kaolin concentrations determined at 343K (Figs. 29 and 30) may be the effect of the heat of sulfur vulcanization process (66) evolved during the determination of k. The evolved heat reduces the magnitude of dT across the sample, hence increasing k, as shown in equation 3.1. The rheographs of the compounds with concentrations at 190 and 210 phr for carbon black (Figs. 26 to 27), show that the vulcanization region appears to take longer than composites with filler concentrations lower than 190 phr. This phenomenon suggests continuity of vulcanization process in composites with filler

concentration higher than 190 phr, when optimal temperatures are reached.

Considering evidence of Fig. 25 where the rate of change of modulus is initially high but decreases with time of cure, the upsurge in k, determined at 343K, for concentrations higher than 150 phr, is sustained as long as vulcanization process continues during which, the rate of change of modulus is still high. After some time of continuous heating, vulcanization process ceases or may continue at such low rates as to have no significant contributions to the k determined. This confirms the result in Fig. 31 that shows k, decreasing with increasing temperature of measurement.

The relationship between k, and the temperature of measurement is linear in the temperature range 303K to 403K (Fig. 31). The decline in k with increasing temperature may be explained in terms of thermal agitation of the polymer chains that increase with increasing temperature. Thermal agitation at a given temperature impedes thermal transmission by scattering the thermal energy in transit across the composite medium. The degree of scattering increases with increasing chain agitation, this causes declining thermal conductivity with increasing temperature. Similar results have been observed in amorphous

polymers (12,71).

The hardness of rubber composites filled with kaolin and carbon black increase with increasing filler concentration (curve I and II of Fig. 32). Curve I shows a rapid linear increase of hardness with increasing filler volume fraction of carbon black (N339) in the section between A and B, where B correspond to a filler volume fraction of about 0.32. This rapid change in hardness with increasing filler concentration may be due to the increasing percentage of bound rubber and crosslinking density in the rubber composites. Section BC of the same curve shows a slight increase in hardness with increasing filler concentration of the composites. This indicates that a high filler content density has been reached and any additional fillers have no effect on the hardness of the composite. This agrees with the measured DBP values ($124 cm^3/100g$) of carbon black (N339), which predicts a maximum volume fraction of 0.28, of the filler, that can be dispersed in a rubber matrix (44).

Curve II in Fig. 32 shows increasing hardness values with increasing volume fraction of kaolin. The change in hardness from the minimum at A' to the maximum at B' of 17 I.R.H.D. is small compared to a corresponding change in carbon black filled rubber composite of 45 I.R.H.D. in curve I. This difference

in the change of hardness values suggests the presence
of a higher percentage of bound rubber and crosslinking
density in carbon black than in kaolin filled
composites. The small change in hardness of kaolin
filled rubber composites with increasing filler volume
fraction may have been the result of poor filler-polymer
interaction, that may have lead to low percentage
increase in bound rubber and crosslinking density
content. A maximum in the hardness of kaolin filled
composites was not observed, perhaps because the maximum
filler volume fraction of 0.52, that is dispersible in
a matrix, had not been reached (Figs. 32 and 33).

Charcoal filled rubber composites showed a low
increase in hardness values with increasing filler
concentration. The low increase may be caused by the
low crosslinking density and the absence of bound
rubber in the composites.

The thermal conductivity linearly increases with
increasing hardness of kaolin, carbon black and charcoal
filled composites, see curves I, II and III in Fig. 33.
In curve I, k of carbon black linearly increases with
increasing hardness between F and G. This linear
increase may be caused by the increasing percentage of
bound rubber and crosslinking density and is similar to
the observation made in curve I of Fig. 32 between A
and B. The rapid increase in k, with increasing

hardness shown between G and H in curve I of Fig. 33 shows the effect of increasing packing density of the filler in the composite. This decreases the average filler-filler distance and, increases the inter-filler contacts which results in increasing thermal conductivity of the composites, given that the thermal conductivity of the filler (carbon black) has a higher value than the matrix used (rubber). The rapid increase in k begins at a value of hardness that corresponds to a filler volume fraction of 0.33. This filler volume fraction value is slightly higher than the maximum filler volume fraction of carbon black (N339) dispersable in a rubber matrix as is predicted by DBP value ($124cm^3$ /100g) of 0.28 (44), and therefore indicates the presence of undispersed filler agglomerates in the rubber composite. This may be responsible for the observed increase in k caused by the creation of short thermal paths that increase with increasing filler volume fraction above 0.28.

Curve II of Fig. 33 also shows a rapid change in k, with increasing hardness values of kaolin filled rubber composites and is similar to sections GH of curve I in Fig. 33. The rapid increase in k with increasing hardness, may have been mainly due to the decreasing filler-filler distance and increasing filler-filler contacts as the filler concentration increased. The absence of a behavior similar to

section FG of curve I in Fig. 33 suggests the
insignificant contributions to thermal conductivity
made by bound rubber and crosslinking density changes
in kaolin filled composites.

Charcoal filled composites also showed increasing
k, with increasing hardness of the rubber composites
(curve III of Fig. 33) and is in agreement with curve
III of Fig. 32 that shows increasing hardness with
increasing filler volume fraction. The incompartibility
of the charcoal filler to the rubber used limits proper
analysis for the results obtained.

Tensile strength increased with increasing filler
concentration until a critical concentration, when the
strength started decreasing (Fig. 34 and 35). Given
that the area under the stress-strain curve represents
the energy required by the material to break, this may
also be taken as an index of the polymer-polymer and
polymer-filler interaction energy. The energy required
to rupture the composite is affected by the filler
concentration and seems to increase upto a critical
concentration, then decreases. Curve 1 in Figs. 32, 33
and Fig. 34 show that there is a critical filler
concentration at which the conductivity, hardness and
tensile strength changes occur for carbon black filler,
and agree with the DBP values. At the critical
concentration the adhesive energy density reaches its

maximum, but is increasingly lowered as the filler concentration increases. This would be the result of dilution effect. There would be more filler-filler interaction than polymer-filler interactions in the composite. Beyond this crictical concentration the rubber matrix would be inadequate and cannot hold the filler particles together sufficiently so as to withstand high tensile strengths. The tensile strength rapidly decreases, because the filler-filler cohesive energy is then lower than that of the filler-polymer. This is the case in composites with concentrations that are higher than the critical filler concentration.

Carbon black filled rubber composite had much higher tensile strength and thermal conductivity values, than those of kaolin and charcoal for the same filler concentration (Figs. 34 and 35). The high tensile strengths may be taken as an indicator of the interaction energy arising from bound rubber and thereby can be associated with the substantially high increase in k values. This may also be partly due to the finer particle size of carbon black used than those of kaolin and charcoal, in which it agrees with Boonstra's observations on EPDM rubber (44). The high tensile strength in carbon black filled composites indicates that there exists high adsorption energy on the carbon black surface, leading to bound rubber on carbon black, which is minimal in kaolin and

charcoal surfaces. These high coupling forces in carbon black filled composites contribute to the high k, values (Figs. 28 and 29) noticed in carbon black composites and minimum in kaolin or charcoal composites.

The low value of breaking energy of EPDM gum compound is largely due to its amorphous nature that cannot sustain high tensile stresses. The addition of fillers improves the breaking energy of the gum compound by providing surfaces of adsorption of the rubber chains. The increasing breaking energy with filler concentration may be associated with the increasing surface area made available for adsorption of the polymer chains.

The maximum breaking energies of carbon black, kaolin and charcoal are relatively close (Fig. 43). This is the effect of the nature of adsorption energies of the filler surface. Carbon black has local adsorption which does not allow for slippage hence most of the energy is dissipated in breaking molecular chains and the chain-filler surface bonds. Carbon black composites showed high stresses at low strains while kaolin and charcoal, which reportedly have mobile adsorption (44), allow the slippage of the polymer chains on the surface of the filler showed high strains at low stresses (Figs. 36 to 42).

The critical concentrations for the maximum tensile strength correspond to those of the maximum breaking energies in the fillers used (Figs. 34, 35 and 43). This is because these maximum values of tensile stength and breaking energy depend on good dispersions of the filler particles in the composites and the maximized filler-polymer interaction. At filler concentrations higher than the critical concentration, the tensile strengths and breaking energies decline because of the weak filler-filler interaction which dominates the composite. Similarly at low filler concentrations the weak polymer-polymer interactions that dominate the composite medium contribute to the low values observed.

(b) COMPARISON BETWEEN THEORETICAL VALUES AND THE
EXPERIMENTAL RESULTS

The effective thermal conductivity determined theoretically using Russell's equation (eq. 3.2) at 303K did not agree with the experimental values. The calculated values were slightly higher (Fig. 44). The experimental values determined at 343K were however higher than the theoretical values for filler volume fractions between 0 and 0.31 (Fig. 45). At the two temperatures the results of carbon black composites are remarkably close, while those of kaolin show substantial difference between the experimental and theoretical values, (Figs. 44 and 45). The theoretical

values were higher than the experimental values.

Kaolin filled rubber composites showed divergence between the experimentally determined values and the theoretical ones at both temperatures 303K and 343K (Figs. 44 and 45). The theoretical values were also higher than the experimental values.

Del'nev and Zarichnyak's equation given in equation 3.5 led to thermal conductivity values that were found to fit the experimentally determined values, for carbon black filled rubber composites, with filler fractions between 0 and 0.25 at the temperature 303K (Fig. 46). Above this filler volume fraction, the theoretical values diverged from the experimental values. This divergence may be the result of the onset of segregated mixing of the filler in the composite which is contrary to the assumptions of the model. From the DBP value ($124cm^3$/100g) of carbon black (N339) the highest volume fraction that is dispersible in rubber on a mixing mill is 0.28 (44). This value of 0.28 is close to the observed volume fraction of 0.25, the point from which deviation between the experimental values and the theoretical values started. At a higher temperature of 343K the theoretical values and the experimental values did not show any concurrence (Fig. 47).

The effective thermal conductivity of kaolin

filled rubber composites determined experimentally were found to be at variance with the theoretical values determined from equation 3.5 of Del'nev and Zarichnyak at both temperatures.

Nielsen's model given as equation 3.10 did not also fit the experimentally determined data (Figs. 48 and 49). The theoretical values of k for kaolin composites were much higher than the experimental values determined at both temperatures, 303K and 343K. Carbon black filled composites showed slight variation for values determined at 303K. Below a filler volume fraction of 0.25, the theoretical values were less than the experimental values of k (Fig. 48). Similar observations were made for values determined at 343K. The deviation may have been the result of the constants k_E and the maximum packing of the filler ϕ_m that may not have been the true values of the particular fillers used.

Values of k calculated using Brailsford and Major's theoretical results (equation 3.7) showed divergence from the experimental values determined at both temperatures, 303K and 343K. The experimental values were higher than the theoretical values between filler fractions of 0 and 0.25 (Fig. 50 and 51). Similar observations were made from the results obtained using Maxwells equation (Fig. 52 and 53),

however the values obtained using Hamiltons equation
(eq. 3.14) agreed with the experimental values of
Hamilton and Crosser (19).

The effective thermal conductivity of kaolin
filled rubber composites that were experimentally
determined at both temperatures 303K and 343K, were at
variance with the theoretical values determined using
the above quoted models. The theoretical values were
higher than the experimental values.

In carbon black filled rubber composites the
effective thermal conductivity values showed
concurrence with the theoretically determined values
using Del'nev and Zarichnyak's equation determined at
303K. At 343K the experimental values of k were much
higher than the theoretical values.

Most of the theoretical models tested showed
lower values of k compared with the experimentally
determined values between filler volume fractions of 0
and 0.32, by volume of filler at both the temperatures,
for carbon black filled composites (Figs. 44 to 53).
The exceptions were values obtained using Russell's
equation, at 303K, which showed agreement with the
experimental results of carbon black composites despite
some slight deviations. Del'nev and Zarichnyak's
equation at 303K agreed with the experimental results.

The high experimental values of k of carbon black filled composites, and the low k values of kaolin filled composite at both temperatures, did not compare with the theoretically determined values, and suggested the presence of influencing factors that are characteristic of the individual filler properties. The deviations may also be explained by the fact that almost all the models used are based on the law of mixtures i.e., that thermal conductivity of the constituent components and their corresponding volume fraction in the binary composition.

In deriving these models, it seems that the main considerations were, those of contributions to the heat transfer process, made by particle size, porosity, geometry, etc. of the filler on the thermal conductivity of the composites. None of the models seems to adequately address itself to the contributions made by the filler-polymer interactions, that apparently plays a major role in thermal conductivity of rubber composites, and perhaps that is why the experimental and the theoretically determined values of k are at variance.

6.2.0 CONCLUSIONS.

From the data collected and, the foregoing discussion the following conclusions may be made.

(i)   Filler free rubber composite had very low
        thermal conductivity values as was
        expected.

(ii)   The thermal conductivity increased with
        increasing concentration of carbon black
        (N339) or kaolin filled rubber composites.

(iii)   The reported value of k (1.97 W/mK), of
        kaolin (3), was higher than that of carbon
        black, (1.59 W/mK at 303K and 1.73 W/mK at
        343K) (2), but the k values of carbon
        black composites were higher than those of
        kaolin composites. This was contrary to
        the expected results. This result is
        accounted for in terms of the effect of
        filler-polymer interaction.

(iv)   The tensile strength and the breaking
        energy increased with increasing filler
        concentration to a critical value. Above
        the critical concentration the values
        declined. The k values of EPDM rubber
        composites also increased with increasing
        filler concentration up to some critical
        value. The composites of the filler with
        higher tensile strengths showed higher k
        values, thus suggesting a relationship

between k and the filler-polymer
interactions.

(v)   The critical volume fraction of the filler
in the composite at which hardness and
tensile strength occur seems to mark the
onset of segregated mixing, and is in
agreement with the available DBP values of
the fillers used.

(vi) The theoretical models in use for thermal
conductivity do not seem to successfully
predict the experimental values observed.
This has been attributed, in the case of
rubber composite to lack of inclusion of
an energy interaction parameter which
accounts for the chain-filler cohesive
energies.

6.3.0   RECOMMENDATIONS

(1)   The degree of filler-rubber (polymer)
interaction, has been neglected in thermal
conductivity models that have been
proposed in literature. This parameter
needs to be included to improve the
correlation between the theoretical and
experimental values of k, of rubber
composites.

(2)   A study of charcoal filler surface
      properties and those from different trees,
      and varied preparation processess is
      necessary. This may improve the rubber-
      filler (charcoal) compartibility, and
      avail it for use in rubber industry.

(3)   Need to determine the effect of processing
      procedures on the percentage of bound
      rubber and crosslinking density in the
      rubber composites, and how they affect the
      thermal conductivities of the composites.

REFERENCES

1. Jean-Baptiste, Donnet and Andries voet, "Carbon black", Marcel Dekker, Inc. New York 1976.

2. Hand book of Chemistry and Physics, 67th Edition, 1986-87, CRC Press, Florida, Ell.

3. Thomas, H. Ferringo, "Principles of filler selection and use", in Hand book of fillers and Reinforcements for plastics, (Eds) Harry S. Katz and John V. Milewiski, Van Nostrand Reinhold Company, New York (1978).

4. Kaolin laboratory sheet, from Athi River Mining Company Kenya Ltd.

5. P. Anderson and G. Backstrom,J. Appl. Phys., $\underline{44}$, 2601 (1973).

6. O. Sandberg and G. Backstrom, J. Appl. Phys., $\underline{50}$, 4720 (1979).

7. A.B. Bashirov and A.M. Manukyan, Mekhanika Polimerov, $\underline{3}$, 564 (1974).

8. Ernest Karawachi, J. Appl. Phys., $\underline{52}$, 2596 (1981).

9. W. Reese, J. Appl. Phys., $\underline{37}$, 864 (1966).

10.   K. Eiremann, Kolloid-Z, 198, 5(1964).

11.   P. Anderson, J. Appl. Phys., 47, 2424(1976).

12.   D.R. Anderson, Chem. Revs., 66, 677(1966).

13.   Mueller, F.H., and Hellmuth, W., Kolloid-Z., 185, No. 2, 159(1962).

14.   Tanaka, J., and Wakae, M., Rept. Ind. Res. Inst. Osaka Prefect., 3, No. 2, 26(1951).

15.   Zanemonets, N.A., and Fogel, V.O., Abstr., 53, 564 (1974).

16.   Dauphinee, T.M., Ivery, D.G., and Smith, T., Phys. Rev., 71, 487 (1947).

17.   Dauphinee, T.M., Ivery, D.G., and Smith, M.D., Can. J. Res., 28A, 596 (1950).

18.   Tantz, H., Kolloid-Z, 174, 128(1961).

19.   Hamilton, R.L., Crosser, O.K., Ind. Eng. Chem. Fundam., 1, 187(1962).

20.   L.E. Nielsen, Ind. Eng. Chem. Fundam., 13, No. 1, 17(1974).

21. J.H. Atkins and J.E. Sullivan, Jr., Rubber Chem. Techn., _42_, 1314(1969).

22. A Voet and R.F. Cook, Unpublished results, J.M. Huber Cook Borger, Texas.

23. F. Keith and W.Z. Black,"Basic Heat Transfer," Harper and Row Publishers, New York (1980).

24. D.M. Dawson and A. Briggs, J. Mater. Scie., _16_, 3346(1981).

25. J.C. Maxwell, "Electricity and Magnetism", Vol. 1 Claredon Press, Oxford,(1904).

26. A. Matsuura, T. Akehata and T. Shirai, Heat Trans. Jap. Res. _4_, 79(1975).

27 G.N. Del'nev and Z.V. Sigalova, Int. Chem. Engng. _5_, 218(1965).

28. H.W. Russell, J. Amer. Ceram. Soc. 18(1935).

29. W. Woodside and J.H. Messmer, J. Appl. Phys. _32_, 1688(1961).

30. E.H. Ratcliff, J. Appl. Chem., _18_, 25, (1968)

31. G.N. Del'nev and Yu. p. Zarichnyak, Heat Transfer Sov. Res. $\underline{2}$, 89 (1970).

32. R.A. Crane and R.I. Vachon, Int. J. Heat Mass Trans., $\underline{20}$, 71 (1977).

33. M.R.J. Wyllie and P.S. Southwick, J. Petrol. Tech. $\underline{6}$, 44 (1954).

34. A.D. Brailsford and K.G. Major, Br. J. Appl. Phys. $\underline{15}$, 313 (1964).

35. D.R. Chaudhary and R.C. Bhandari, Brit. J. Appl. Phys. $\underline{2}$, 609 (1969).

37. L.E. Nielsen. J. Appl. Phys., $\underline{41}$, 4626 (1970).

38. T.B. Lewis and L.E. Nielsen, J. Appl. Polym. Sci., $\underline{14}$, 1449 (1970).

39. E.H. Kerner, Proc. Phys. Soc. (London), $\underline{B69}$, 802, 808 (1956).

40. J.C. Halpin, J. Compos. Mater., $\underline{3}$, 732 (1969).

41. R.L. Hamilton, PhD. thesis, University of Oklahoma, 1960.

42. J.C. Maxwell, "A Treatise on Electricity and Magnetism," Vol. I, 3rd Ed., Dover, New York, 1954.

43. H. Fricke, Phys. Rev. 24, 575-87 (1924).

44. B.B. Boonstra, "Reinforcement by fillers", in
     Rubber Technology and Manufacture, (Eds) C.M. Blow
     and C. Hepburn, Butterworths (1982).

45. G.L. Taylor and J.H. Atkins, J. Phys. Chem. ithaca,
     70, 1678 (1966).

46. S. Ross and J.P. Oliver,"Physical Adsorption,"
     Willey, New York, (1964).

47. B.B. Boonstra and G.L. Taylor, Rubb. Chem. Technol.
     38. 943 (1965).

48. J.J. Brennman and Jermya, T.E., J. Appl. Poly. Sci.,
     91,2749 (1964).

49. H.A. Braendle, Rubber Age, 72, 205 (1952).

50. W.F. Watson, Proc. 3rd. Rubber Techn. Conf. pp.
     553 (1953).

51. F.B. Stickney and R.D. Falb, Rubber Chem. Tech.,
     1299 (1964).

52. W.F. Watson, Ind. Engng. Chem., 74, 1281 (1955).

53. Silas E. Gustafsson, Ernest Karawachi and M.
     Nazim Khan, J. Phys., D, 12, 1411 (1979).

54. P. Anderson and G. Backstrom, J. Appl. Phys., 14, 2601(1973).

55. J.H. Blackwell, J. Appl. Phys., 25, 137(1954).

56. Method of Testing for Thermal Conductivity of materials by means of the guarded hot plate C 177-45 , 1955 Book of ASTM Standard, Part 3, pp. 1084.

57. International thermocouple reference tables, BS 4937, Parts 1 to 7, British Standards Institute, 1973, 1974.

58. W. Woodside, "Analysis of Errors due to Edge Heat loss in Guarded hot Plate", Symposium on Thermal Conductivity measurements and Application of thermal insulation, ASTM STP 217, ASTTA, Am. Soc. Testing Mats., pp. 49-64(1957).

59. W. Woodside and A.G. Wilson, "Unbalance Errors in Guarded Hot Plate Measurement", Symposium on Thermal Conductivity measurements and Application of thermal insulation, ASTM STP 217, ASSTA, A. Soc. Testing Mats., pp. 32-48(1957).

60. C.F. Gilbo, "Experiments with a Guarded Hot Plate Thermal Conductivity Set", Symposium on thermal

insulating materials, Am. Soc. Testing Mats.
pp. 45-55(1955).

61.   F.D. Polte and P. Di Fillipo, "Design criteria for
      guarded thermal insulations ASTM STP 544, ASTTA,
      Am. Soc. Testing Mats., 97(1974).

62.   E.V. Somers and J.A. Cyphers, Analysis of Errors in
      Measuring Thermal Conductivity of Insulating
      Materials, "Review of Scientific Instruments",
      RSINA, pp. 583-586(1961).

63.   Encyclopedia of Chemical Technology, Vol. 13, pp
      355, 2nd Edition, 1967, John Wiley and Sons, Inc.
      (New York).

64.   B.G. Growther, H.M. Edmondson and M. Elias,
      "Processing Technology", in Rubber Technology and
      manufacture (Eds) C.M. Blows and C. Hepburn,
      Butterworths (1982).

65.   Encyclopedia of Chemical Technolgy, Vol. 20, pp.
      369, 3rd Edition 1982, John Wiley and Sons, Inc,
      (New York).

66.   P.I. Bruce, R. Lyle and J.T. Blake, Ind. Engng.
      Chem., 36, 37(1944).

67. Encyclopedia of Chemical Technology, Vol. 20, pp 375, 3rd Edition, 1982, John and Wiley and Sons, Inc. (New York).

68. R.P. Brown,"Physical Testing of Rubbers," Applied Sci. Publishers Ltd., London (1979).

69. P. Anderson and G. Backstrom, Rev. Sci. Insrum., 47, 205 (1976).

70. R.W. Powell, "Thermal Conductivity determined by thermal comperator method", Chapt. 6 in R.P. Tye, (Eds), Thermal Conductivity, Vol. 2, Academic Press, New York, 1969.

71. D. Hansen and Chong, C. Ho, J. Poly. Sci. 3, 659 (1965).

72. Bueche, F.,"Physical Properties of Polymers," Interscience publishers (1962).

APPENDIX I

FILL. CONC.	FILL. VOL. FRAC.	DEL'N. k	NILL. k	RUSSE. k	MAX. k	BRAI. k	EXPER. k
0	0	0.170	0.170	0.170	0.170	0.170	0.170
20	0.088	0.221	0.213	0.236	0.205	0.209	0.232
40	0.163	0.267	0.258	0.278	0.239	0.254	0.270
80	0.280	0.340	0.347	0.348	0.303	0.354	0.345
100	0.327	0.371	0.393	0.378	0.331	0.405	0.355
120	0.368	0.400	0.440	0.406	0.359	0.456	0.390
150	0.421	0.438	0.514	0.444	0.400	0.528	0.419
170	0.452	0.461	0.564	0.470	0.423	0.573	0.432
190	0.480	0.482	0.620	0.490	0.447	0.617	0.434
210	0.505	0.502	0.676	0.515	0.472	0.657	0.450

TABLE 10: Calculated and the experimental values of carbon black filled composites at 303K based on the models abbreviated as follows:

DEL'N. = Del'neve and Zarichnyaks equation given by equation 3.5.

NIEL. = Nielsens conductivity model given by equations 3.10.

RUSSE. = Russell's conductivity equation given by equation 3.2.

MAX. = Maxwell's conductivity equation given by equation 3.17.

BRAI. = Equation developed by Brailsford and Major given by equation 3.6.

EXPER. = Experimental results.

FILL. CONC.	FILL. VOL. FRAC.	DEL'N. k	NIEL. k	RUSSE. k	MAX. k	BRAI. k	EXPER. k
O	O	O.155	O.155	O.155	O.155	O.155	O.155
20	O.088	O.205	O.191	O.214	O.189	O.193	O.210
40	O.163	O.253	O.234	O.256	O.222	O.238	O.264
80	O.280	O.331	O.321	O.323	O.283	O.343	O.330
1OO	O.327	O.365	O.366	O.351	O.312	O.399	O.349
120	O.368	O.396	O.414	O.375	O.340	O.454	O.370
150	O.421	O.434	O.490	O.419	O.380	O.535	O.397
170	O.452	O.458	O.545	O.442	O.404	O.586	O.419
190	O.480	O.481	O.603	O.467	O.429	O.635	O.451
210	O.505	O.502	O.664	O.487	O.452	O.680	O.464

TABLE 11: Calculated and the experimental values of carbon
black filled composites at 343K based on the
models abbreviated as is shown in table 10.

| FILL. | FILL. | DEL'N. | NIEL. | RUSSE. | MAX. | BRAI. | EXPER. |
| CONC. | VOL. | | | | | | |
	FRAC.	k	k	k	k	k	k
0	0	0.170	0.170	0.170	0.170	0.170	0.170
20	0.071	0.220	0.207	0.240	0.200	0.200	0.193
40	0.133	0.265	0.245	0.271	0.229	0.240	0.218
50	0.161	0.286	0.263	0.289	0.243	0.261	0.235
60	0.187	0.306	0.282	0.306	0.257	0.283	0.230
80	0.235	0.342	0.321	0.335	0.284	0.329	0.245
100	0.277	0.375	0.361	0.365	0.310	0.377	0.272
120	0.315	0.405	0.402	0.392	0.336	0.427	0.291
150	0.365	0.447	0.466	0.429	0.372	0.503	0.295
170	0.394	0.470	0.509	0.452	0.384	0.552	0.316
190	0.421	0.493	0.556	0.474	0.419	0.601	0.335
210	0.446	0.515	0.606	0.497	0.442	0.648	0.332

TABLE 12: Calculated and the experimental values of kaolin filled
composites at 303K based on the models abbreviated as
is shown in table 10.

FILL. CONC.	FILL. VOL. FRAC.	DEL'N. k	NIEL. k	RUSSE. k	MAX. k	BRAI. k	EXPER. k
0	0	0.155	0.155	0.155	0.155	0.155	0.155
20	0.071	0.206	0.190	0.214	0.183	0.186	0.180
40	0.133	0.250	0.225	0.252	0.210	0.221	0.190
50	0.161	0.270	0.243	0.269	0.223	0.241	0.200
60	0.187	0.290	0.261	0.283	0.236	0.242	0.210
80	0.235	0.351	0.298	0.313	0.262	0.307	0.237
100	0.277	0.358	0.335	0.339	0.286	0.355	0.250
120	0.315	0.388	0.374	0.382	0.310	0.405	0.269
150	0.365	0.428	0.436	0.399	0.344	0.481	0.309
170	0.394	0.452	0.479	0.422	0.369	0.530	0.347
190	0.421	0.475	0.523	0.442	0.389	0.580	0.362
210	0.446	0.496	0.572	0.464	0.411	0.628	0.384

TABLE 13: Calculated and the experimental values of kaolin filled composites at 343K based on the models abbreviated as is shown in table 10.
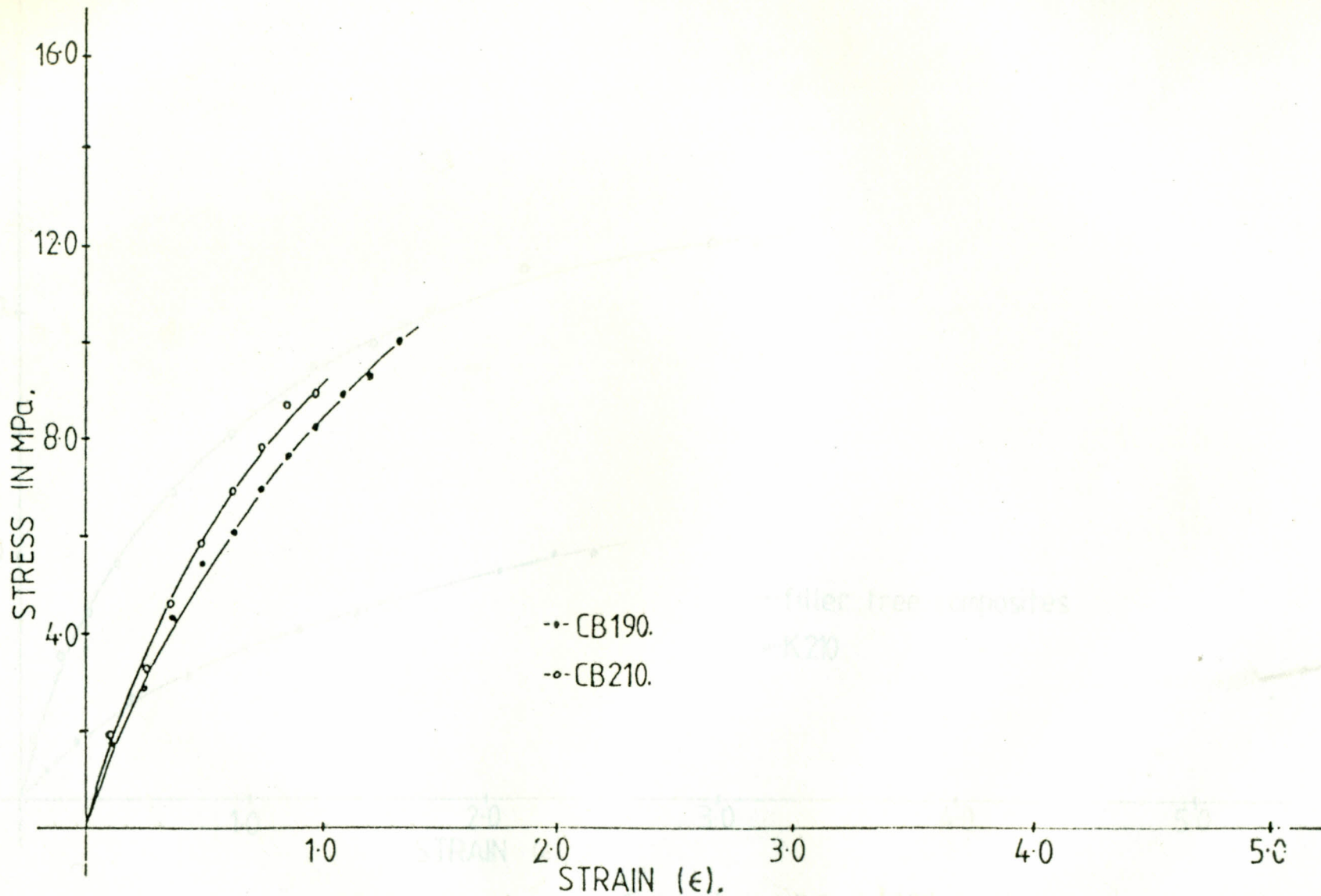
Fig. 36   Stress versus strain curves of samples type CB190 and CB210.
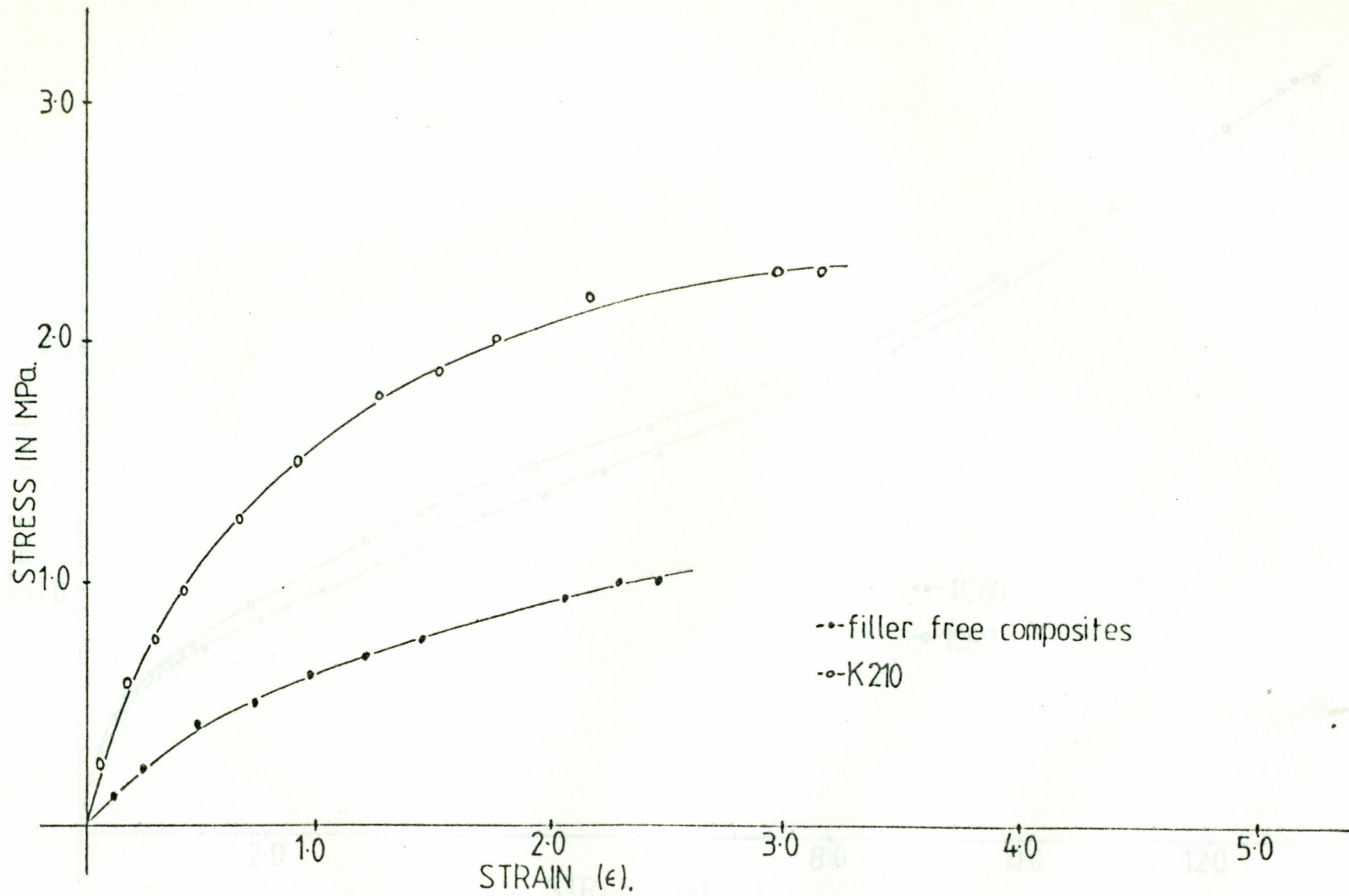
Fig. 37   Stress   versus strain curves of samples type A and K210.

Fig 38   Stress versus strain curves of samples types 1C60 and 1C30.

Fig. 39   Stress versus strain curves of samples types CB60, CB120, CB100 and CB40.
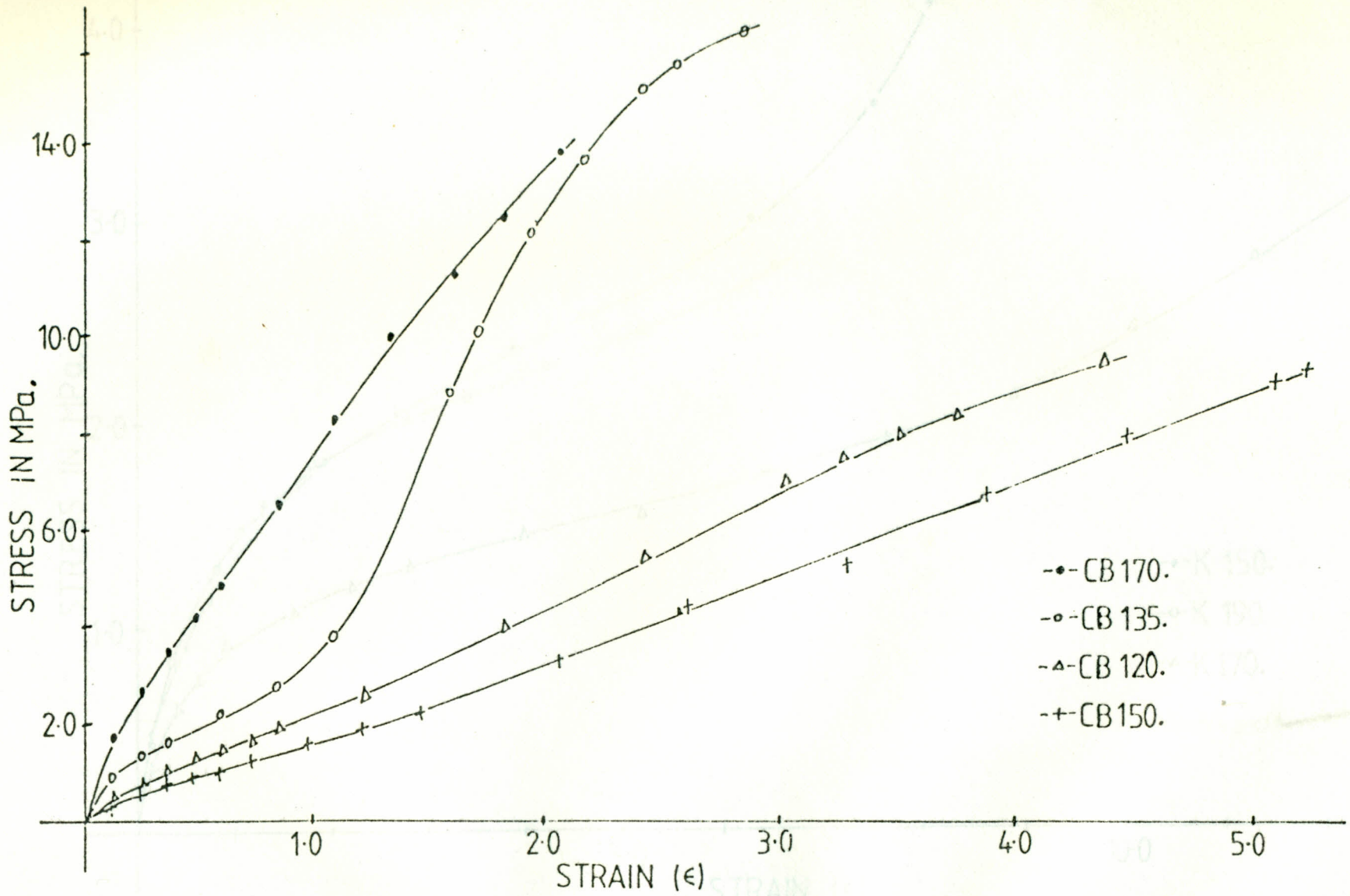
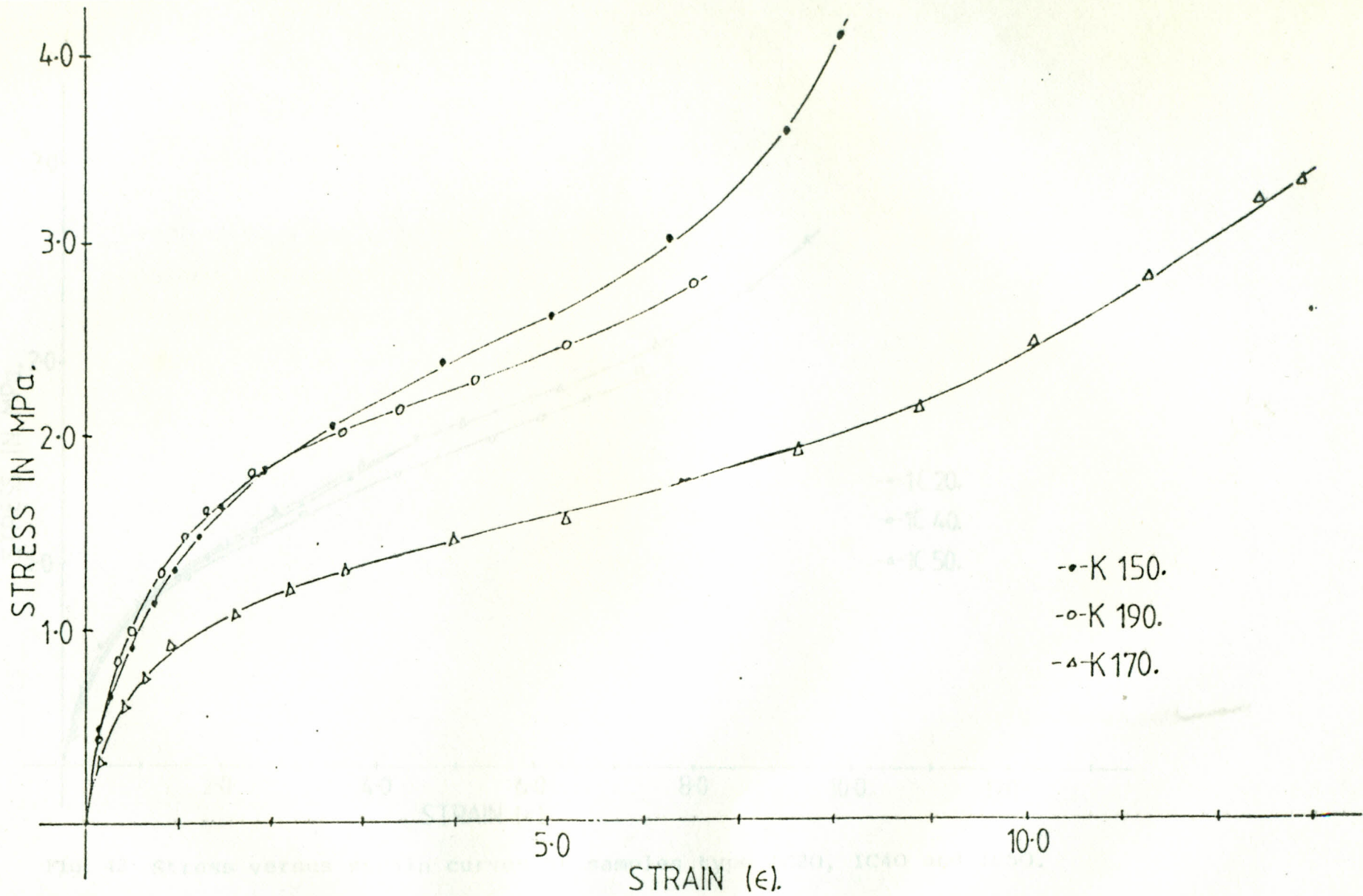Fig. 40   Stress versus strain curves of samples types CB170, CB135, CB120 and CB150

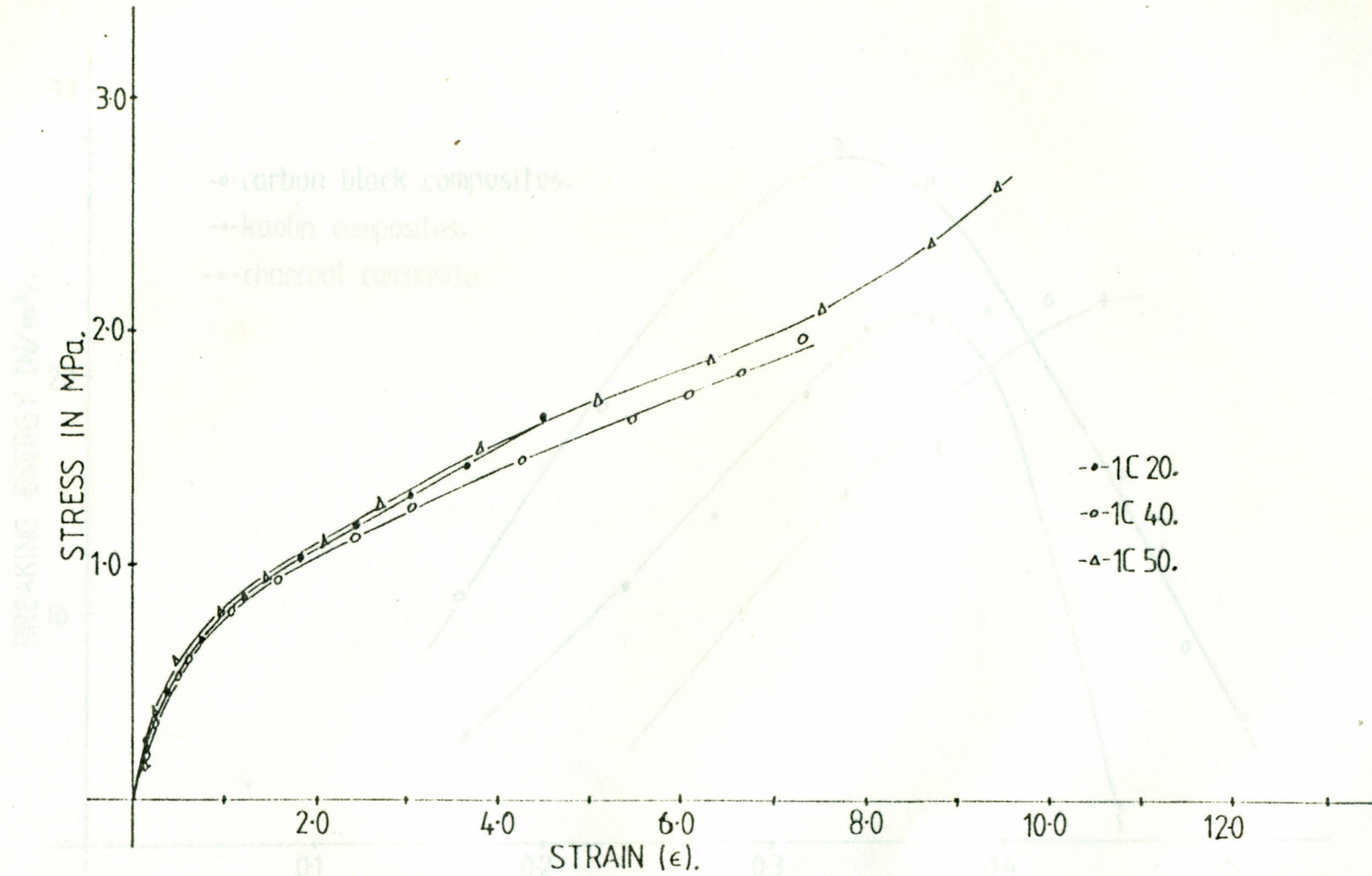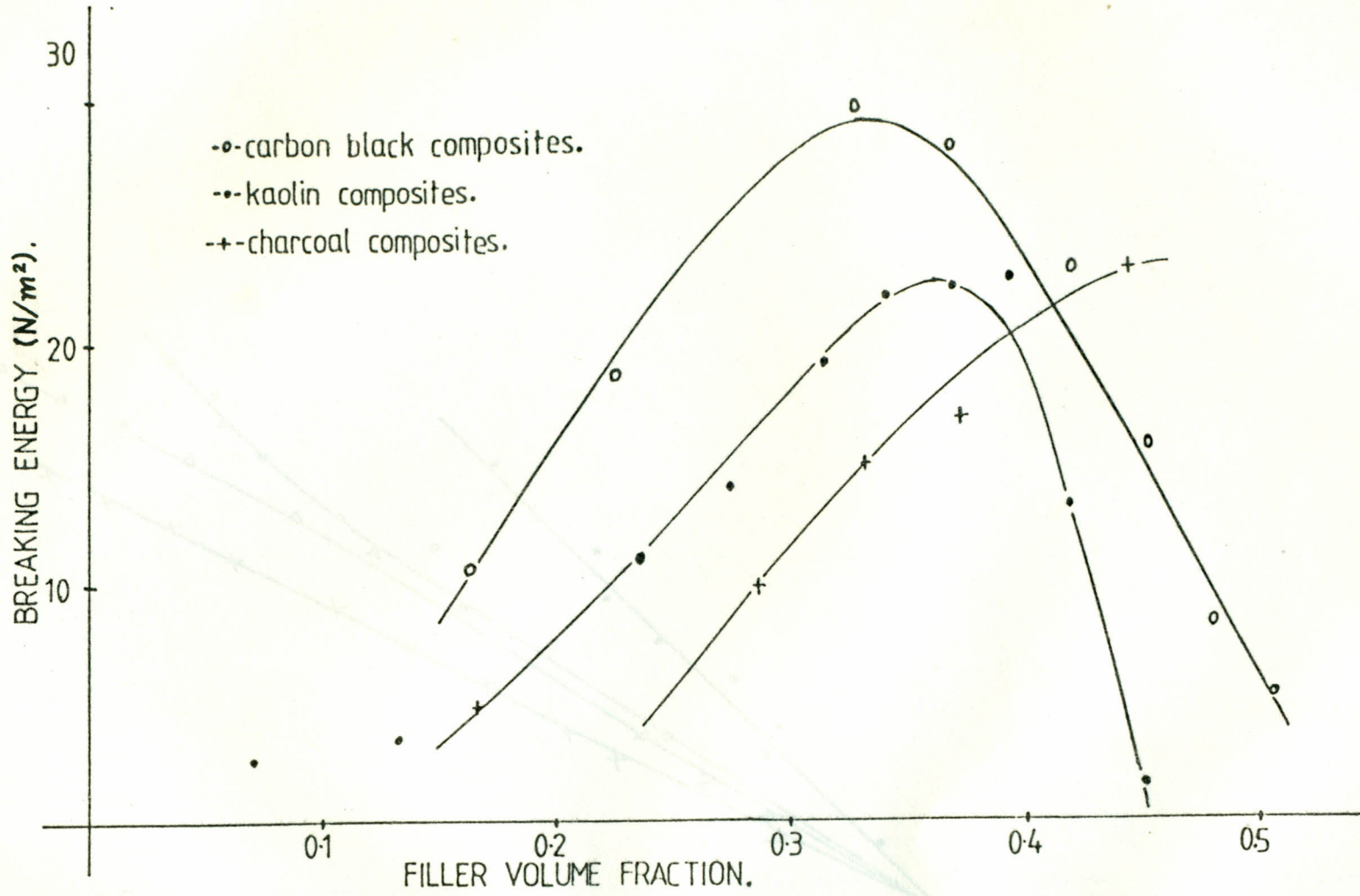Fig. 41   Stress versus strain curves of samples types K150, K190 and K170.

Fig. 42 Stress versus strain curves of samples type IC20, IC40 and IC50.

Fig. 43   Breaking energy versus filler volume fraction of EPDM rubber

Fig. 44   Russell's conductivity equation at 303K, x and
. are the theoretical and experimental values
of k of kaolin composites; Δ and o are theore-
tical and experimental results of k of carbon
black composites.
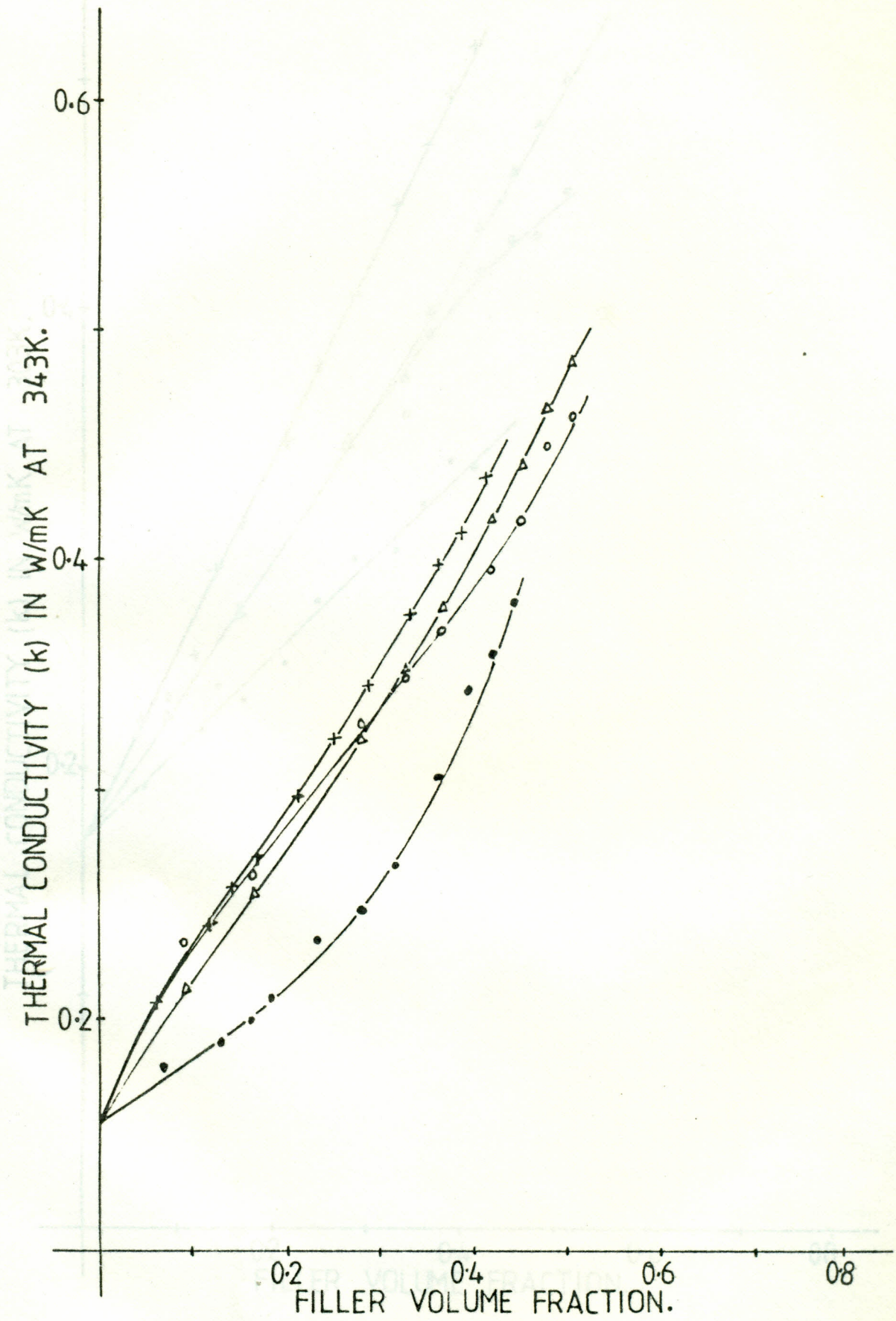
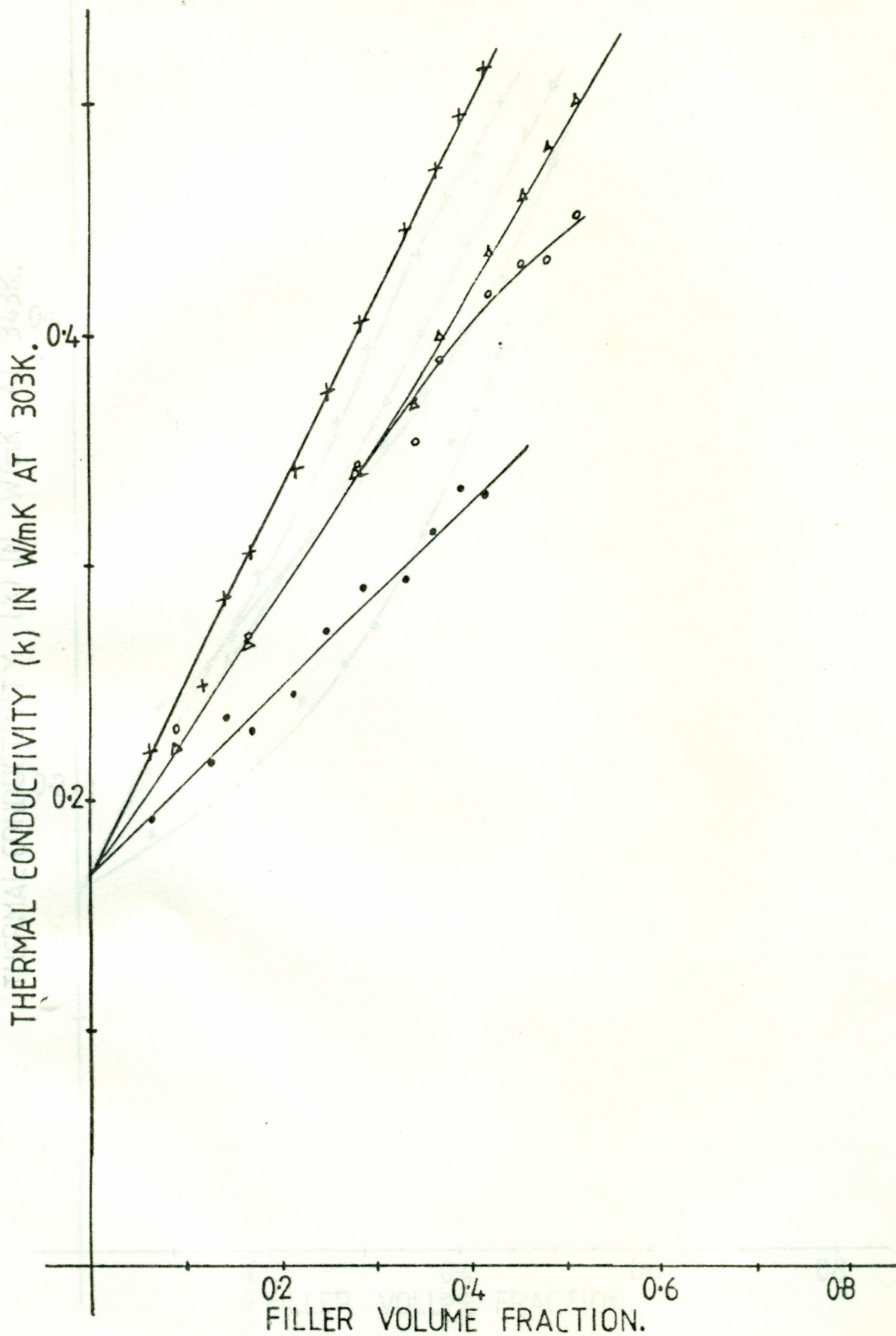Fig. 45   Russell's conductivity equation at 343K, x and
           . are the theoretical and experimental values
           of k, of kaolin filled composites; Δ and o are
           the theoretical and experimental values of k
           of carbon black filled composites

Fig. 46   Del'nev and Zarichnyak's equation at 303K, x
           and . are the theoretical and experimental
           values of k of kaolin composites; Δ and o
           are the theoretical and experimental results
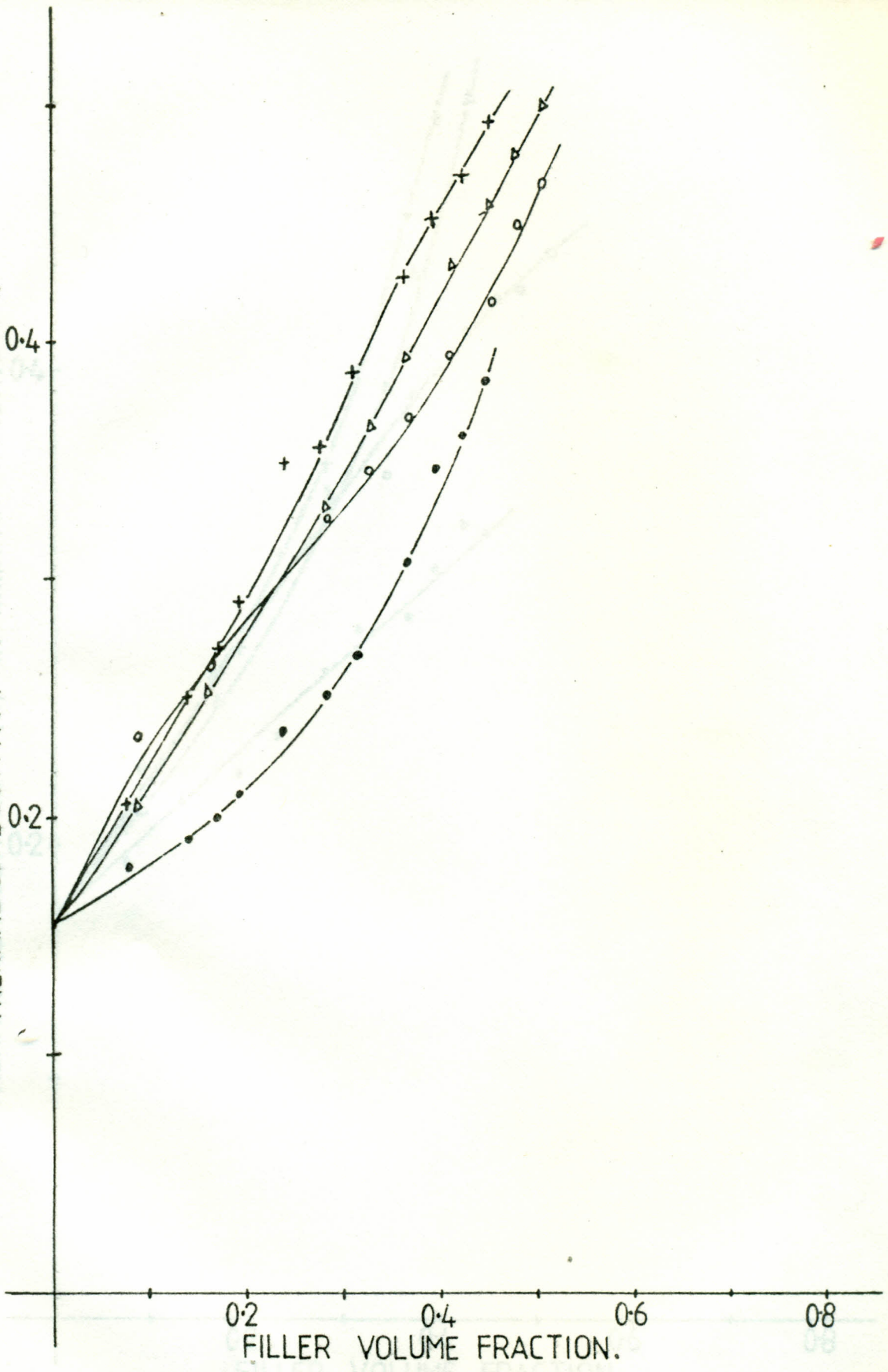   of k of carbon black filled composites.

Fig. 47   Del'nev and Zarichnyak's equation at 343K, x
and . are the theoretical and experimental
values of k of kaolin filled composites; Δ
and o are the theoretical and experimental
results of k of carbon black filled composites.
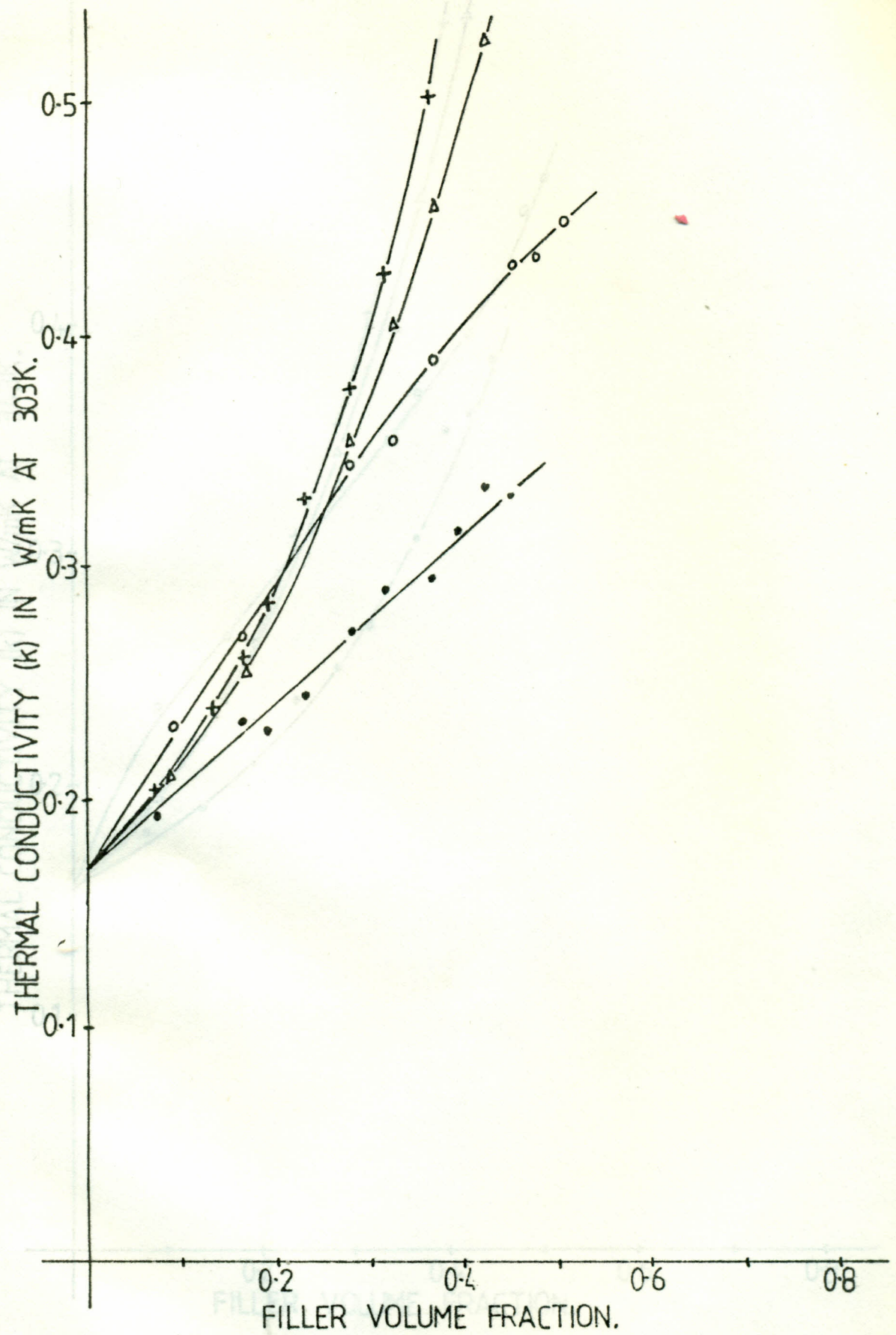
Fig. 50   Brailsford and Major's equations at 303K; x and
               . are the theoretical and experimental values of
               kaolin filled composites; Δ and o are the
               theoretical and experimental results of k of
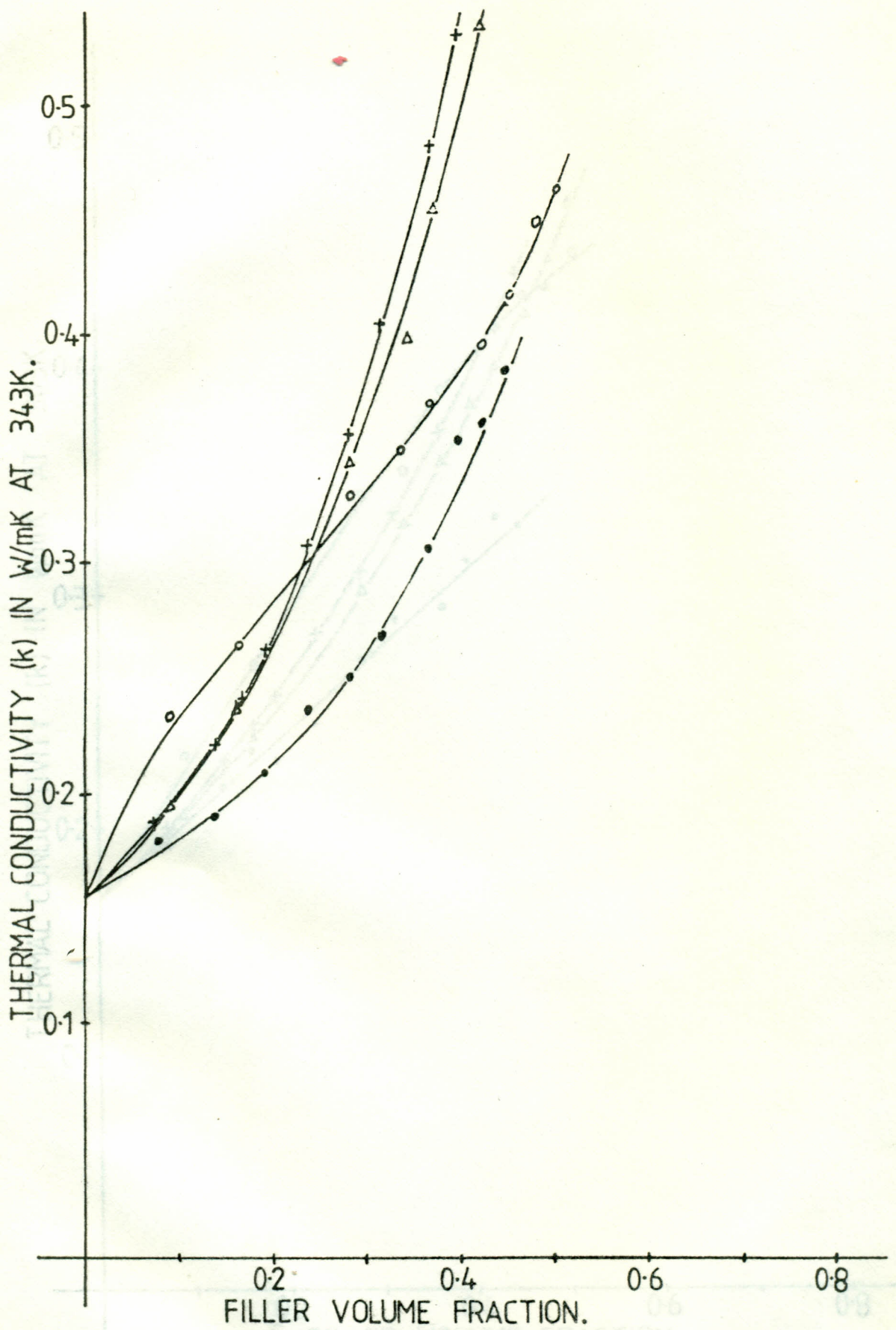   carbon black filled composites.

Fig. 51   Brailsford and Major's equation at 343K; x and
           . are the theoretical and experimental values of
           k of kaolin filled composites; Δ and o are the
           theoretical and experimental results of k of
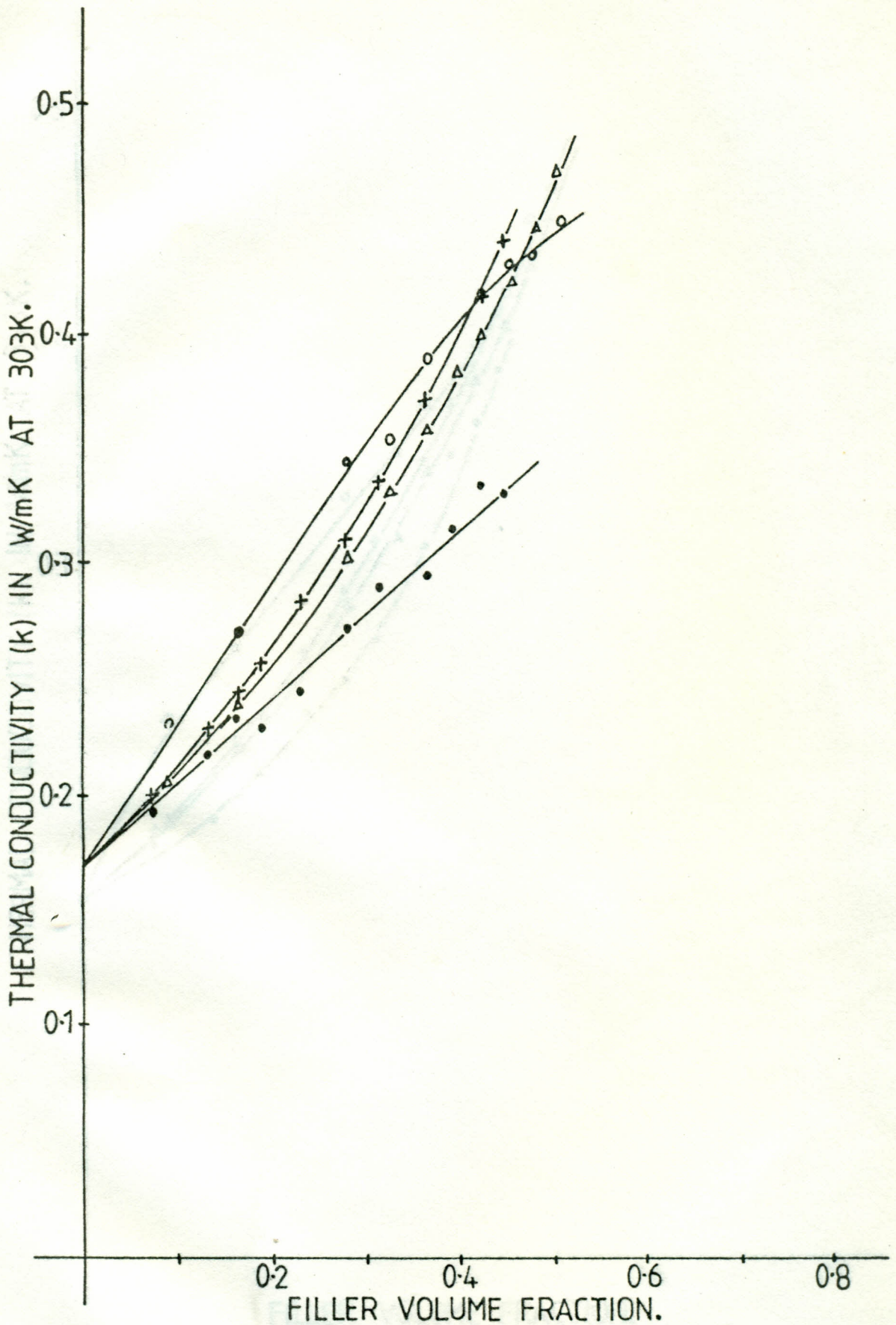   carbon black filled composites.

Fig. 52   Maxwell's equation at 303K, x and . are the
theoretical and experimental values of k of
kaolin filled composites; Δ and o are the
theoretical and experimental results of k of
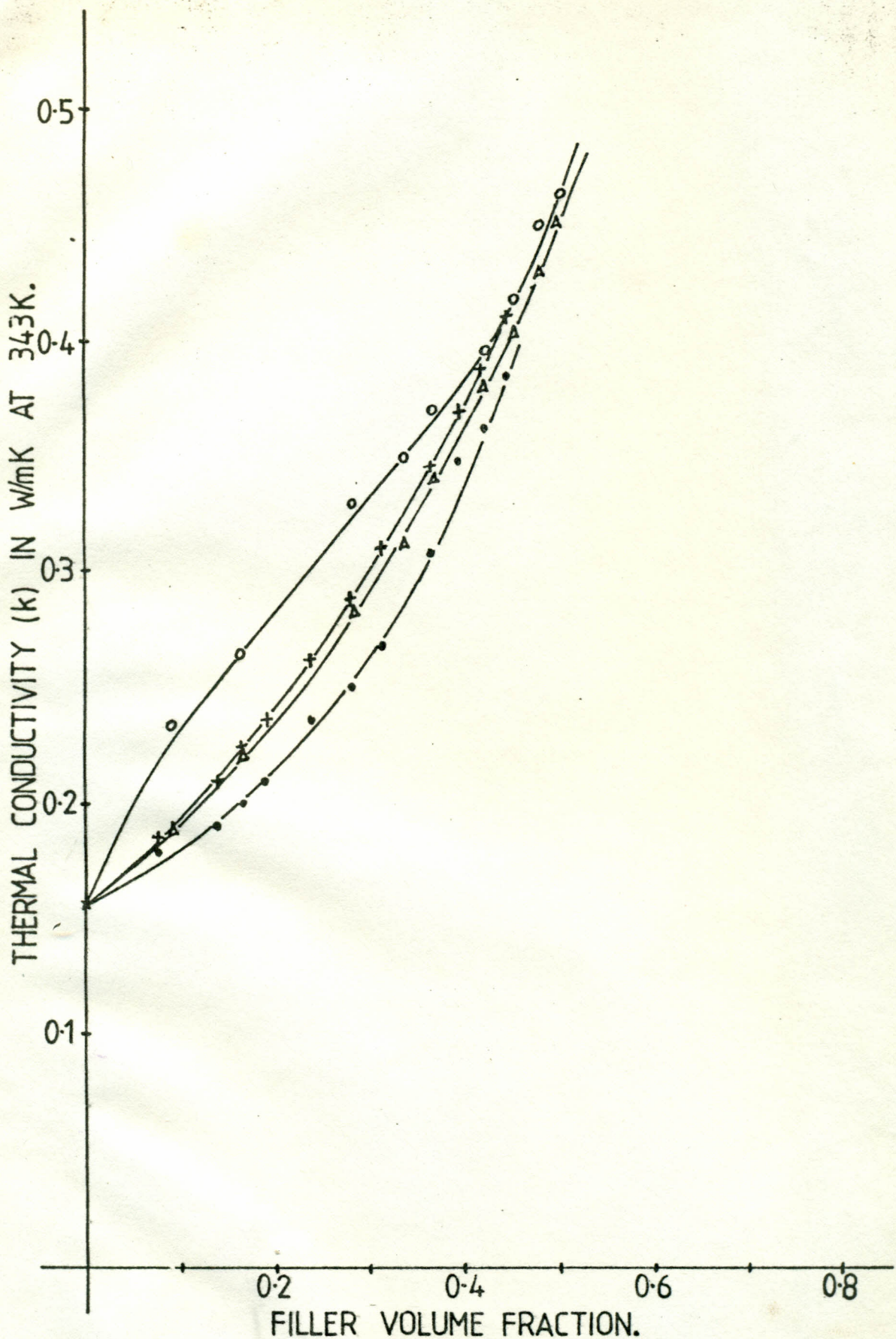carbon black filled composites.

Fig. 53   Maxwell's equation at 343K, x and . are the
theoretical and experimental values of k of
kaolin filled composites; Δ and o are the
theoretical and experimental results of k of
carbon black filled composites.